Micro- and Nano- Fabrication and Replication Techniques

Why do we have to write thing small and replicate fast ?

Plenty of Room at the Bottom

Richard P. Feynman, December 1959

How do we *write* it? We have no standard technique to do this now. But let me argue that it is not as difficult as it first appears to be. We can reverse the lenses of the electron microscope in order to demagnify as well as magnify. A source of ions, sent through the microscope lenses in reverse, could be focused to a very small spot. We could write with that spot like we write in a TV cathode ray oscilloscope, by going across in lines, and having an adjustment which determines the amount of material which is going to be deposited as we scan in lines. **This method might be very slow** because of space charge limitations. There will be more rapid methods. We could first make, perhaps by some **photo process**, a screen which has holes in it in the form of the letters. Then we would strike an arc behind the holes and draw metallic ions through the holes; then we could again use our system of lenses and make a small image in the form of ions, which would deposit the metal on the pin.

Plenty of Room at the Bottom

Richard P. Feynman, December 1959

A simpler way might be this (though I am not sure it would work): We take light and, through an optical microscope running backwards, we focus it onto a very small photoelectric screen. Then electrons come away from the screen where the light is shining. These electrons are focused down in size by the electron microscope lenses to impinge directly upon the surface of the metal. Will such a beam etch away the metal if it is run long enough? I don't know. If it doesn't work for a metal surface, it must be possible to find some surface with which to coat the original pin so that, where the electrons bombard, a change is made which we could recognize later.

Plenty of Room at the Bottom

Richard P. Feynman, December 1959

There is no intensity problem in these devices---not what you are used to in magnification, where you have to take a few electrons and spread them over a bigger and bigger screen; it is just the opposite. The light which we get from a page is concentrated onto a very small area so it is very intense. The few electrons which come from the photoelectric screen are demagnified down to a very tiny area so that, again, they are very intense. **I don't know why this hasn't been done yet!**

Building a computer

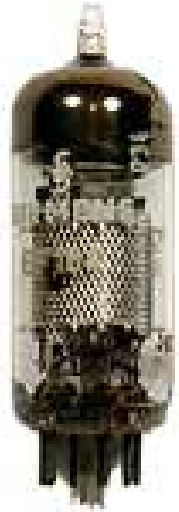

First Integrated Circuit

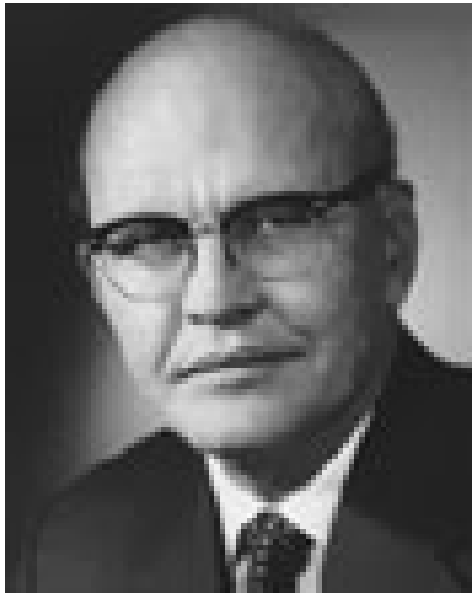

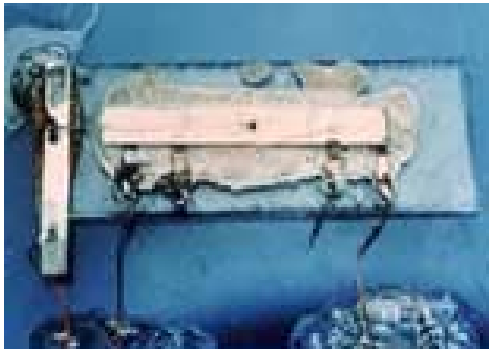

"What we didn't realize then was that the integrated circuit would reduce the cost of electronic functions by a factor of a million to one, nothing had ever done that for anything before" - Jack Kilby 2000 Nobel Prize

1958 Texas Instruments

Moore's Law

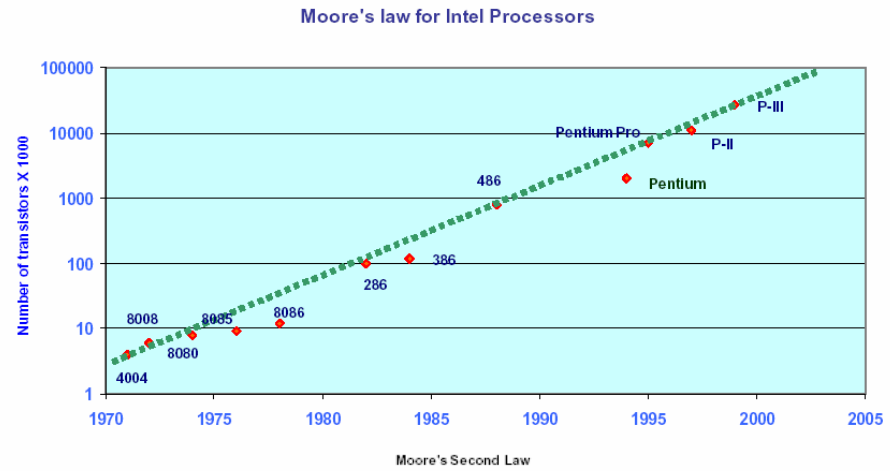

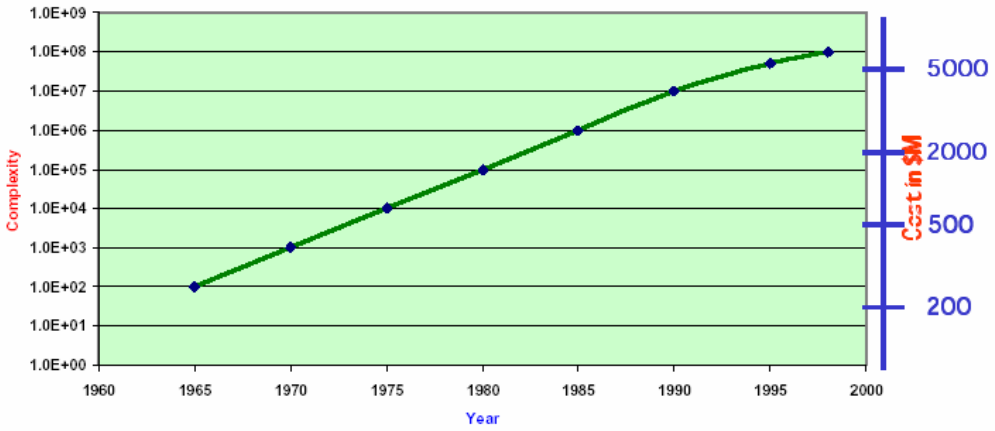

Moore's Laws

First Law: Number of components in a chip (IC) will double roughly every 18 months (1965, in *Electronics*). This has held true more or less since then.

Second Law: Facility costs increase on a semilog scale (terminology due to Eugene Meieran, Intel Fellow). Fab costs double approximately every four years.

Tool Cost

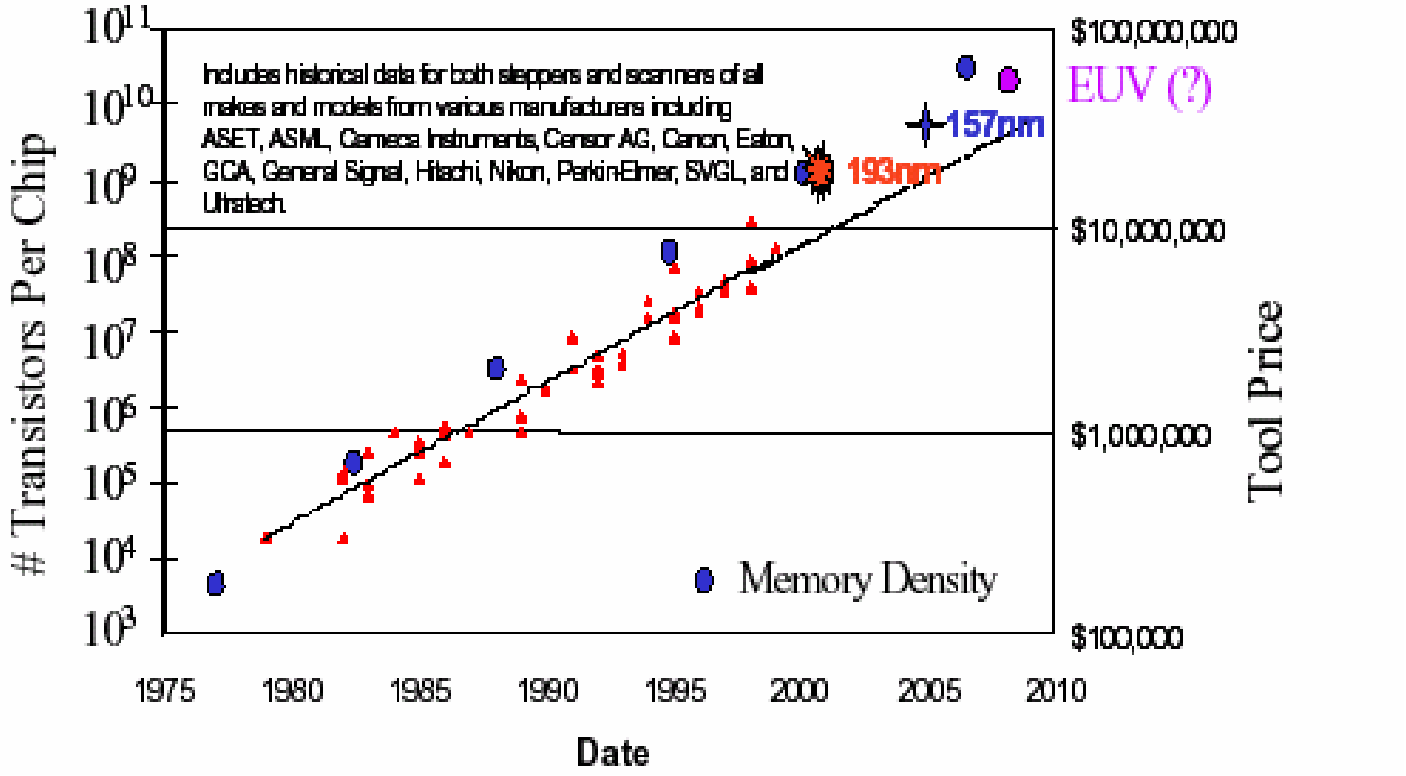
Includes historical data for both steppers and scanners of all makes and models from various manufacturers including ASET, ASML, Cameca Instruments, Censor AG, Canon, Eaton, GCA, General Signal, Hitachi, Nikon, PerkinElmer, SVGL, and Ultratech.
157nm
193nm
EUV (?)
Memory Density
Transistors Per Chip
Tool Price
Date
10^{11}
10^{10}
10^{9}
10^{8}
10^{7}
10^{6}
10^{5}
10^{4}
10^{3}
$100,000,000
$10,000,000
$1,000,000
$100,000
1975
1980
1985
1990
1995
2000
2005
2010

metal-oxide-semiconductor field-effect transistor (MOSET)

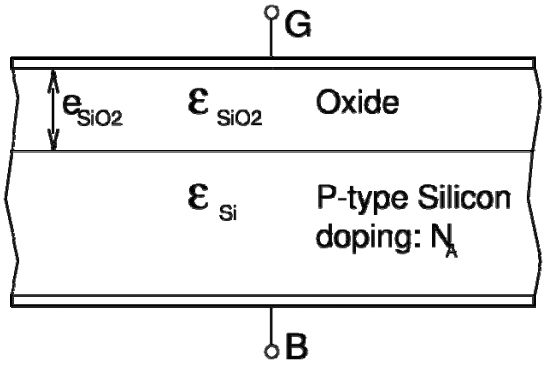

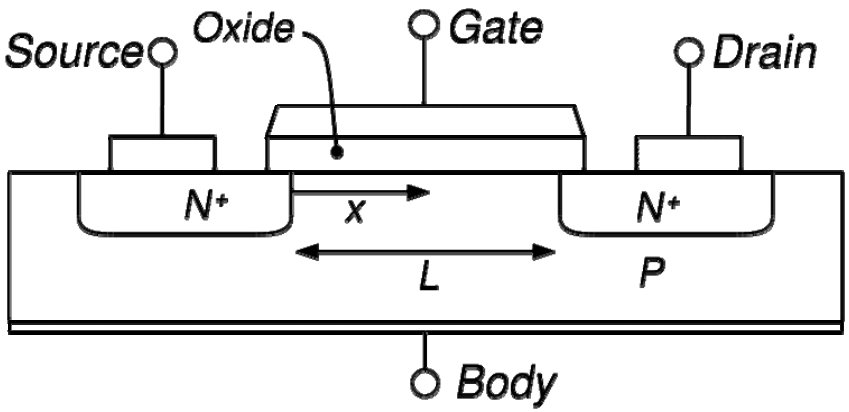

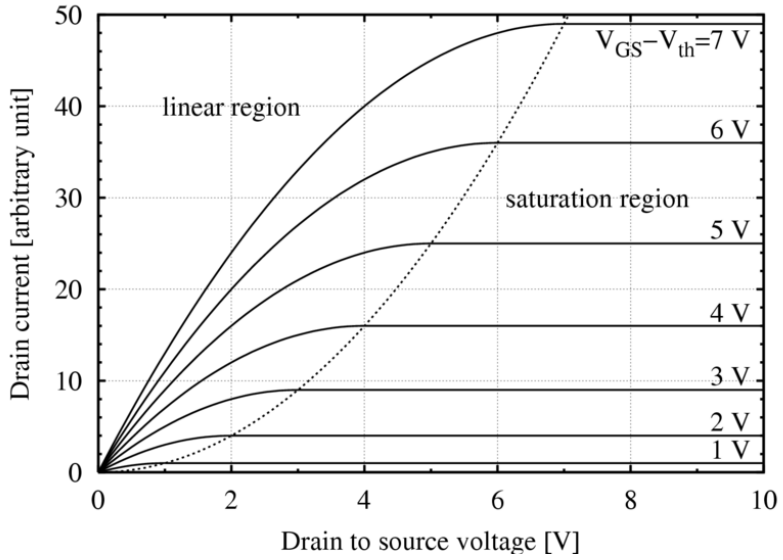

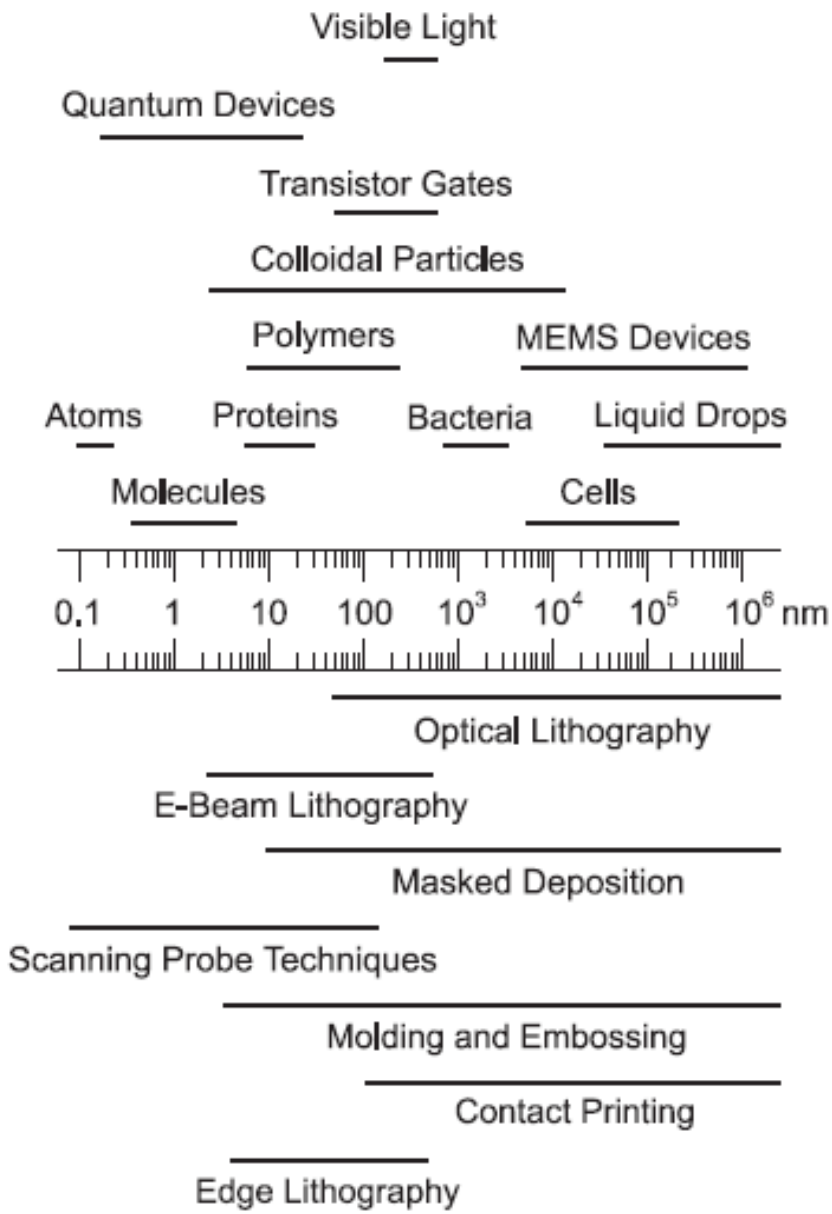
Visible Light
Quantum Devices
Transistor Gates
Colloidal Particles
Polymers
MEMS Devices
Atoms
Proteins
Bacteria
Liquid Drops
Molecules
Cells
0.1
1
10
100
10^3
10^4
10^5
10^6 nm
Optical Lithography
E-Beam Lithography
Masked Deposition
Scanning Probe Techniques
Molding and Embossing
Contact Printing
Edge Lithography

Optical Microscope

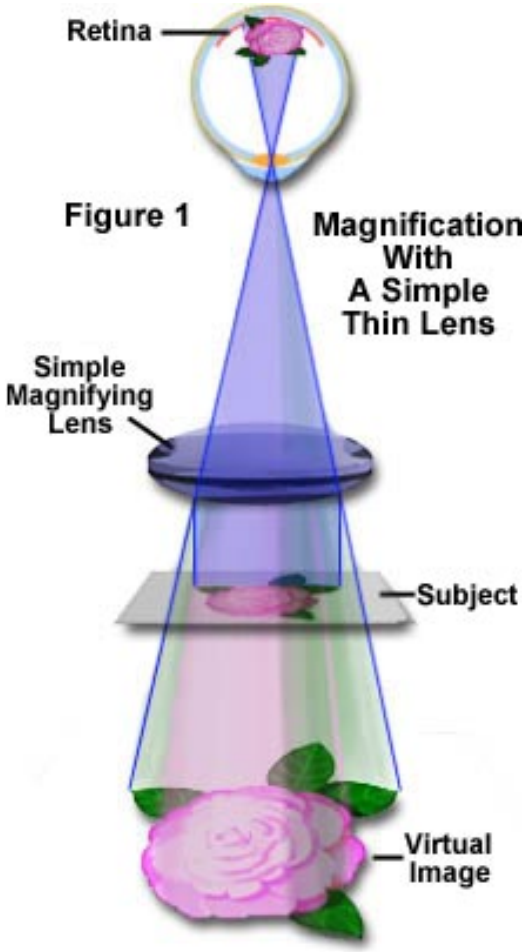

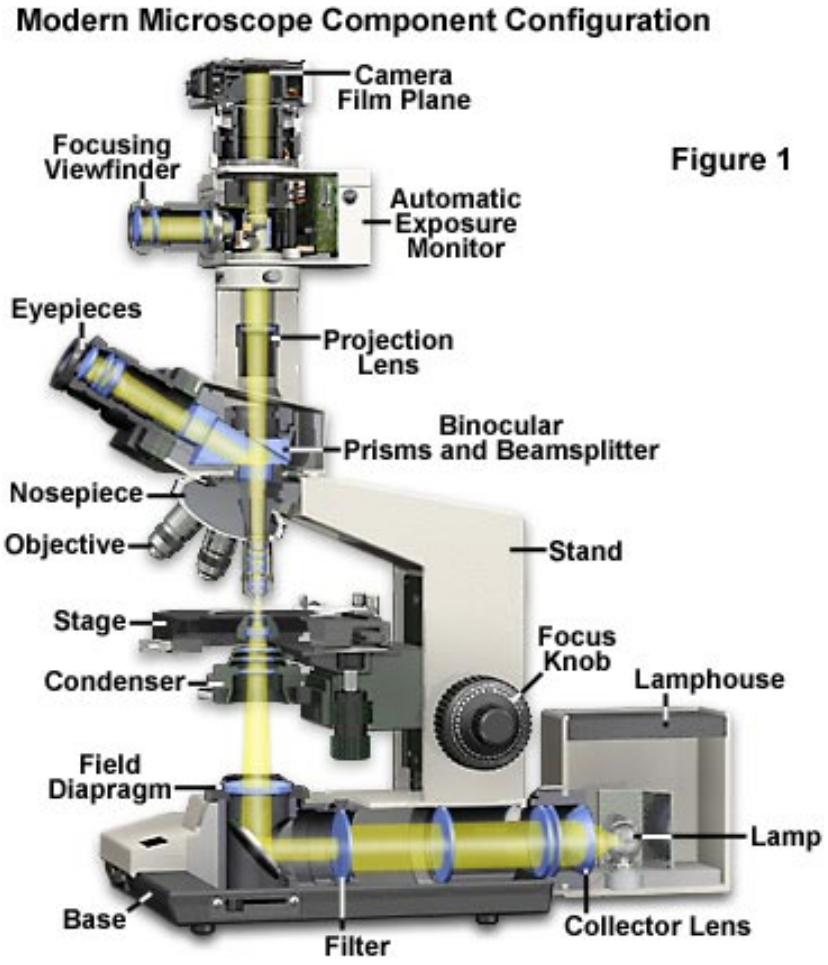

Limit of Photolithography

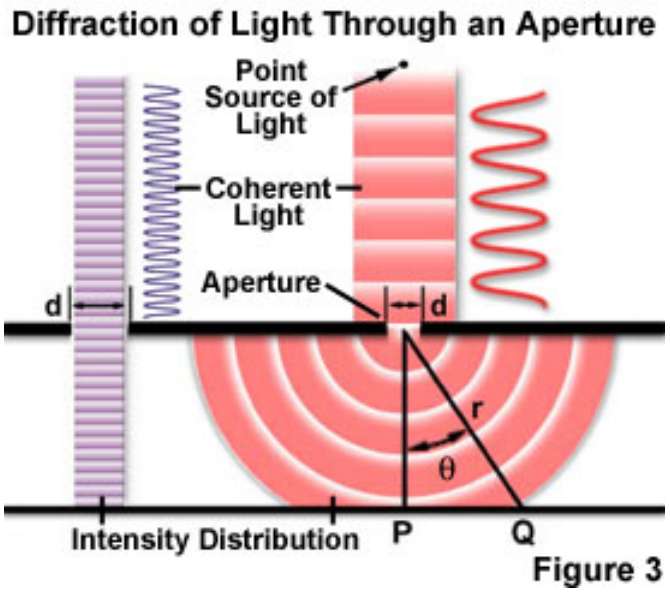

Figure 3

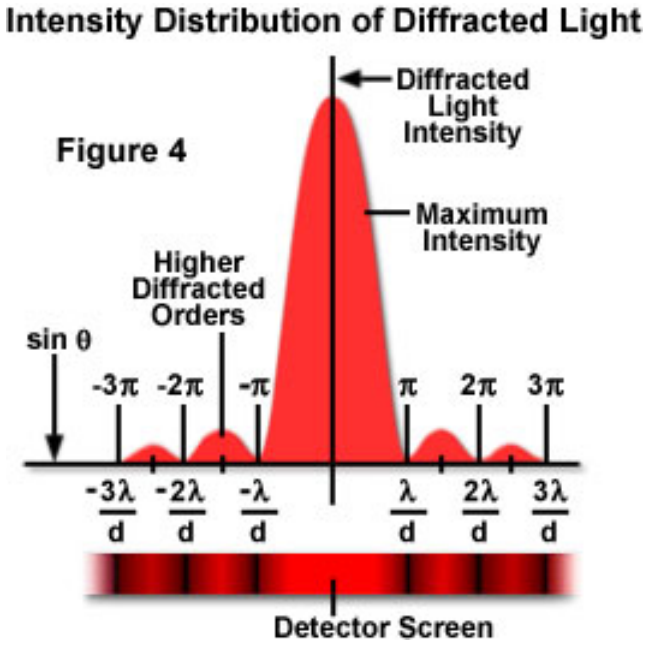

Figure 4

r = 1.22 x λ/(2 x N.A.)

N.A. = n x sin(θ)

Diffraction Limit

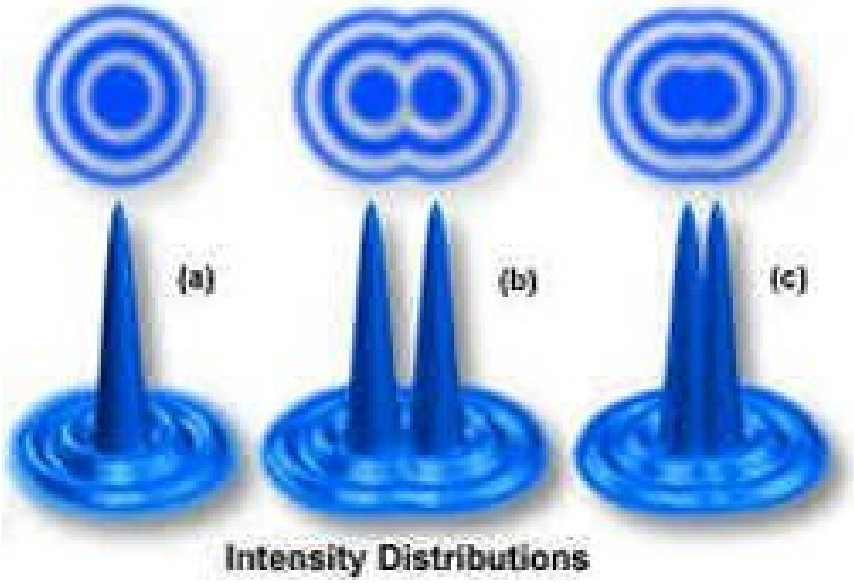

Resolution = K x λ/(N.A.)

Depth of Focus = λ/(N.A.)^2

K = 0.61

Photolithography

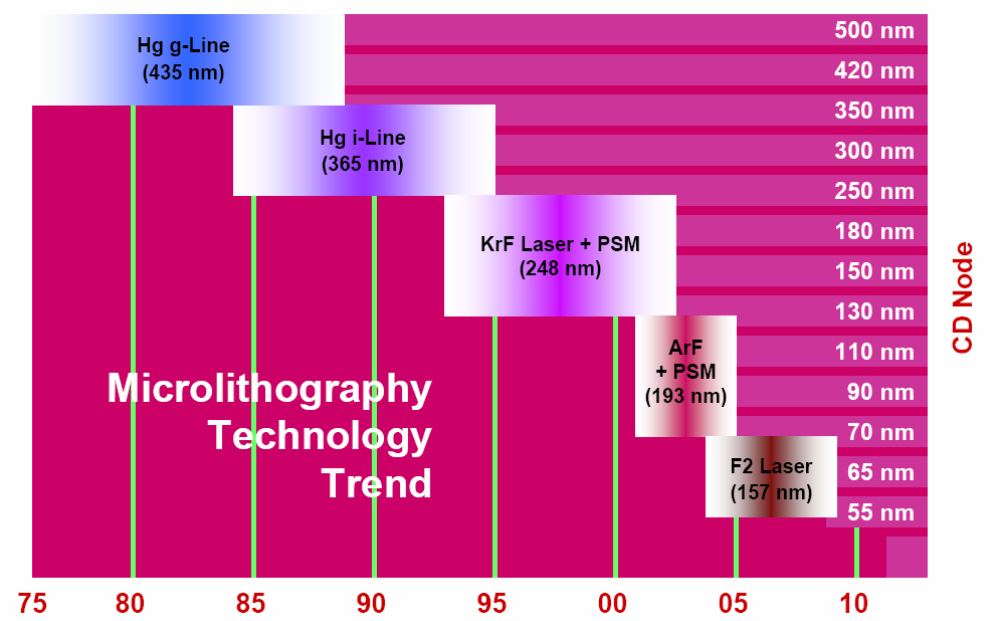

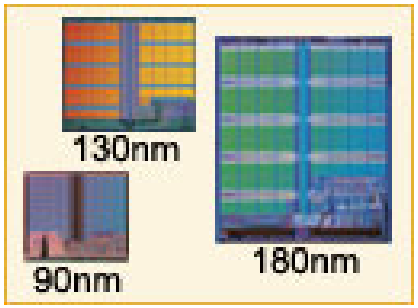

Methods of Photolithography

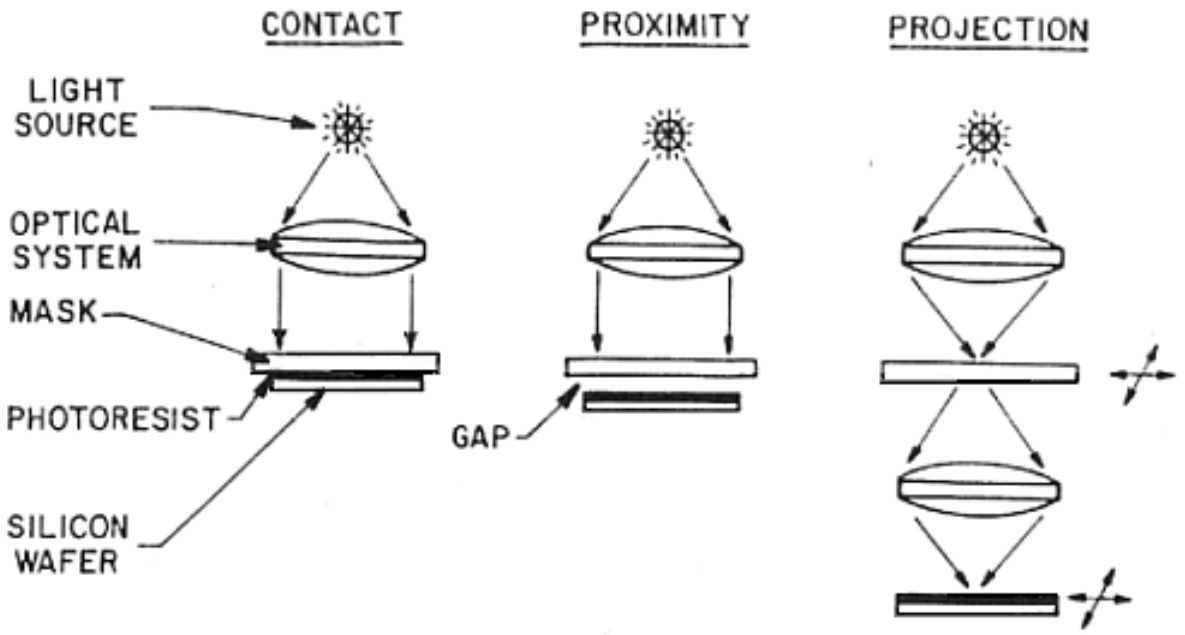

UV Wavelength (nm)	Wavelength Name	UV Emission Source
436	g-line	Mercury arc lamp
405	h-line	Mercury arc lamp
365	i-line	Mercury arc lamp
248	Deep UV (DUV)	Mercury arc lamp or Krypton Fluoride (KrF) excimer laser
193	Deep UV (DUV)	Argon Fluoride (ArF) excimer laser
157	Vacuum UV (VUV)	Fluorine (F_2) excimer laser

Water Immersion Lithography

Year	Linewidth (nm)	Wavelength (nm)
1986	1200	436 g-line mercury lamp
1988	800	436/365
1991	500	365 i-line mercury lamp
1994	350	365/248
1997	250	248 KrF excimer laser
1999	180	248
2001	130	248
2003	90	248/193
2005	65	193 ArF excimer laser
2007	45	193/157

Resolution (R) = K x λ/(N.A.)
K = 0.25, NA ~1.4, λ = 193
R = 35 nm

Air n= 1.0003
Water n = 1.437

Year	Linewidth (nm)	Wavelength (nm)
1986	1,200	436
1988	800	436/365
1991	500	365
1994	350	365/248
1997	250	248
1999	180	248
2001	130	248
2003	90	248/193
2005 (fcst)	65	193
2007 (fcst)	45	193

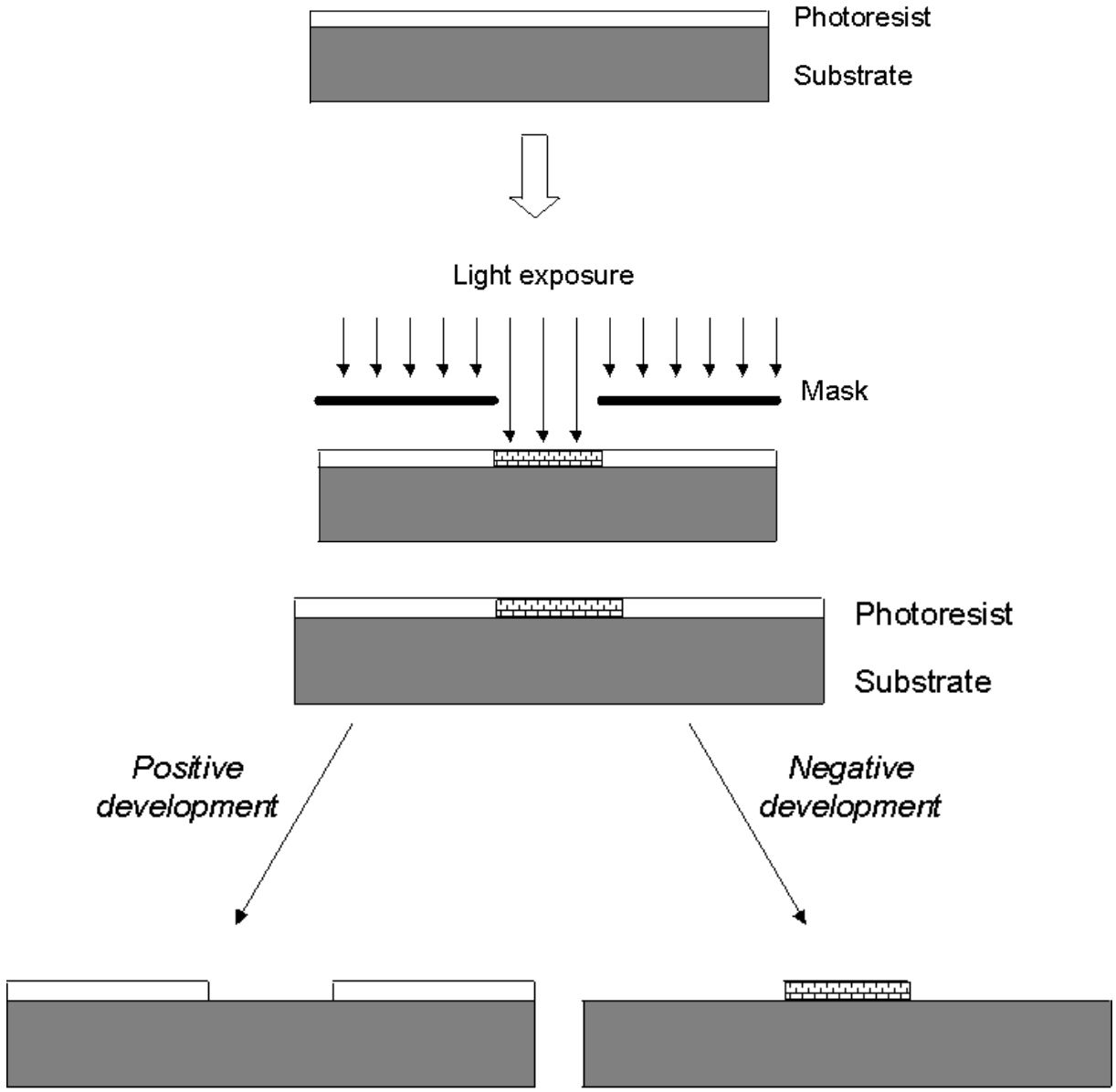
Photoresist
Substrate
Light exposure
Mask
Photoresist
Substrate
Positive development
Negative development
Polymer is more soluble after exposure.
Polymer is less soluble after exposure.

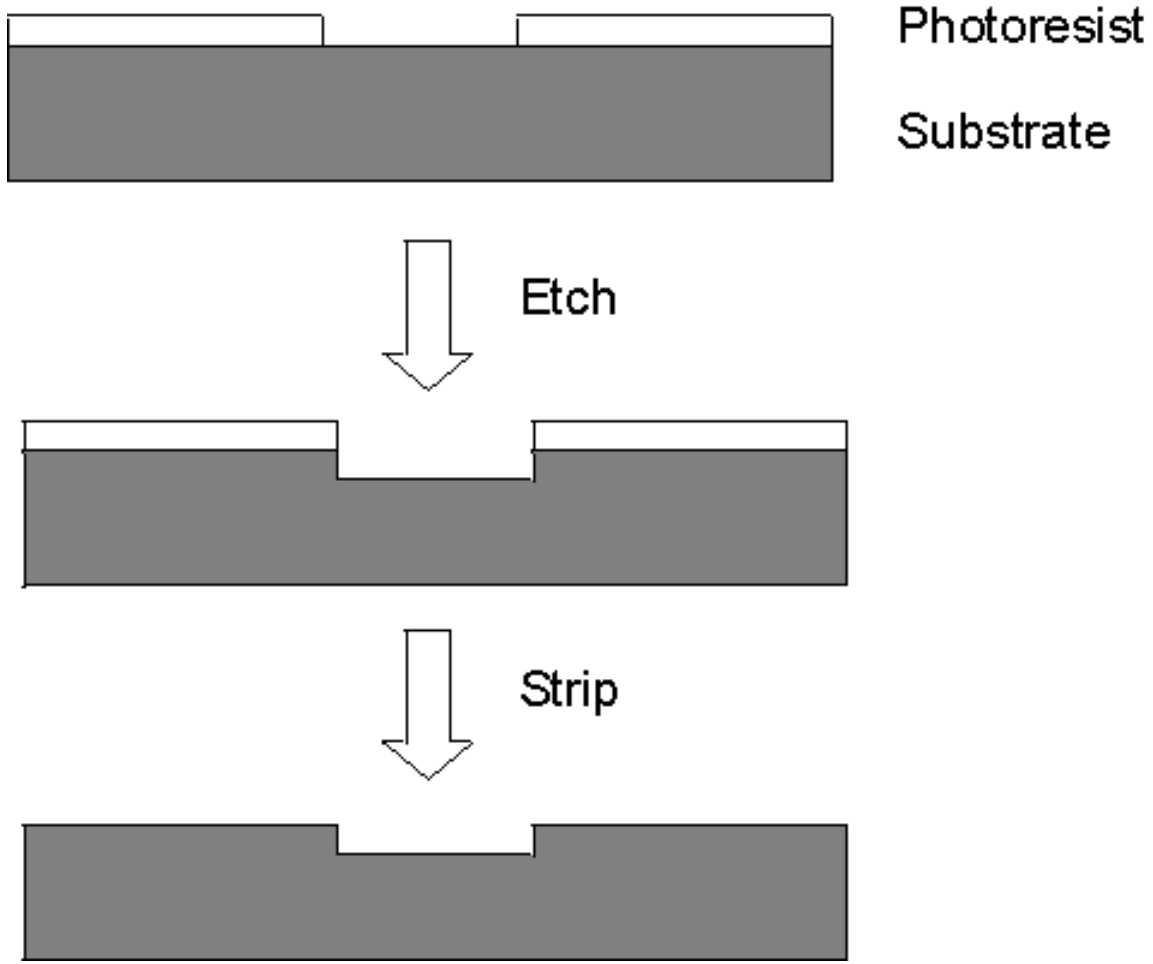
Photoresist
Substrate
Etch
Strip

RCA Cleaning (By Radio Corporation of America in 1965)

Chemicals	Volume ratio	Procedure Time (min)	Operation Temperature	Function
Trichlorothane		5	Room T	Dissolve Organic
Acetone		5	Room T	Dissolve Organic
DI Water		5	Room T	Washing
H_2SO_4 (98%)-H_2O_2 (30%) (Piranha Solution)	3:1	10-20	～90℃	Oxide and Dissolve Organic and Metals
DI Water		5	Room T	Washing
HF(49 wt %)-H_2O	～2:100	10-20	Room T	Dissolve surface $Si0_2$
NH_4OH(29%)-H_2O_2(30%)-H_2O	1:1:5	10-20	～90℃	Oxide and Dissolve Metals
DI Water		5	Room T	Washing
HCl(37%)- H_2O_2(30%)-H_2O	1:1:5	10-20	～90℃	Oxide and Dissolve Metals
DI Water		5	Room T	Washing
Spin Dry (In lad – N_2 blow)				

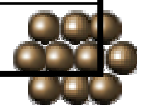

Spin Coating Photoresist on Wafer

1

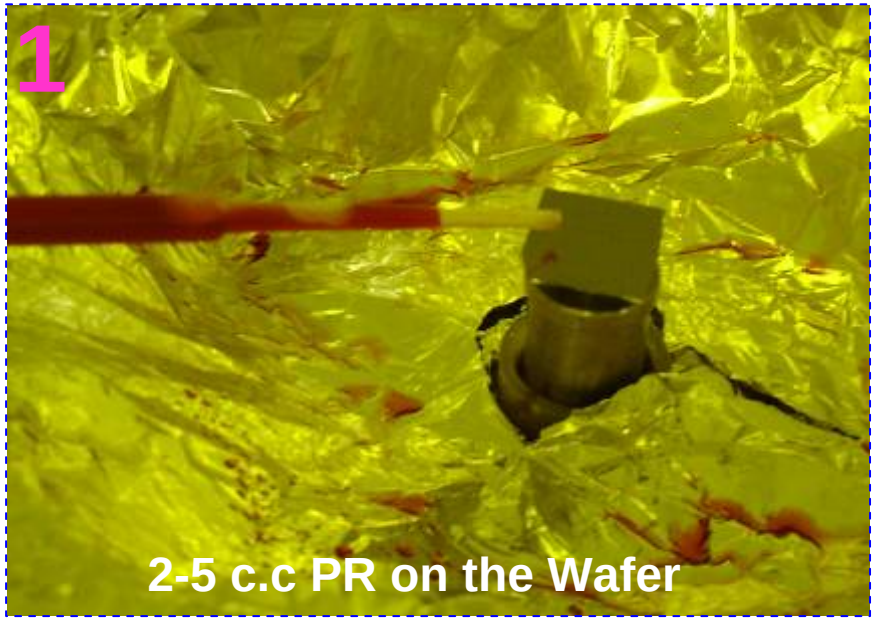

2-5 c.c PR on the Wafer

2

Wait for 5 to 15 second

3

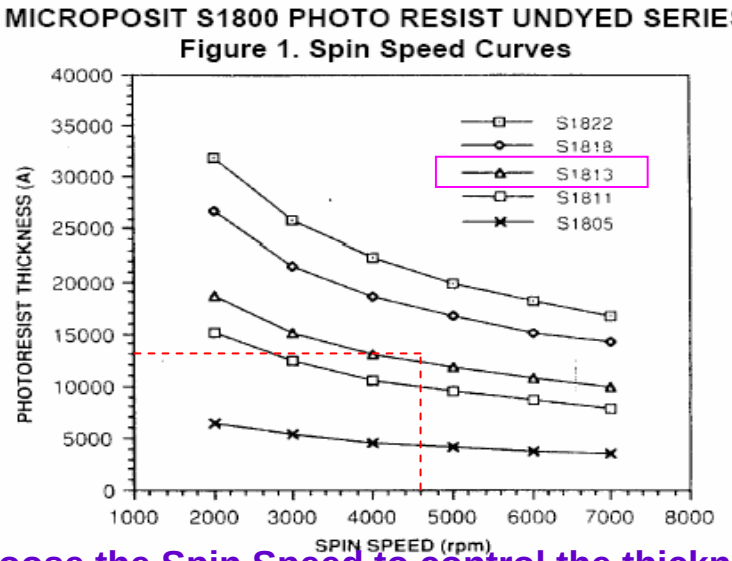

Choose the Spin Speed to control the thickness

- Photo resist：Shipley **1813**
- **Spin： 2000 rpm 5 s**
  4500 rpm 15 s
- Soft Bake：110℃ 60 s
- Exposure：7 s
- Developed：MF319 for 15 s

Align the pattern and Exposure

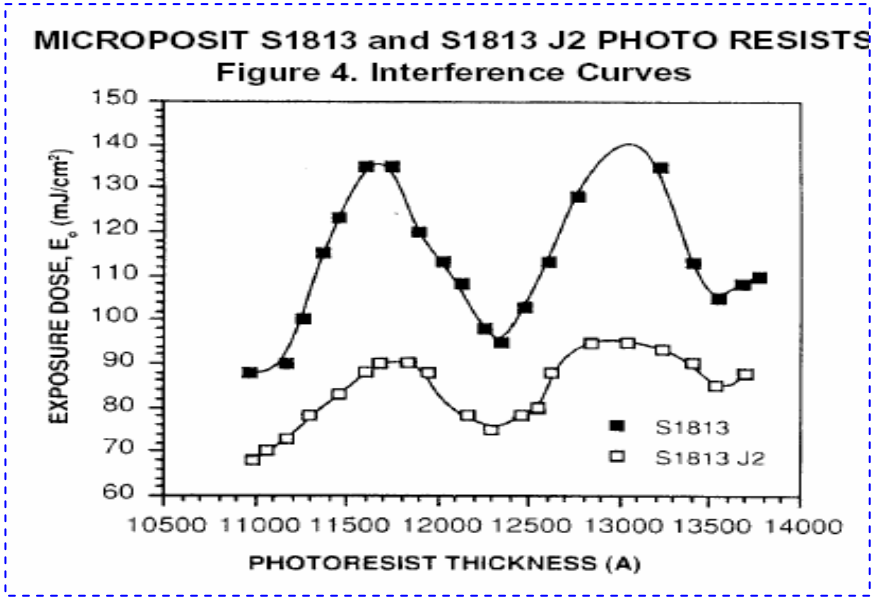

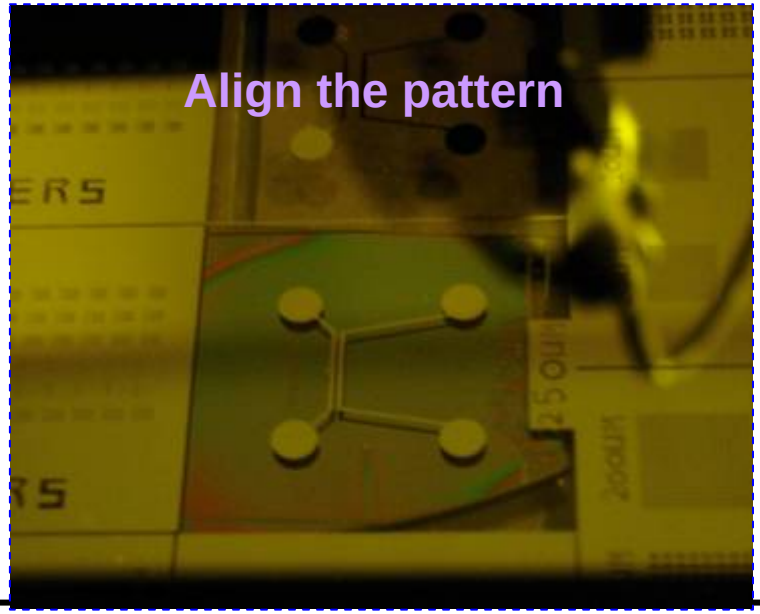

Standard Mask Size: 5” x 5”

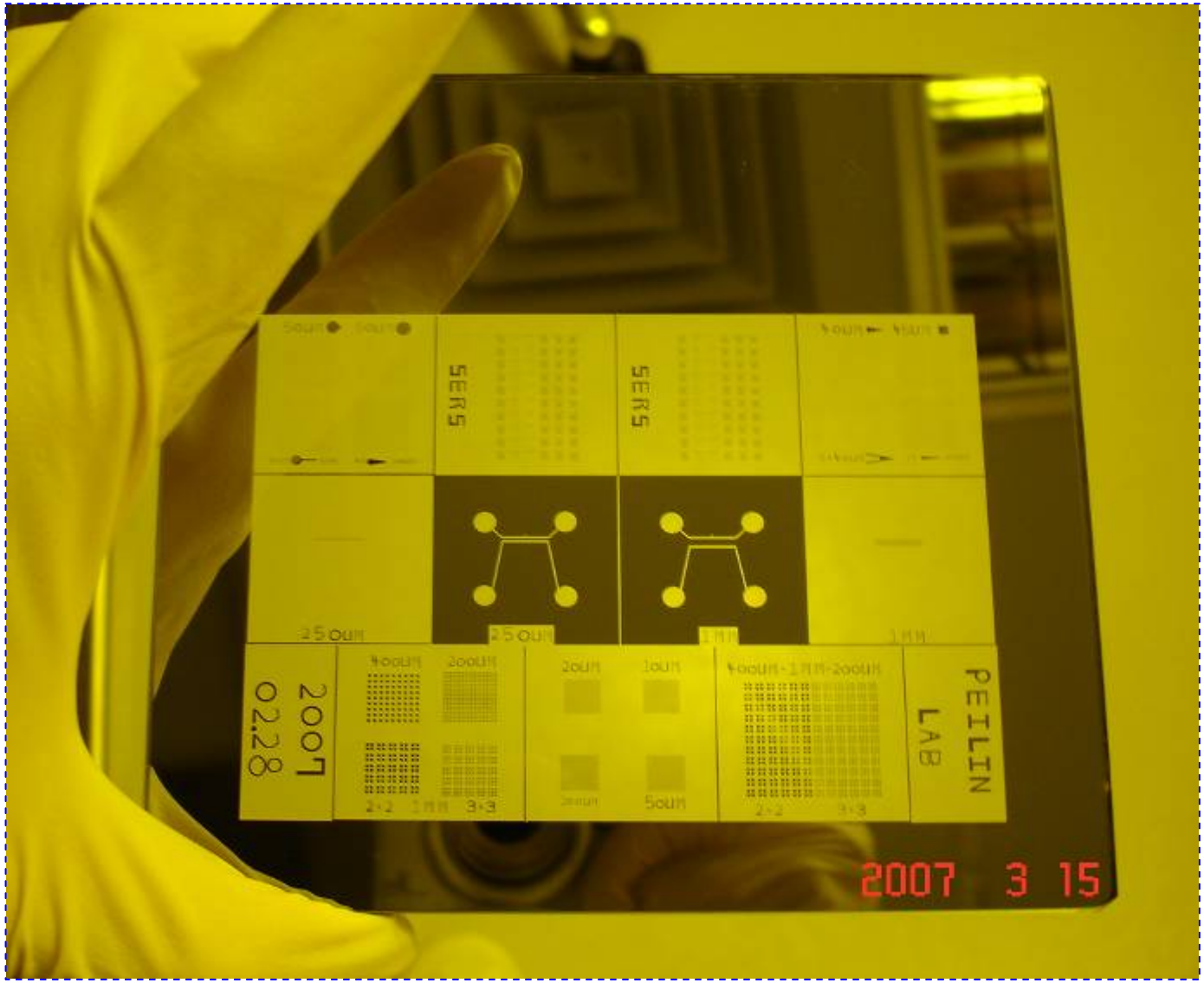

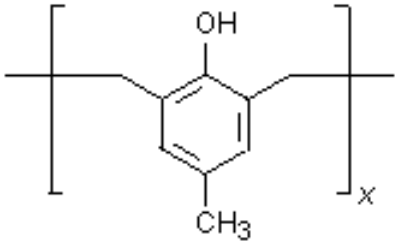

Novolak

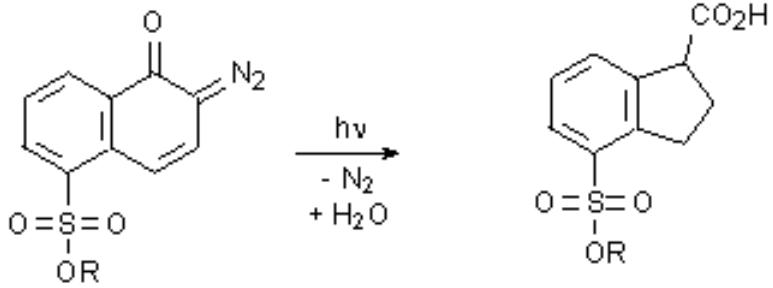

Diazonaphthaquinone additive

Positive tone

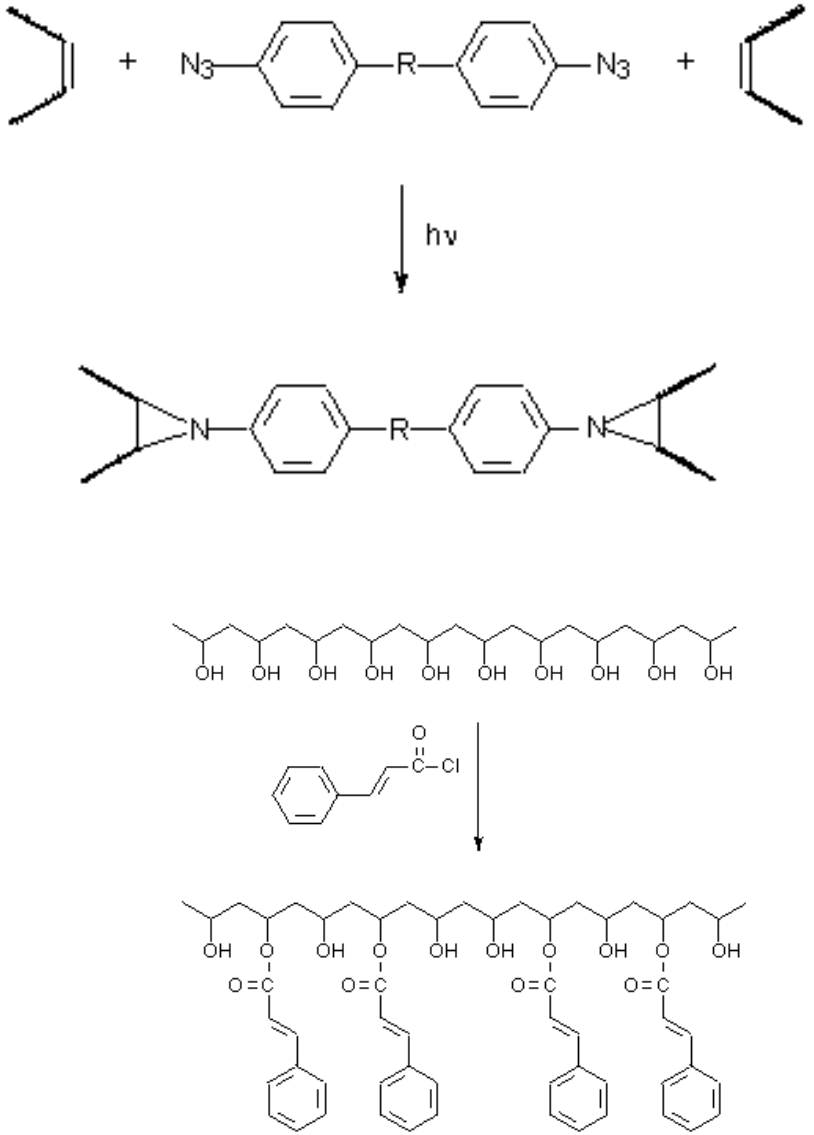

Negative tone

Some Photoresist Need PEB (post exposure Bake)

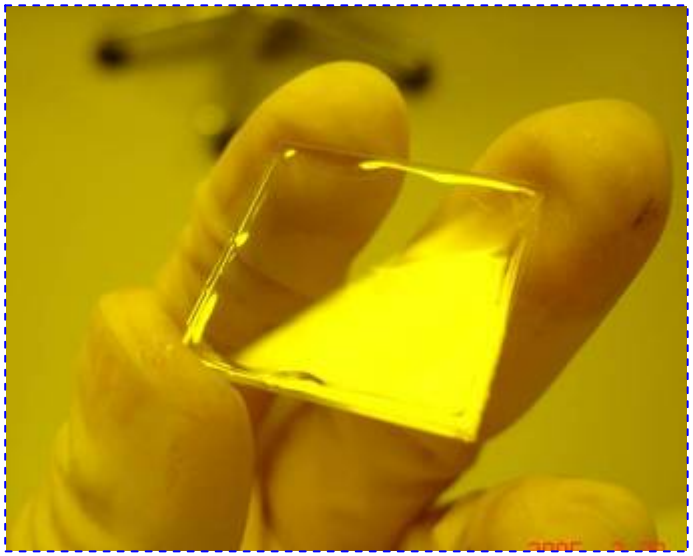

SU-8 2015

65 ℃, 60 s

95 ℃, 60 s

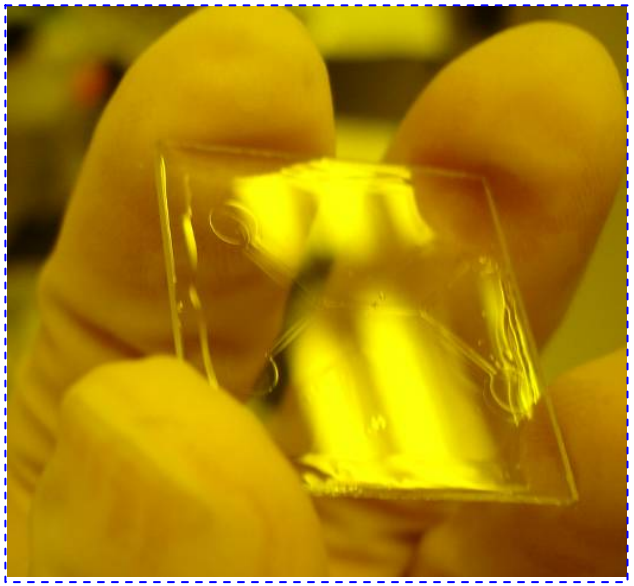

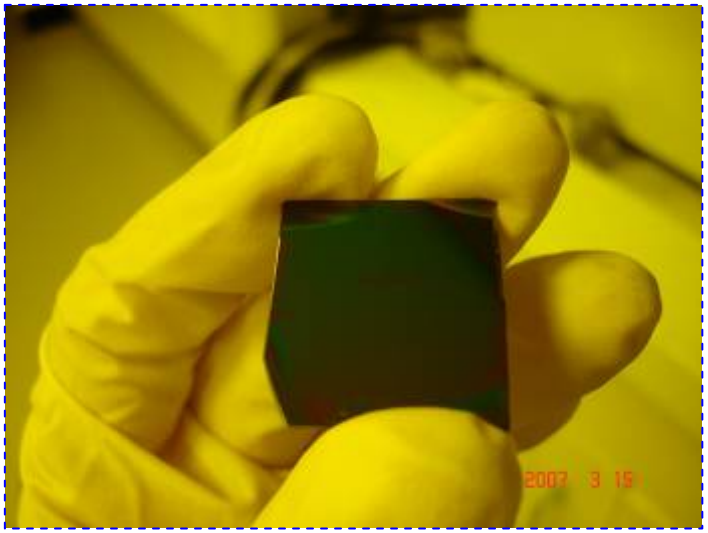

SPR 510A

90 ℃, 90 s

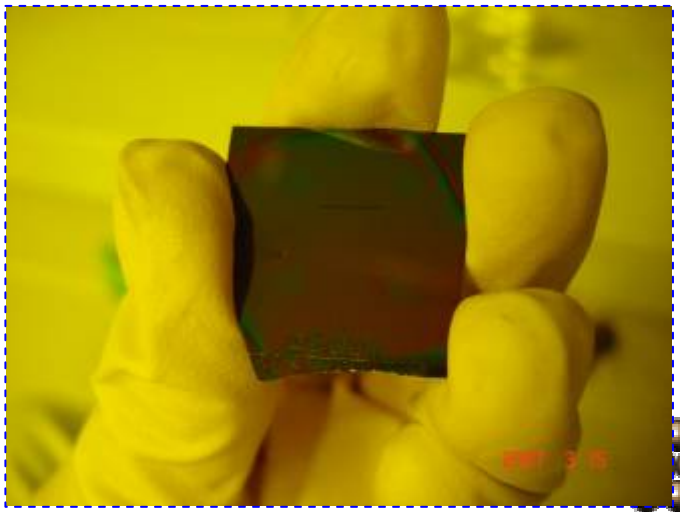

Develop the Photoresis

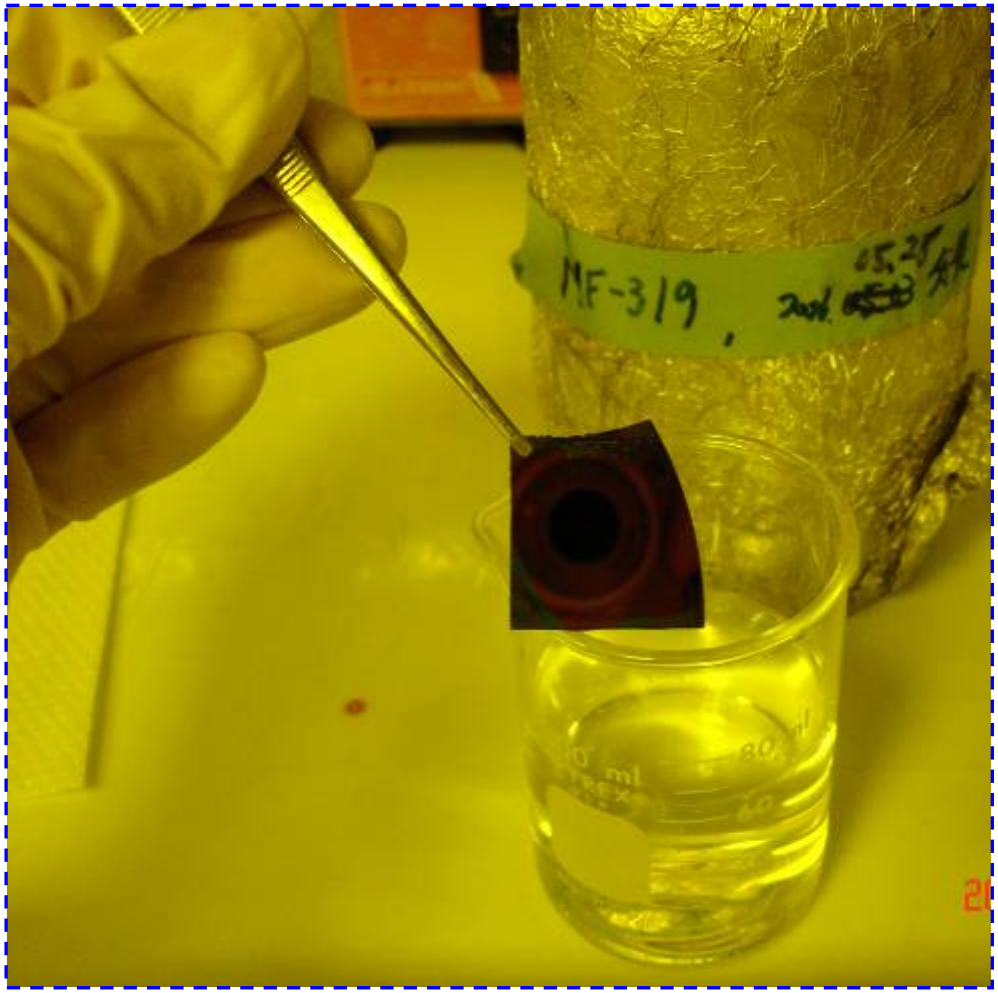

- Photo resist：Shipley **1813**
- Spin： 2000 rpm 5 s
  4500 rpm 15 s
- Soft Bake：110℃ 60 s
- Exposure：7 s
- **Developed：MF319 for 15 s**

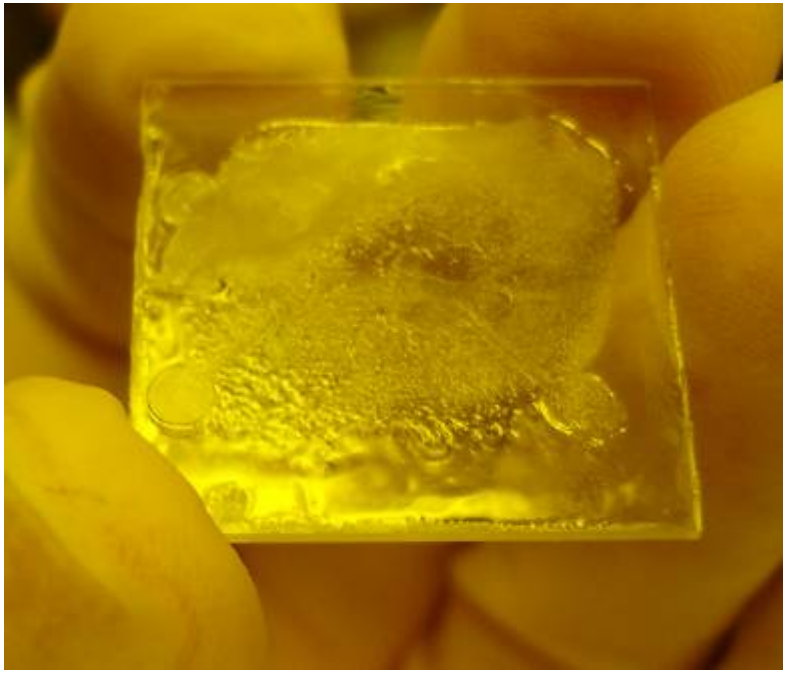

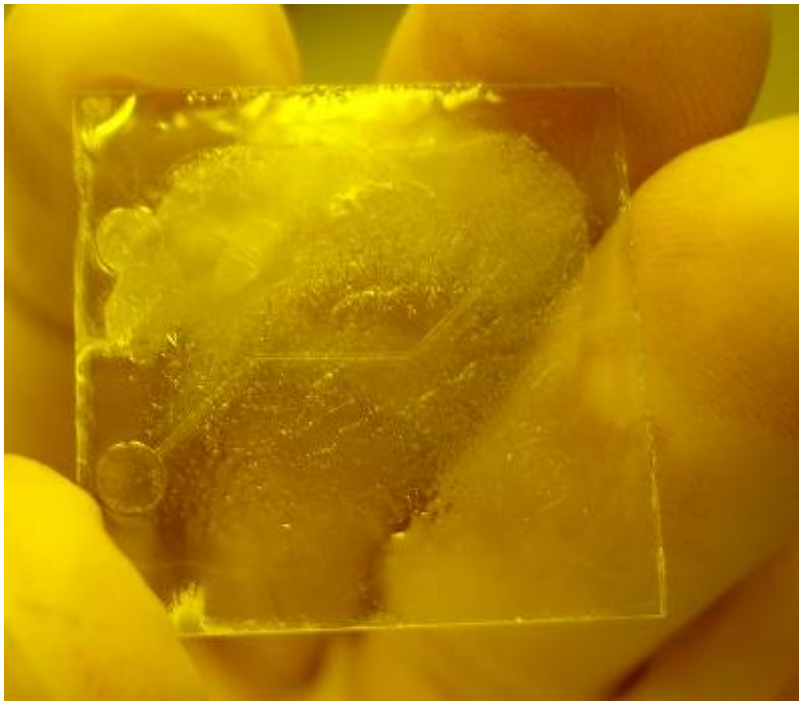

RCAS E-Beam Evaporator

一儀器名稱

中文名稱：電子束蒸鍍系統

英文名稱：E-Beam

二. 儀器廠牌、型號及儀器購置年限

廠牌：聚昌科技 AST

儀器購置年限：民國92年7月

三. 重要規格

蒸鍍金屬: Ni、Ti、 Au、Al、 Pt 、Cr

回儀器配置圖

TI 50 nm

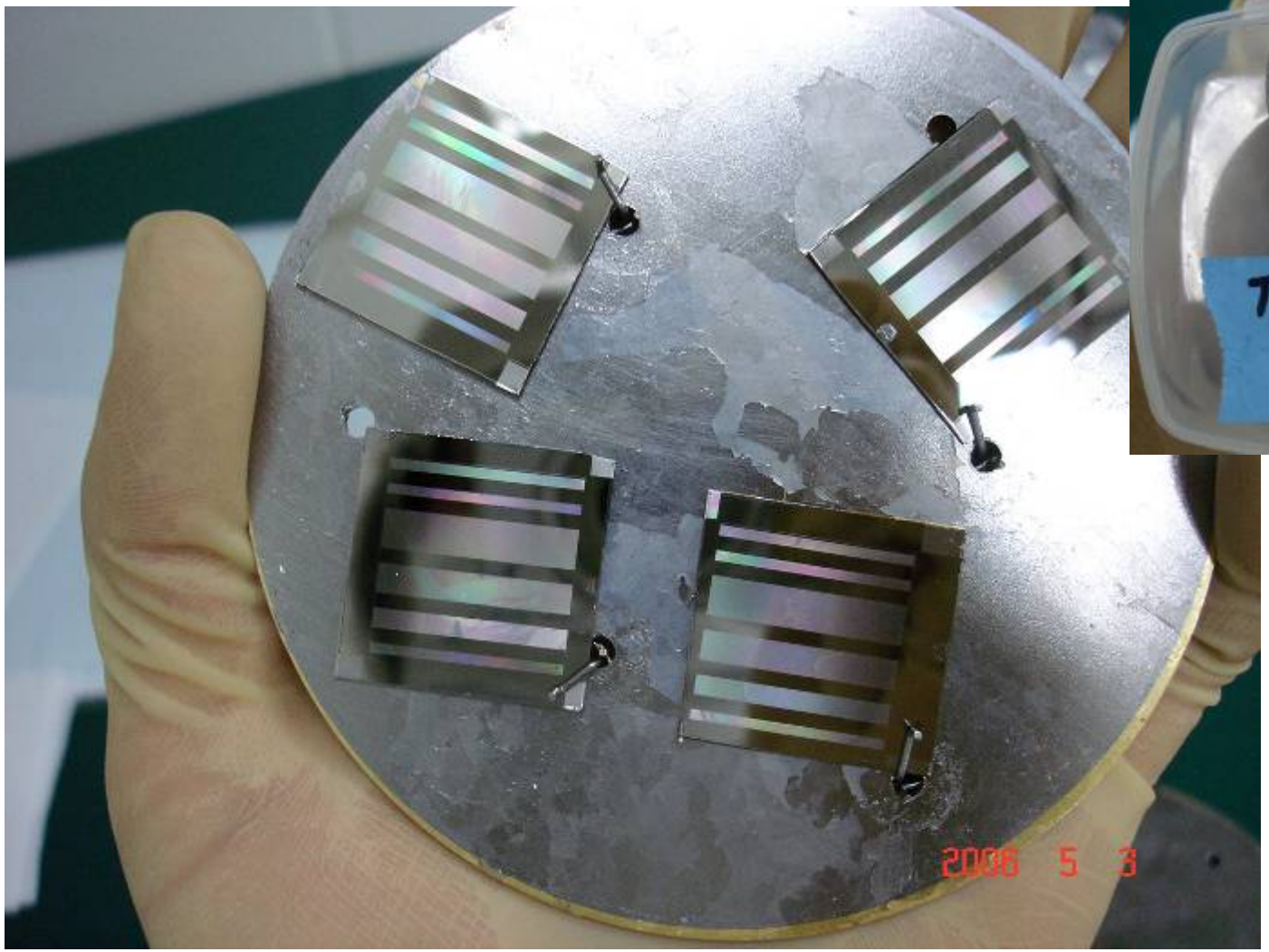

SEM image of Ti 50 nm on Si wafer

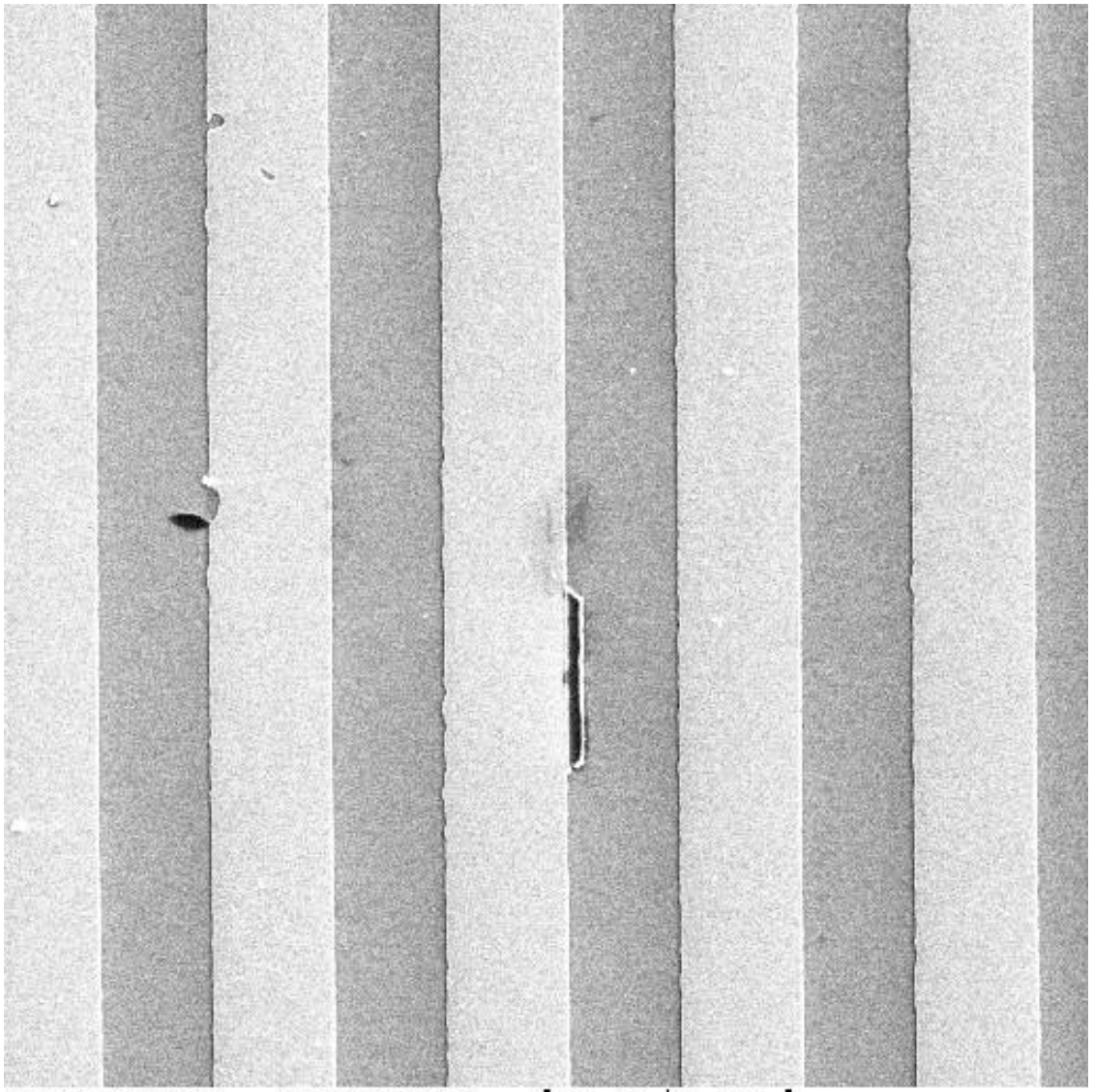

Lift OFF PROCESS BY ACETONE

Ti 50 nm

LIFT OFF

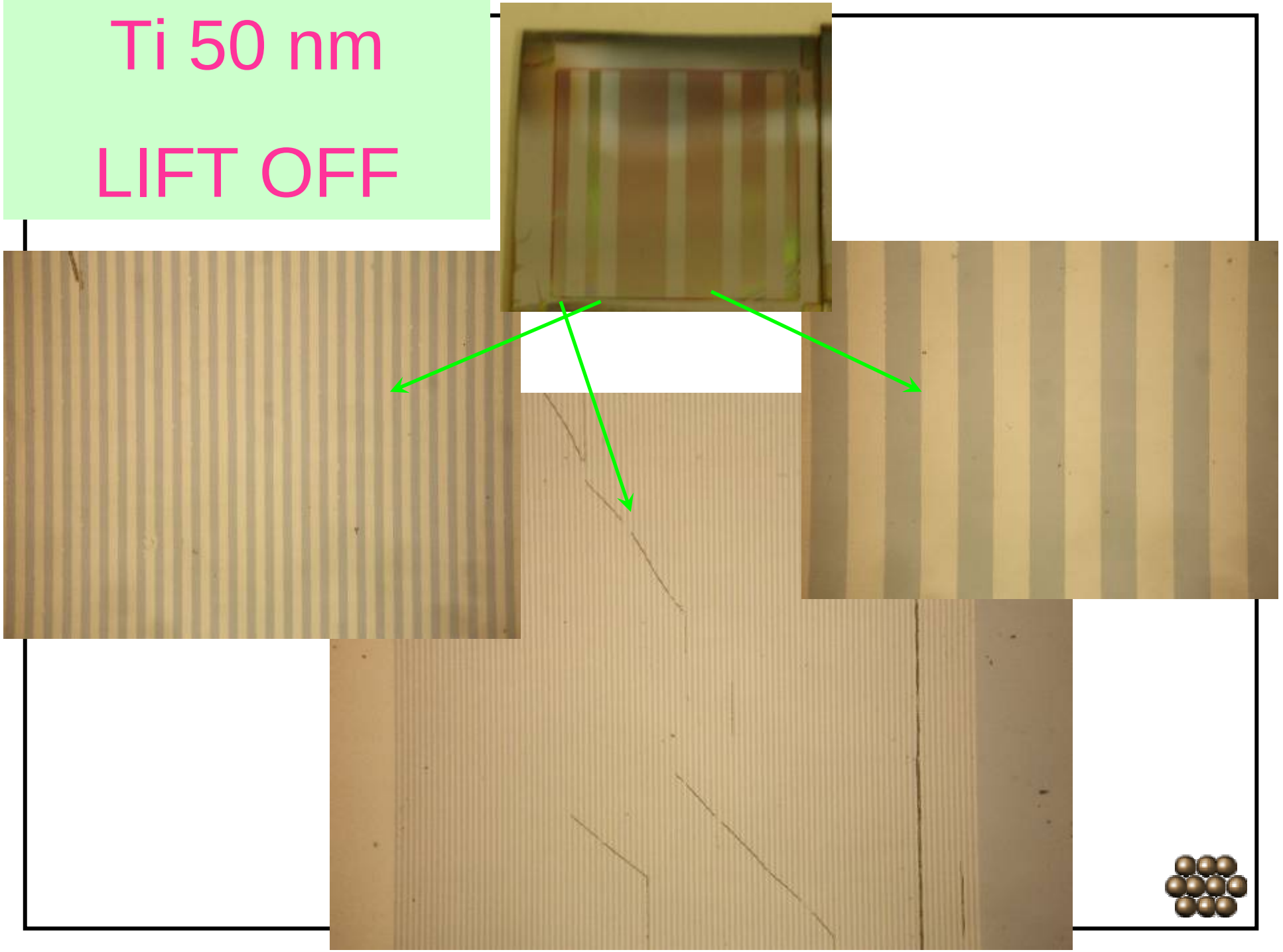

Ti 50 nm on Si 20 um

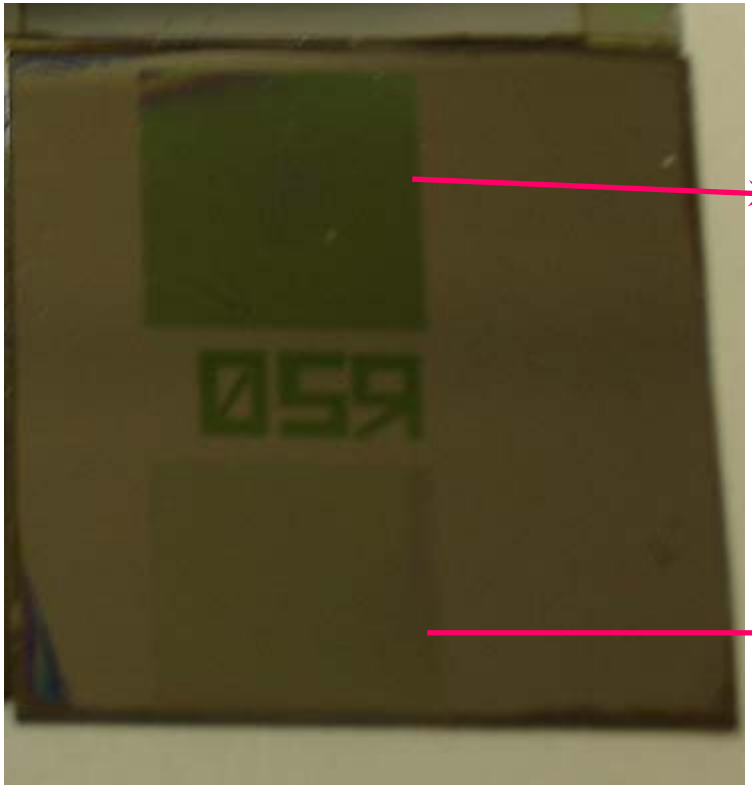

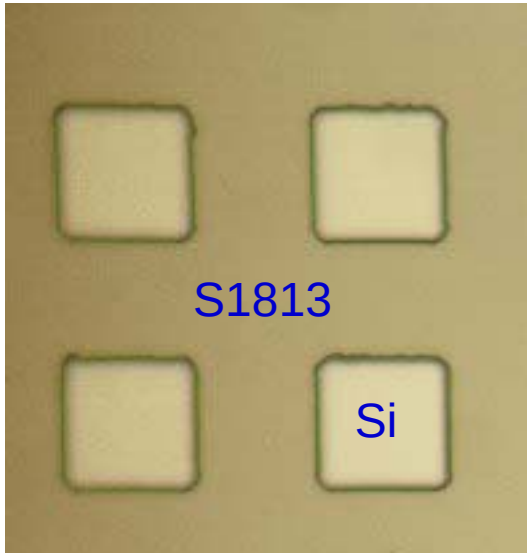

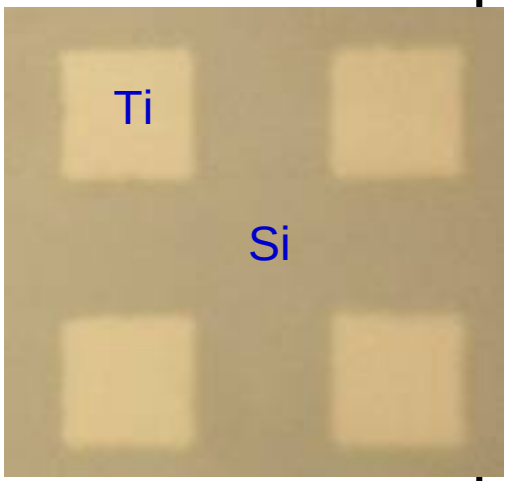

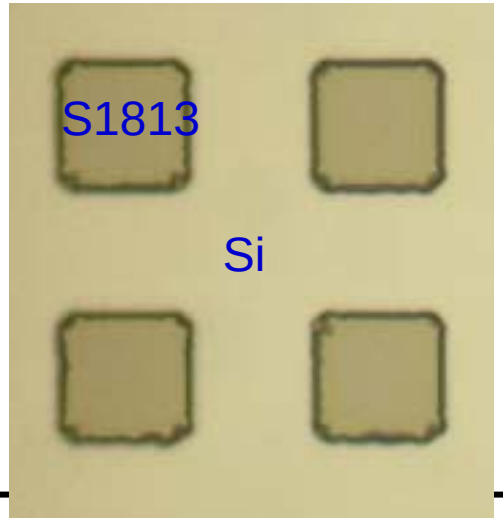

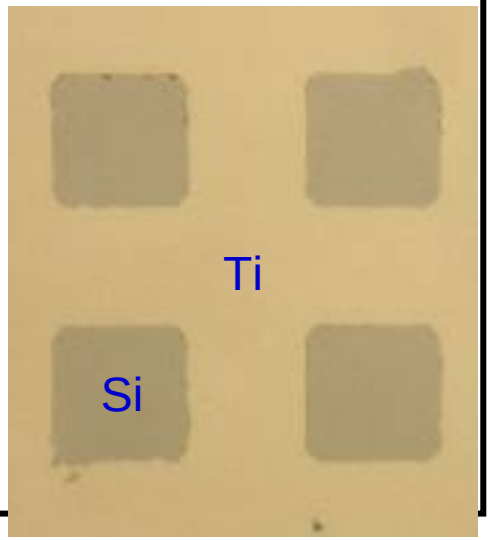

Ti 50 nm on Si 5 um

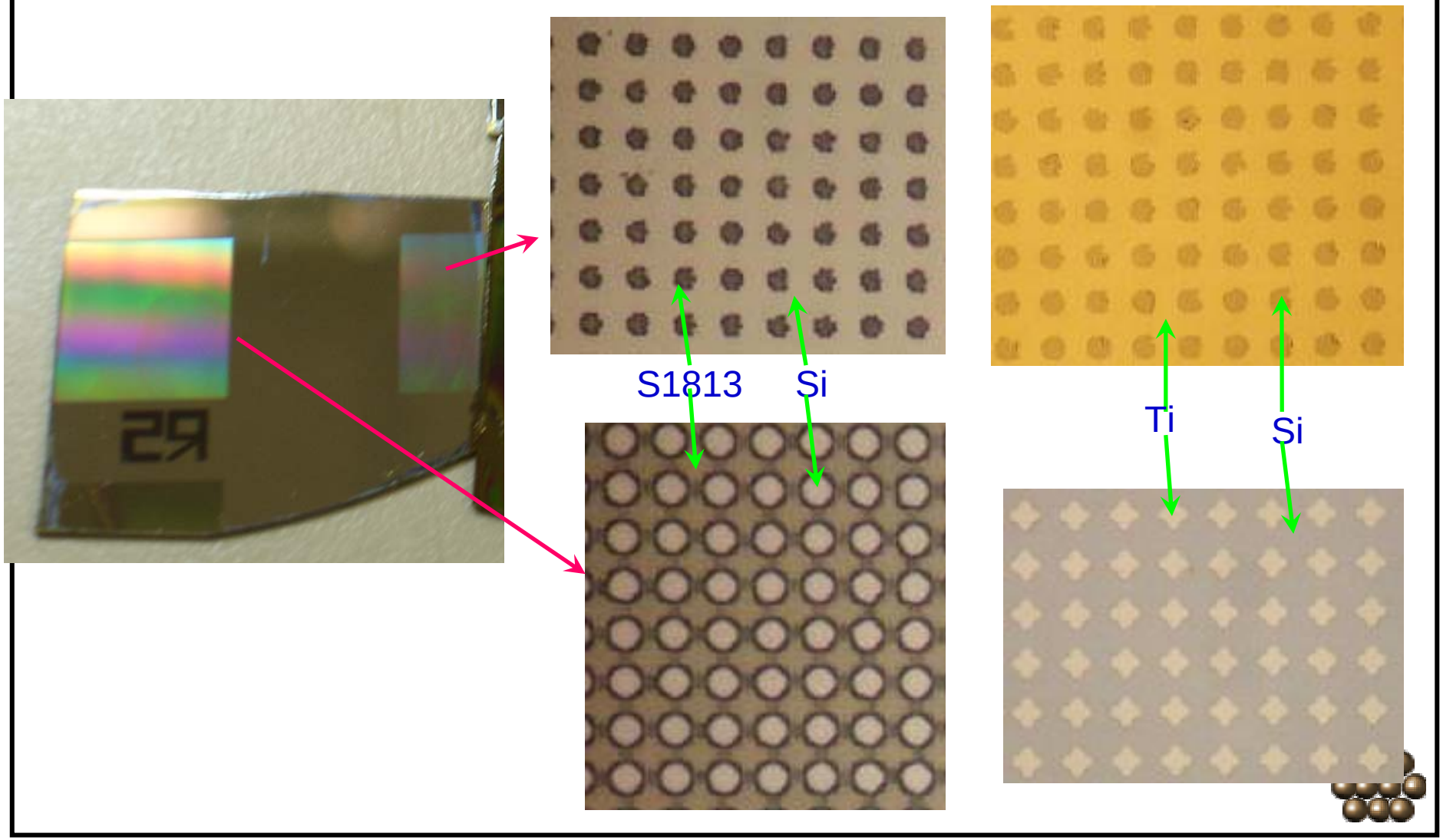

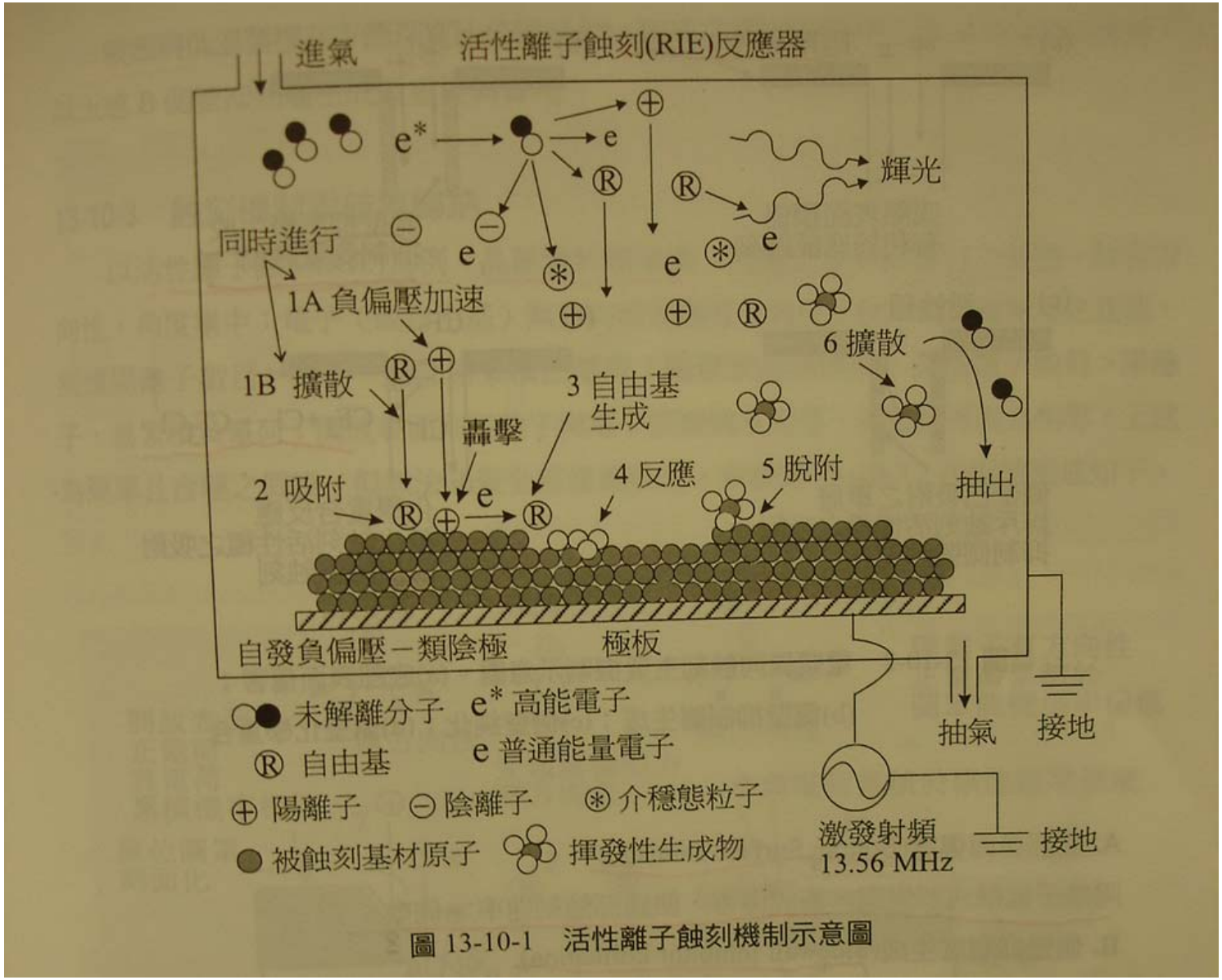

圖 13-10-1　活性離子蝕刻機制示意圖

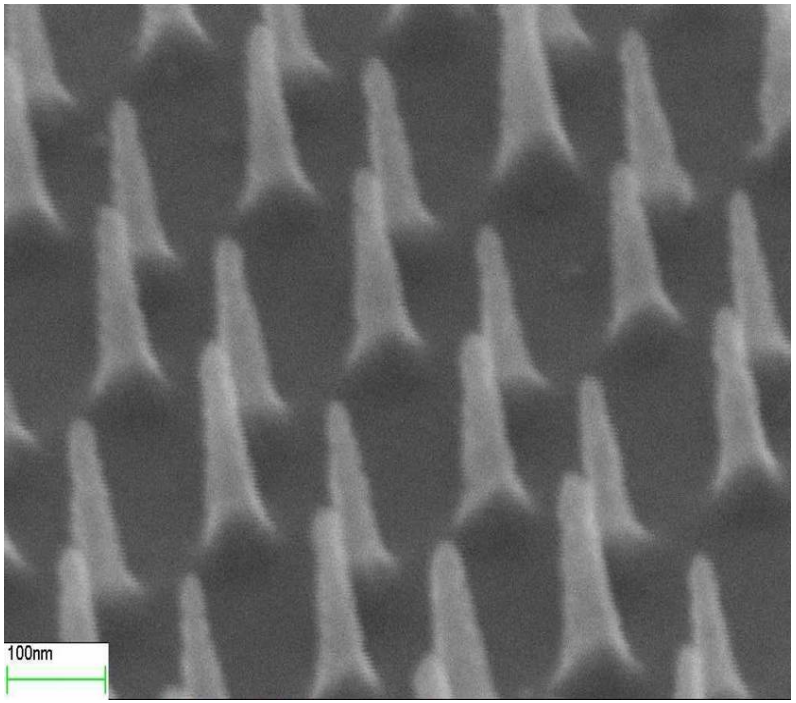
100nm

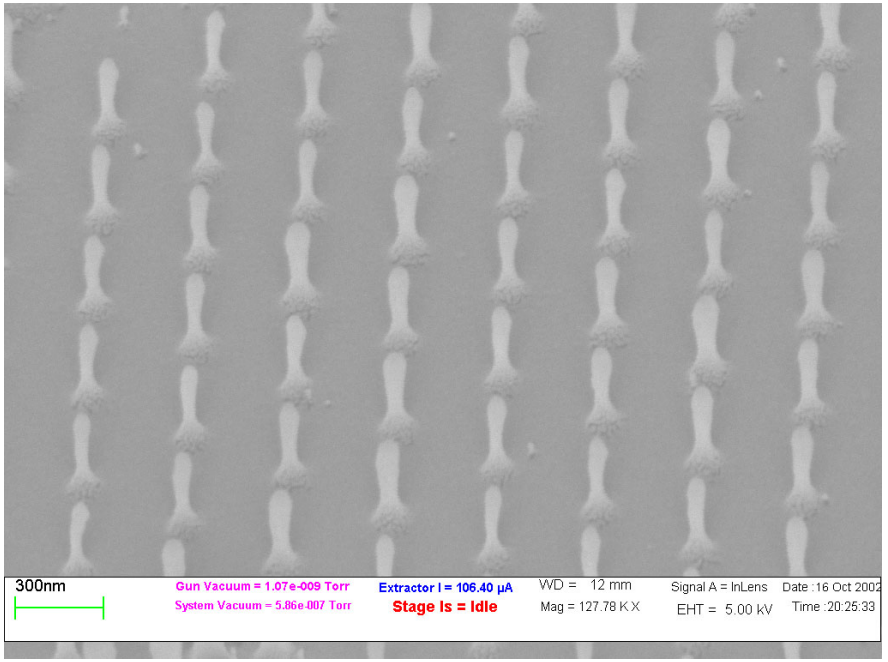
300nm
Gun Vacuum = 1.07e-009 Torr
System Vacuum = 5.86e-007 Torr
Extractor I = 106.40 µA
Stage Is = Idle
WD = 12 mm
Mag = 127.78 K X
Signal A = InLens
EHT = 5.00 kV
Date :16 Oct 2002
Time :20:25:33

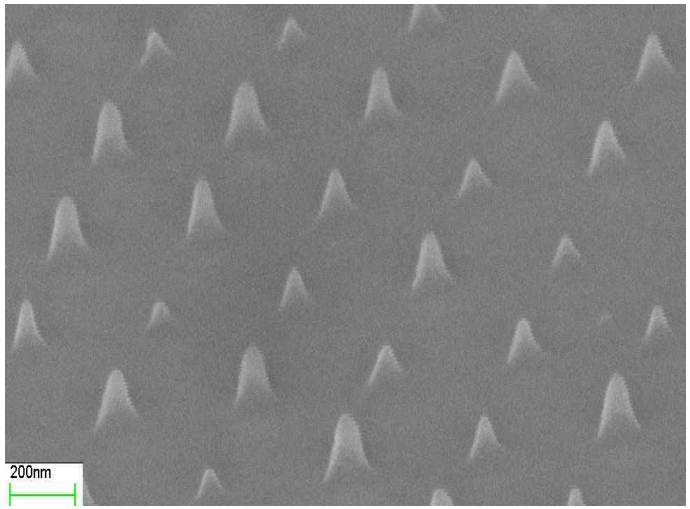
200nm

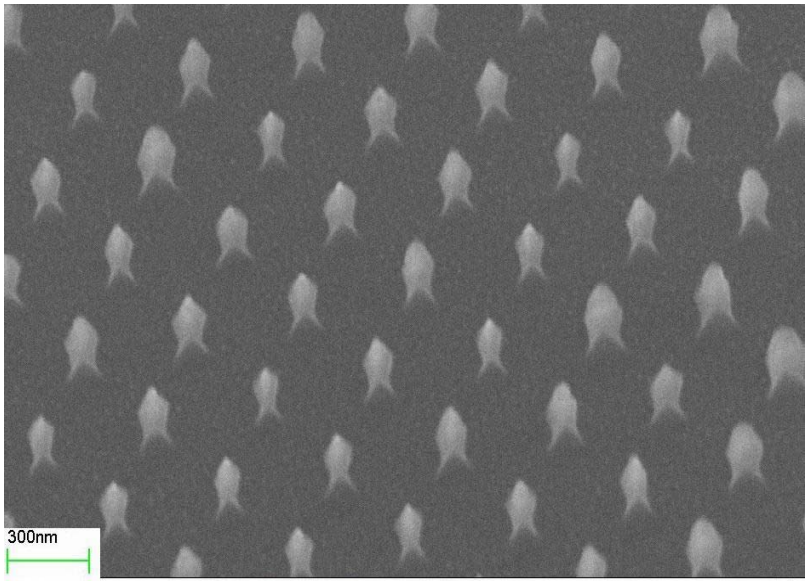
300nm

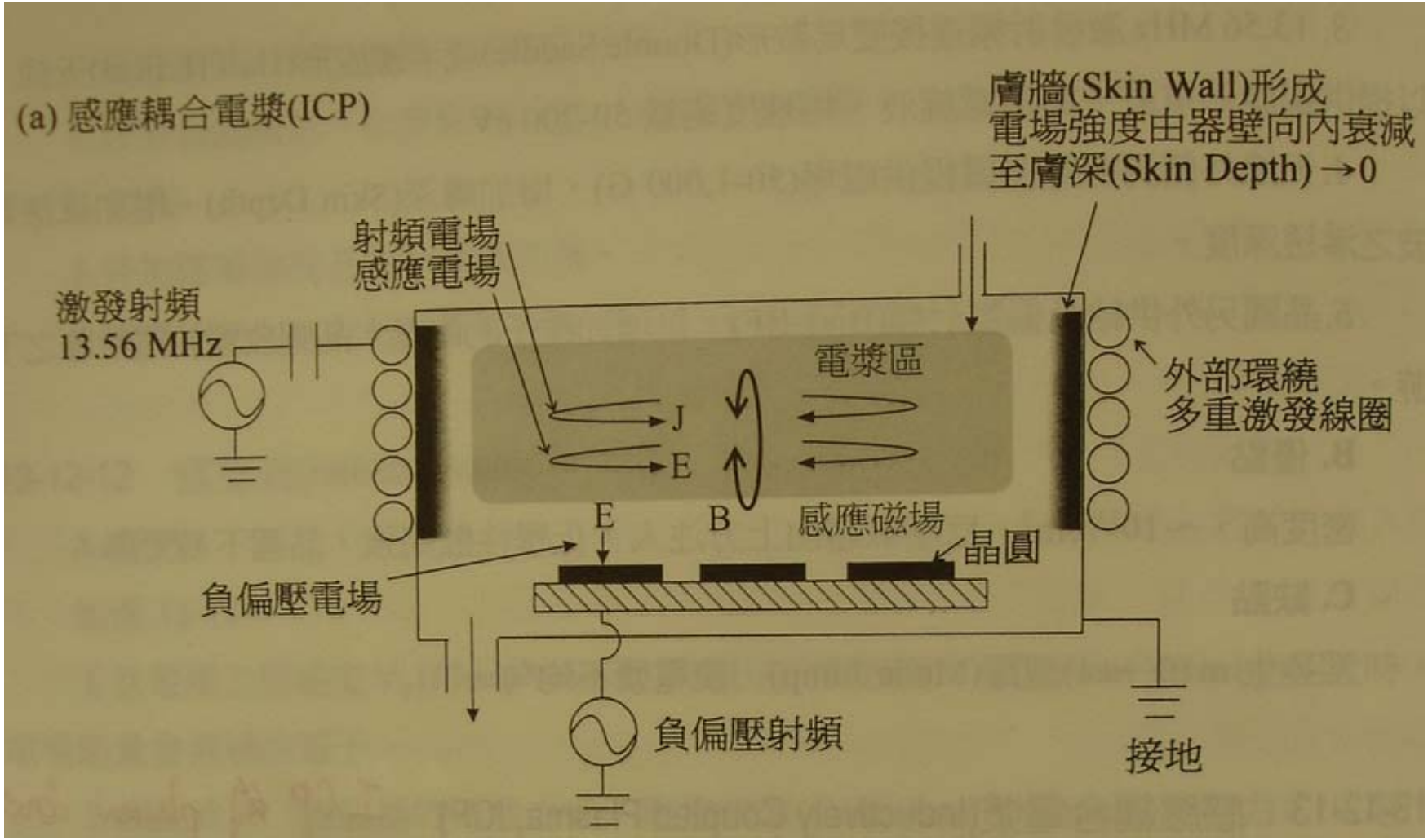
(a) 感應耦合電漿(ICP)
膚牆(Skin Wall)形成
電場強度由器壁向內衰減
至膚深(Skin Depth) →0
射頻電場
感應電場
激發射頻
13.56 MHz
電漿區
外部環繞
多重激發線圈
J
E
E
B
感應磁場
晶圓
負偏壓電場
負偏壓射頻
接地

ICP- “BOSCH” Recipe
Etching & Sidewall Passivation Cycle

(a) Etch Step

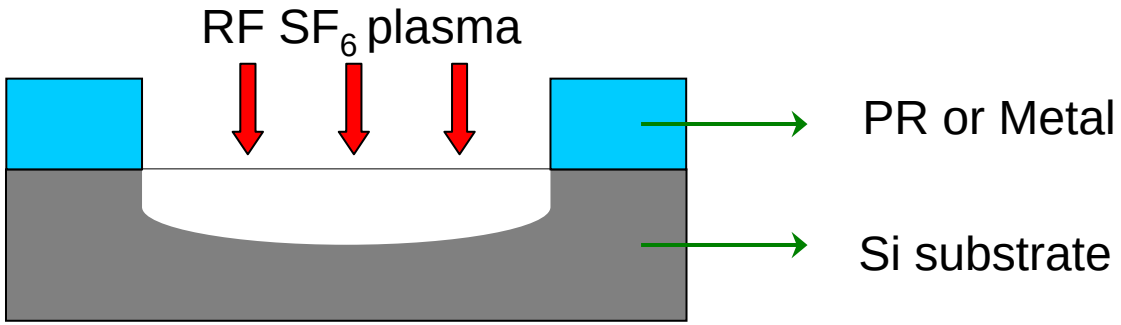

(b) Passivate Step

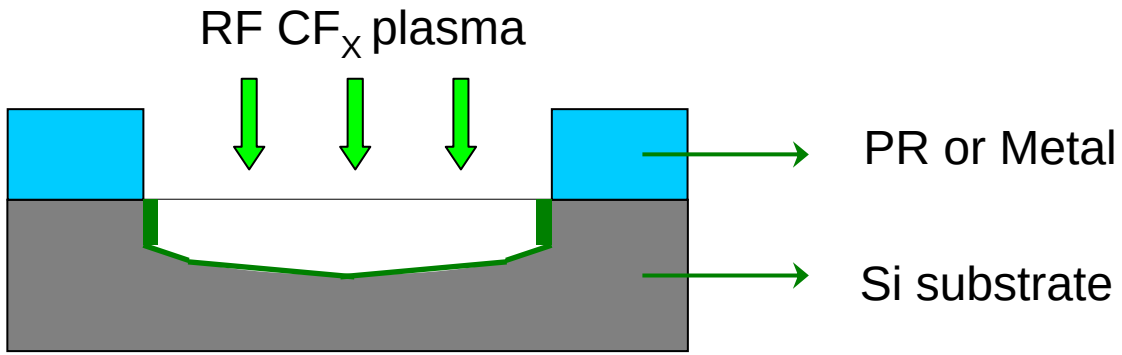

(a’) Etch Step

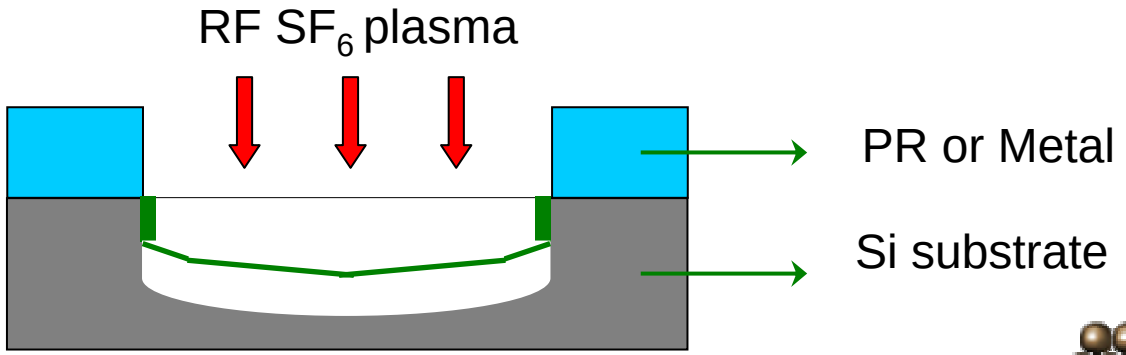

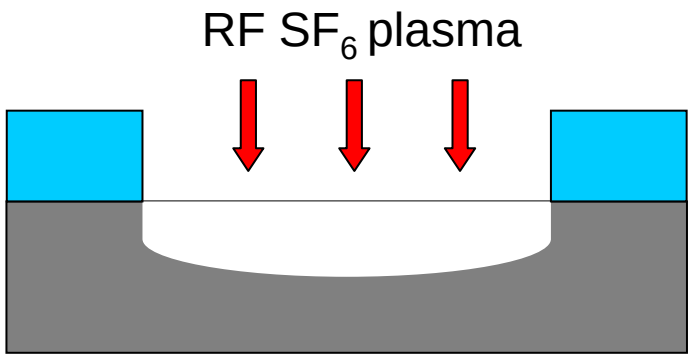

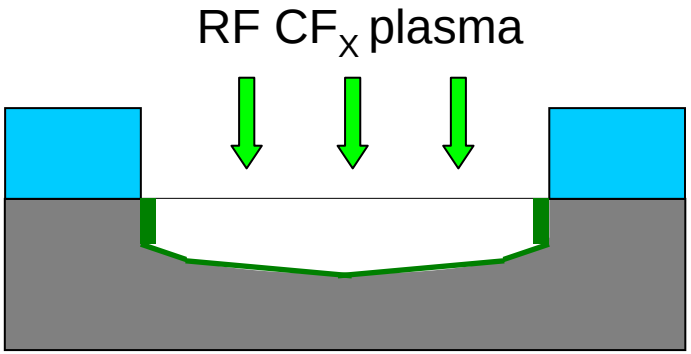

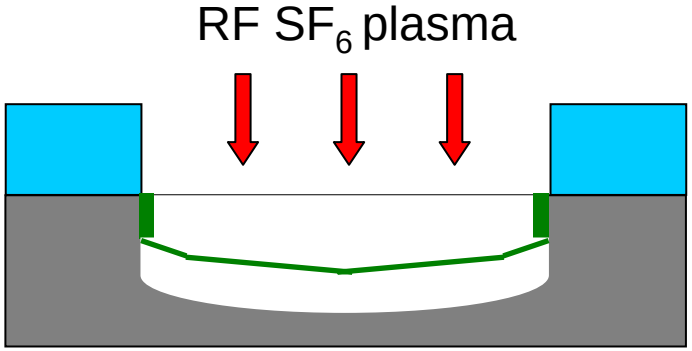

The gases in RCAS

C_4F_8, CF_4, CHF_3, Ar, O_2

SAMCO ICP (RECIPE)

Si etching CF_4 / O_2= 30 / 10

SiO_2 (on Si) CHF_3 / Ar = 15 / 30

The gases in NEMSRC

SF_6, C_4F_8, CF_4, O_2

RECIPE

	TIME	
Etch:	11.5 s	SF_6(130sccm) O_2(13sccm)
Passivate:	7s	C_4F_8(85sccm)

NEMSRC ICP

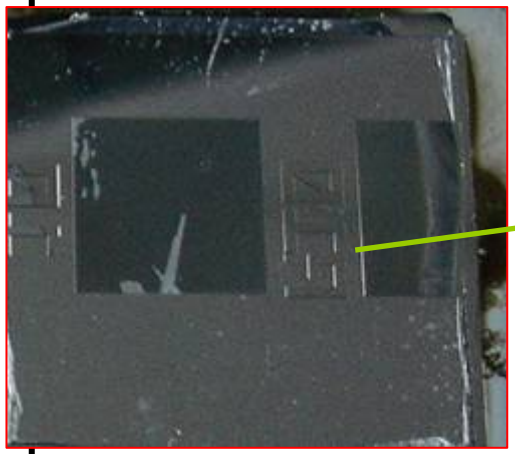

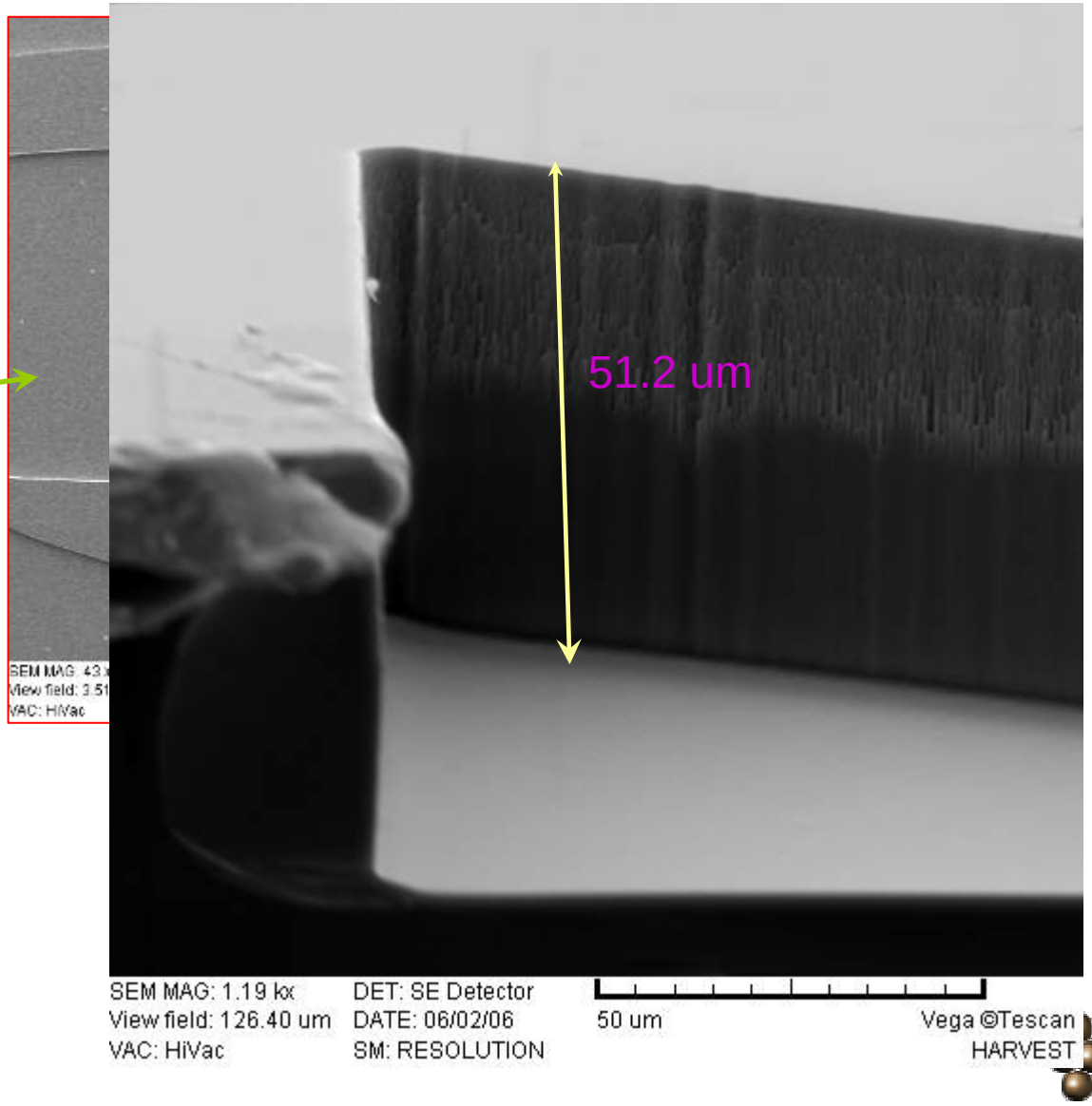
51.2 um
SEM MAG: 1.19 kx
View field: 126.40 um
VAC: HiVac
DET: SE Detector
DATE: 06/02/06
SM: RESOLUTION
50 um
Vega ©Tescan
HARVEST

Si ---S1813---ICP

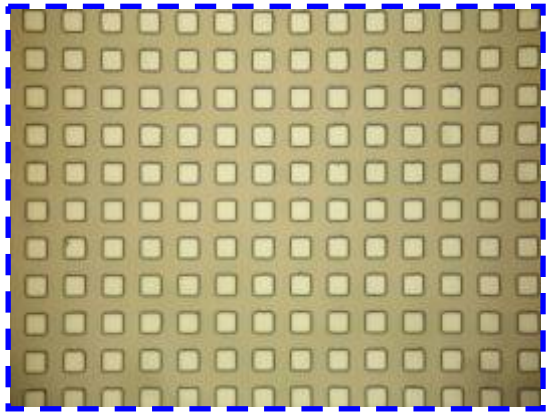

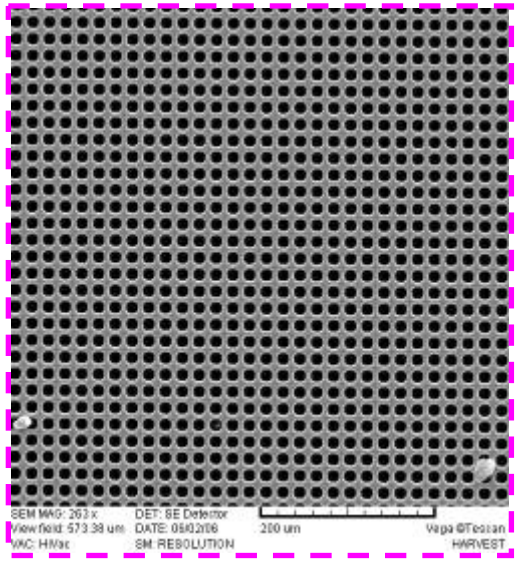

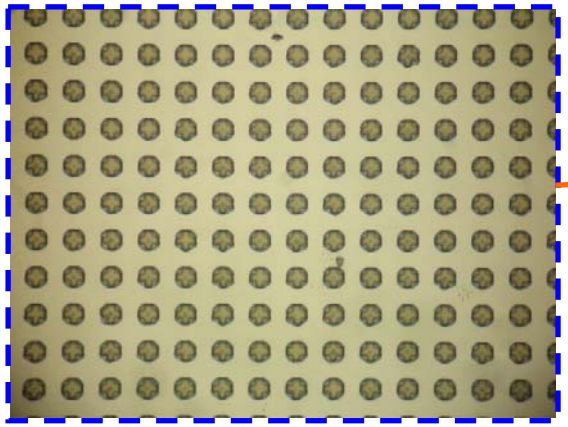

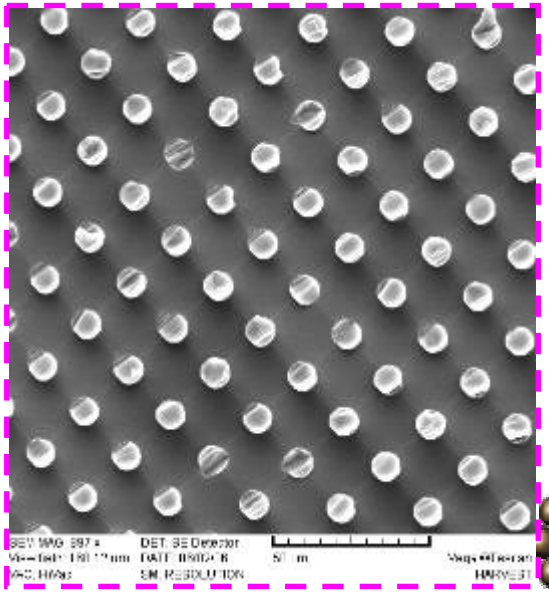

NEMSRC ICP

Si 10 um Line

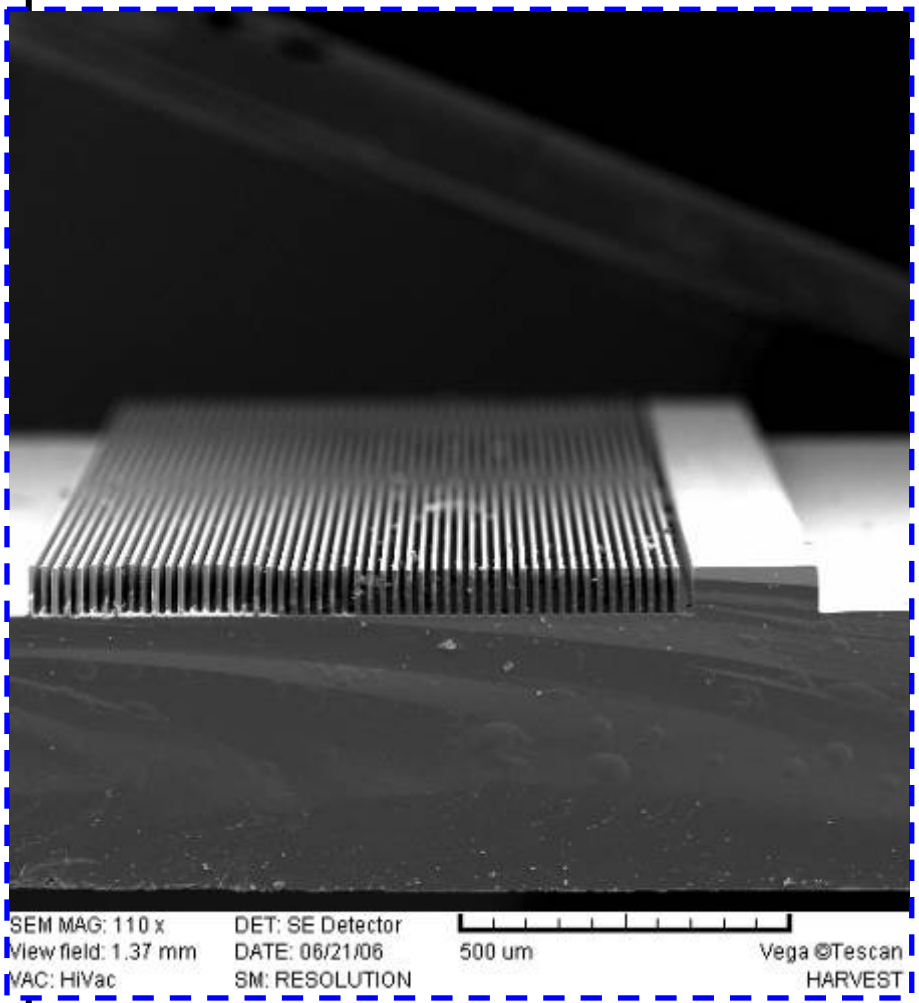

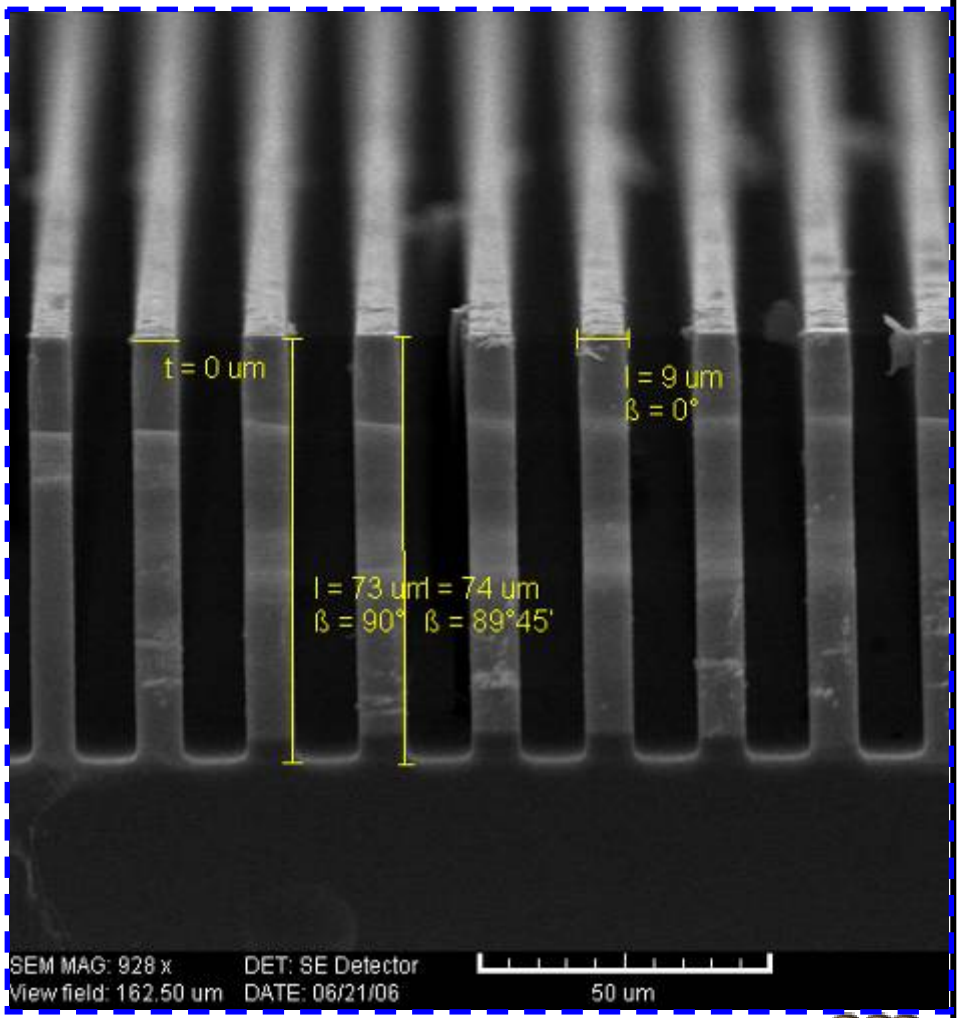

NEMSRC ICP ：S1813 on Si --20 μm array

The gases in NEMSRC

SF_6, C_4F_8, CF_4, O_2

RECIPE

	TIME		
Etch:	11.5 s	SF_6(130sccm)	O_2(13sccm)
Passivate:	7s	C_4F_8(85sccm)	

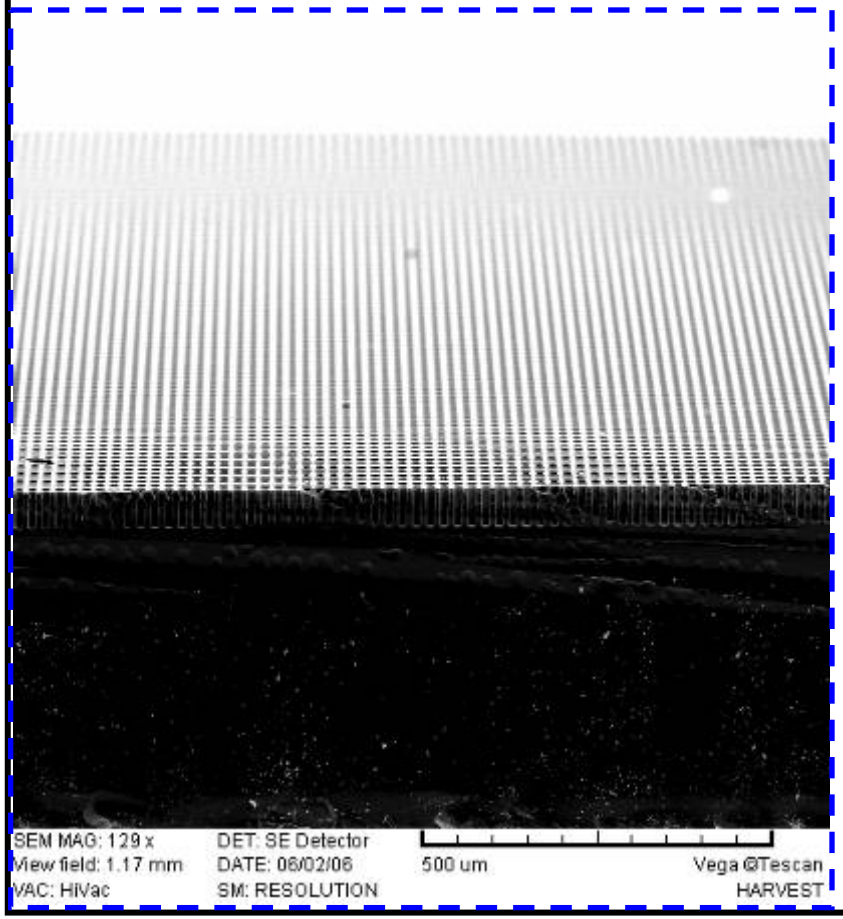

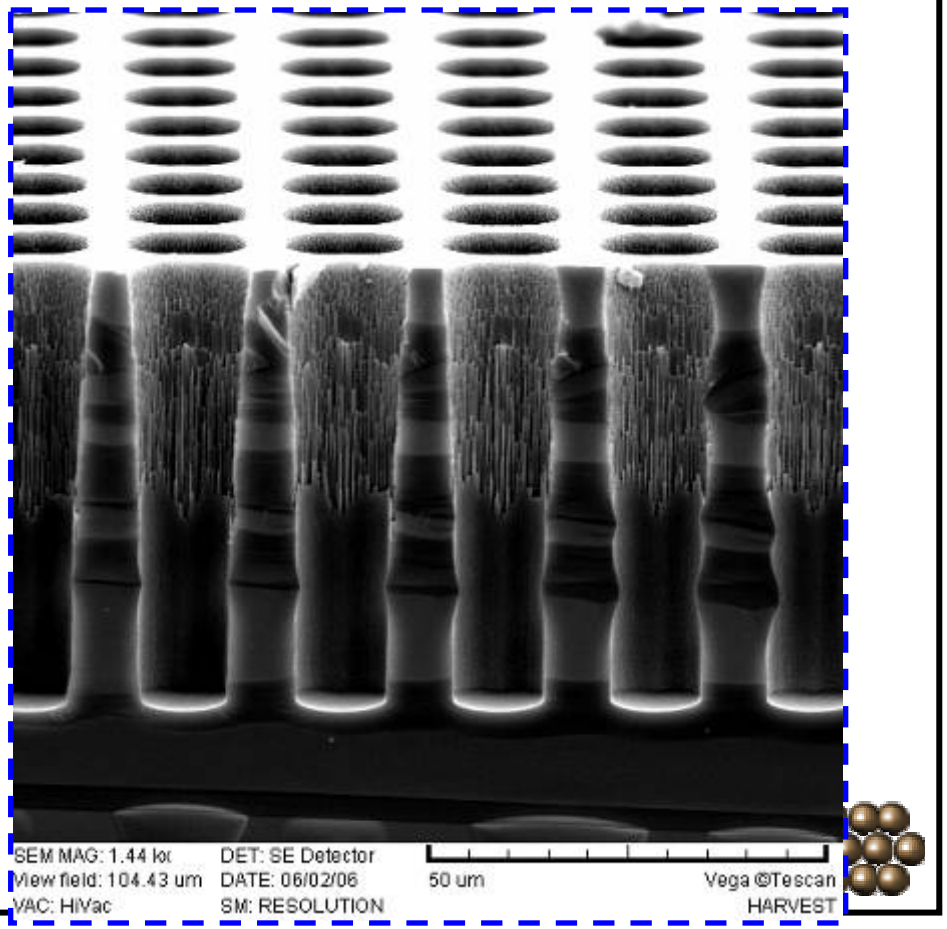

NEMSRC ICP ：S1813 on Si

10 um pillar

The gases in NEMSRC

SF_6, C_4F_8, CF_4, O_2

RECIPE

TIME

Etch: 11.5 s SF_6(130sccm) O_2(13sccm)

Passivate: 7s C_4F_8(85sccm)

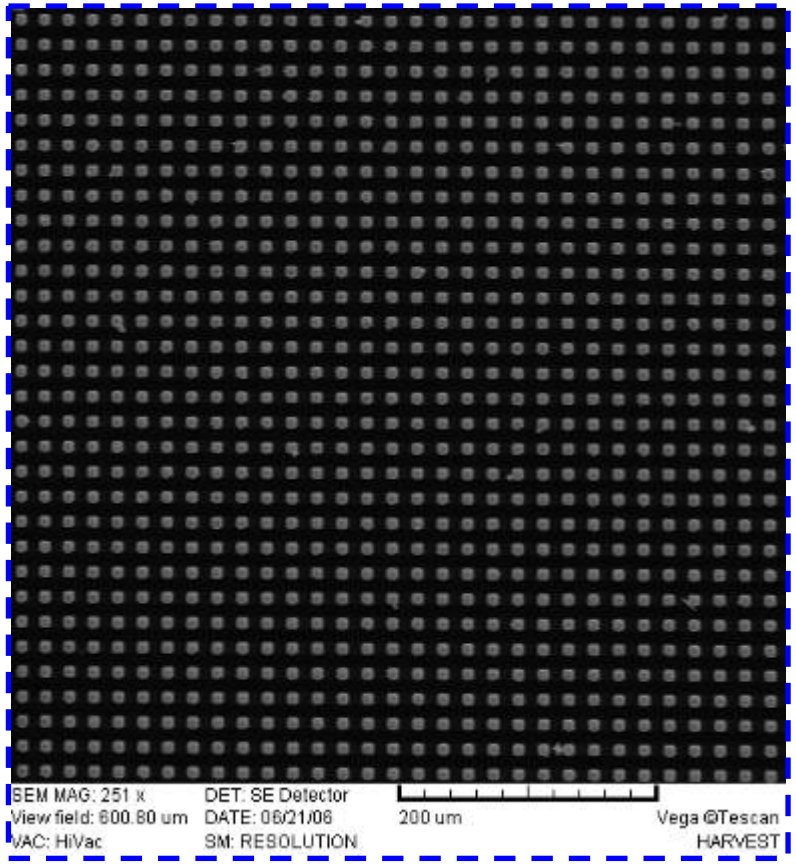

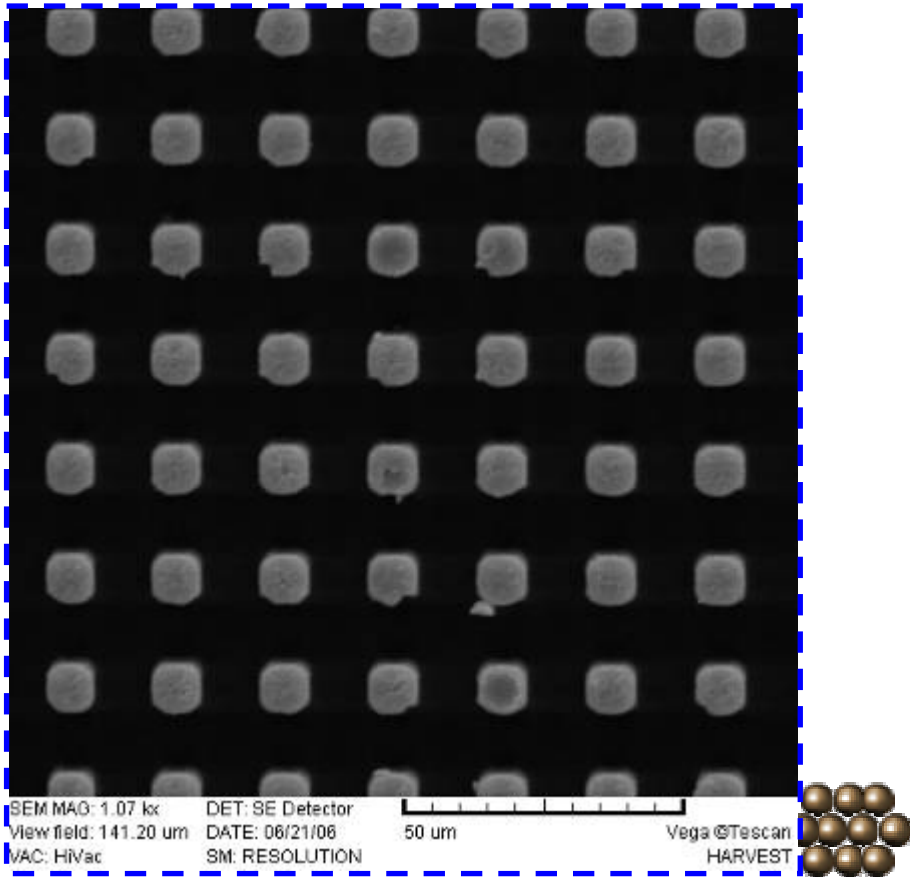

NEMSRC ICP

Si 10 um pillar

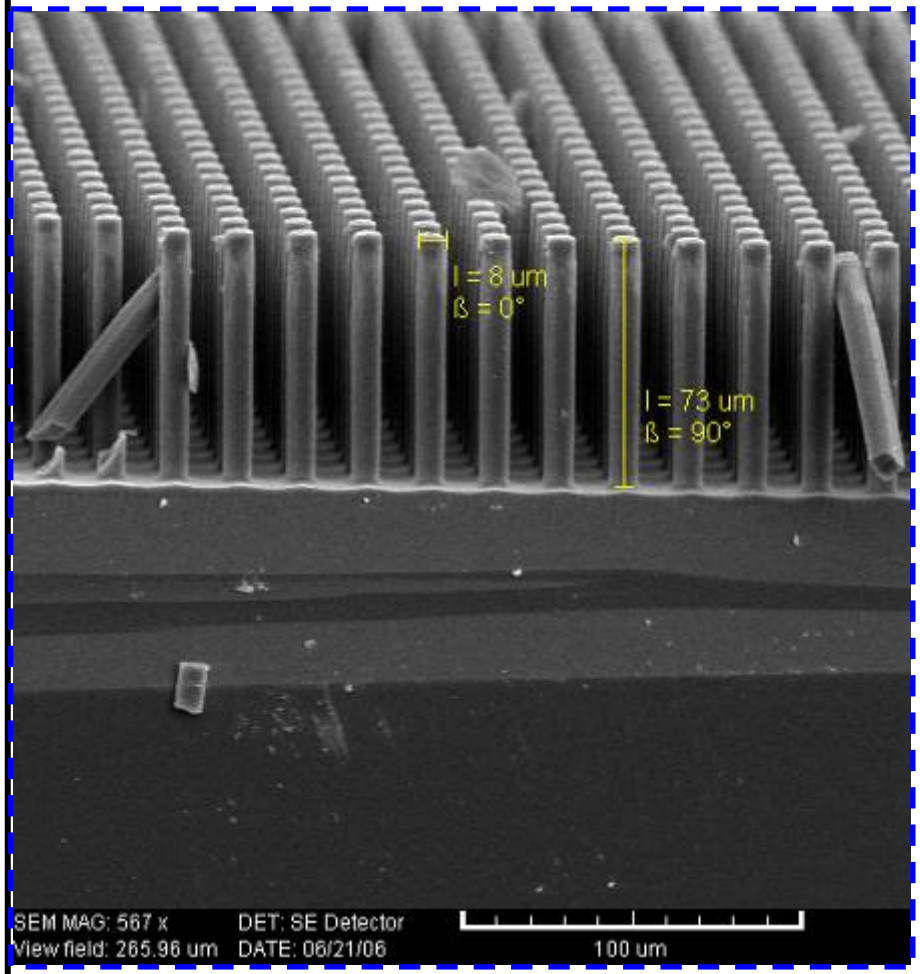

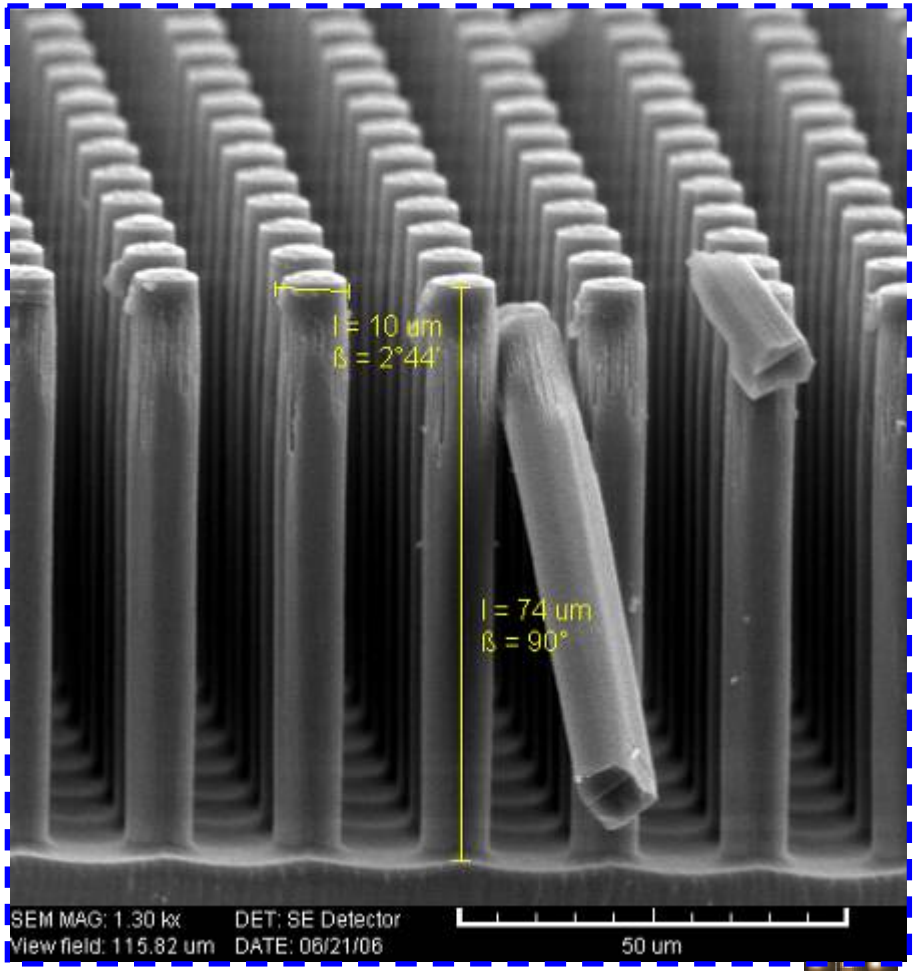

NEMSRC ICP ：S1813 on Si

5 um pillar

The gases in NEMSRC

SF_6, C_4F_8, CF_4, O_2

RECIPE

TIME

Etch: 11.5 s SF_6(130sccm) O_2(13sccm)

Passivate: 7s C_4F_8(85sccm)

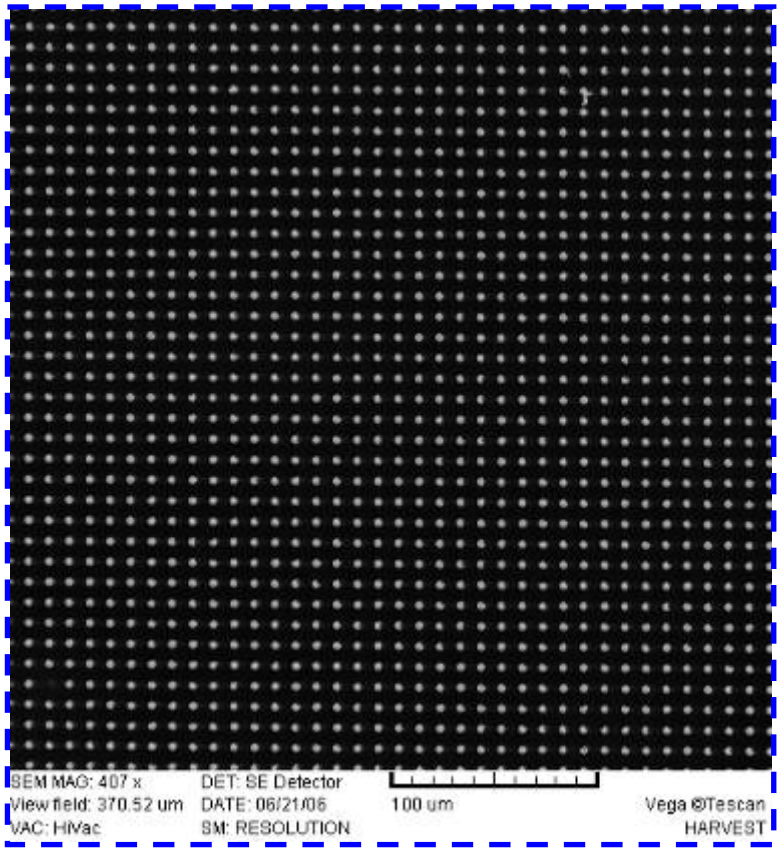

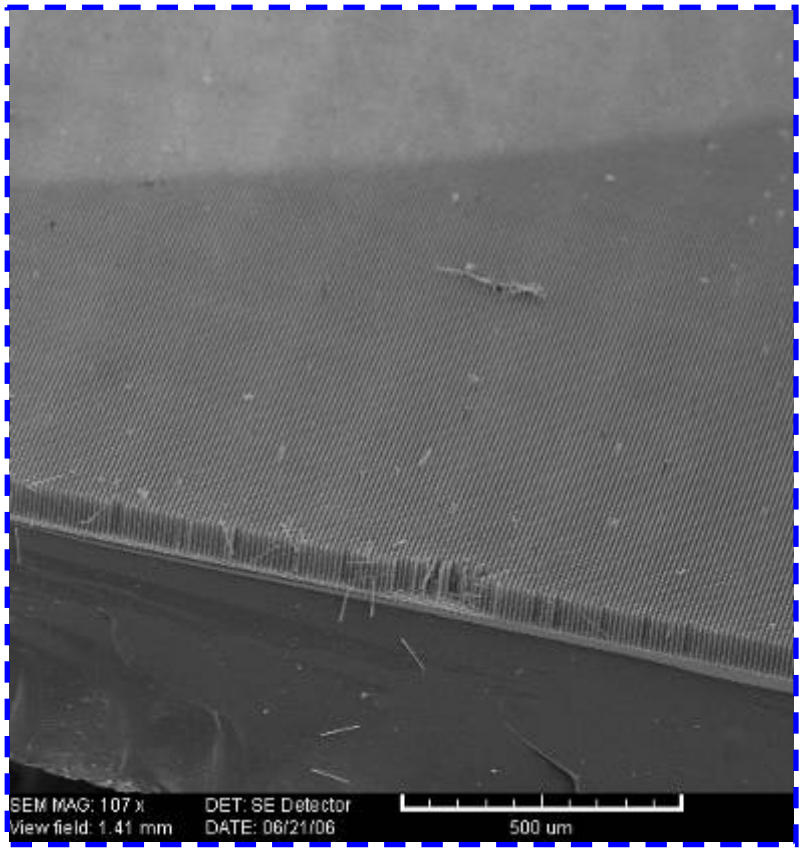

PDMS

Table 1. Physical and Chemical Properties of PDMS

property	characteristic	consequence
optical	transparent; UV cutoff, 240 nm	optical detection from 240 to 1100 nm
electrical	insulating; breakdown voltage, 2×10^7 V/m [71]	allows embedded circuits; intentional breakdown to open connections[43]
mechanical	elastomeric; tunable Young's modulus, typical value of ~750 kPa [24]	conforms to surfaces; allows actuation by reversible deformation;[24] facilitates release from molds
thermal	insulating; thermal conductivity, 0.2 W/(m·K); coefficient of thermal expansion, 310 μm/(m·°C)[71]	can be used to insulate heated solutions;[64] does not allow dissipation of resistive heating from electrophoretic separation
interfacial	low surface free energy ~ 20 erg/ cm^2 [20]	replicas release easily from molds; can be reversibly sealed to materials
permeability	impermeable to liquid water; permeable to gases and nonpolar organic solvents	contains aqueous solutions in channels; allows gas transport through the bulk material; incompatible with many organic solvents
reactivity	inert; can be oxidized by exposure to a plasma; $Bu_4N^+F^-$((TBA)F)	unreactive toward most reagents; surface can be etched; can be modified to be hydrophilic and also reactive toward silanes;[20] etching with (TBA)F can alter topography of surfaces[59]
toxicity	nontoxic.	can be implanted in vivo; supports mammalian cell growth[57,59]

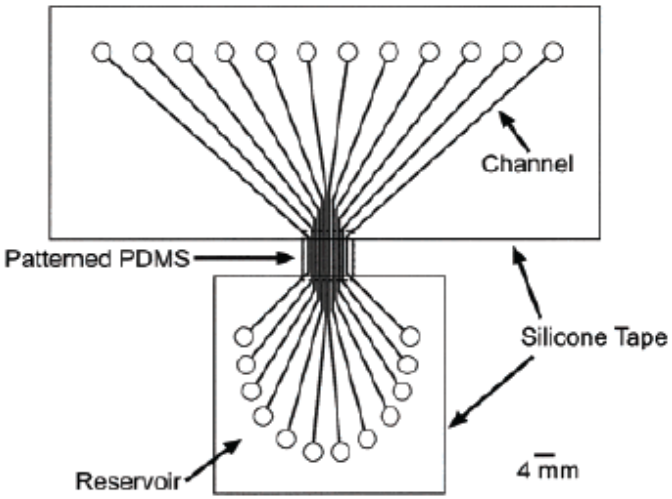

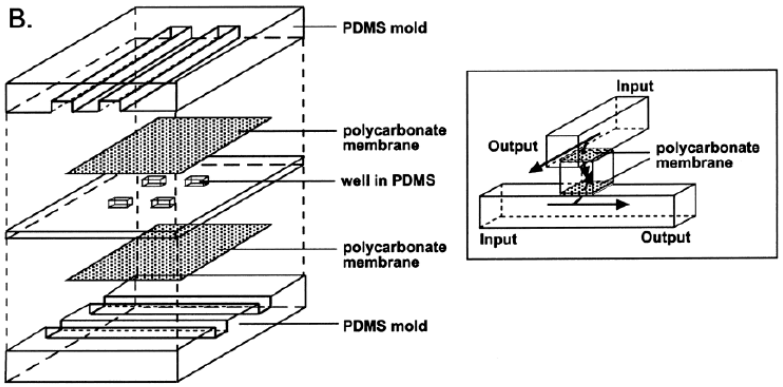

Solvent Compatibility of Poly(dimethylsiloxane)-Based Microfluidic Devices

Anal. Chem. **2003,** *75,* 6544−6554

solvent	δ^a	S^b	μ (D)
perfluorotributylamine	5.6	1.00	0.0
perfluorodecalin	6.6	1.00	0.0
pentane	7.1	1.44	0.0
poly(dimethylsiloxane)	7.3	∞	0.6−0.9
diisopropylamine	7.3	2.13	1.2
hexanes	7.3	1.35	0.0
n-heptane	7.4	1.34	0.0
triethylamine	7.5	1.58	0.7
ether	7.5	1.38	1.1
cyclohexane	8.2	1.33	0.0
trichloroethylene	9.2	1.34	0.9
dimethoxyethane (DME)	8.8	1.32	1.6
xylenes	8.9	1.41	0.3
toluene	8.9	1.31	0.4
ethyl acetate	9.0	1.18	1.8
benzene	9.2	1.28	0.0
chloroform	9.2	1.39	1.0
2-butanone	9.3	1.21	2.8
tetrahydrofuran (THF)	9.3	1.38	1.7
dimethyl carbonate	9.5	1.03	0.9
chlorobenzene	9.5	1.22	1.7
methylene chloride	9.9	1.22	1.6
acetone	9.9	1.06	2.9
dioxane	10.0	1.16	0.5
pyridine	10.6	1.06	2.2
N-methylpyrrolidone (NMP)	11.1	1.03	3.8
tert-butyl alcohol	10.6	1.21	1.6
acetonitrile	11.9	1.01	4.0
1-propanol	11.9	1.09	1.6
phenol	12.0	1.01	1.2
dimethylformamide (DMF)	12.1	1.02	3.8
nitromethane	12.6	1.00	3.5
ethyl alcohol	12.7	1.04	1.7
dimethyl sulfoxide (DMSO)	13.0	1.00	4.0
propylene carbonate	13.3	1.01	4.8
methanol	14.5	1.02	1.7
ethylene glycol	14.6	1.00	2.3
glycerol	21.1	1.00	2.6
water	23.4	1.00	1.9

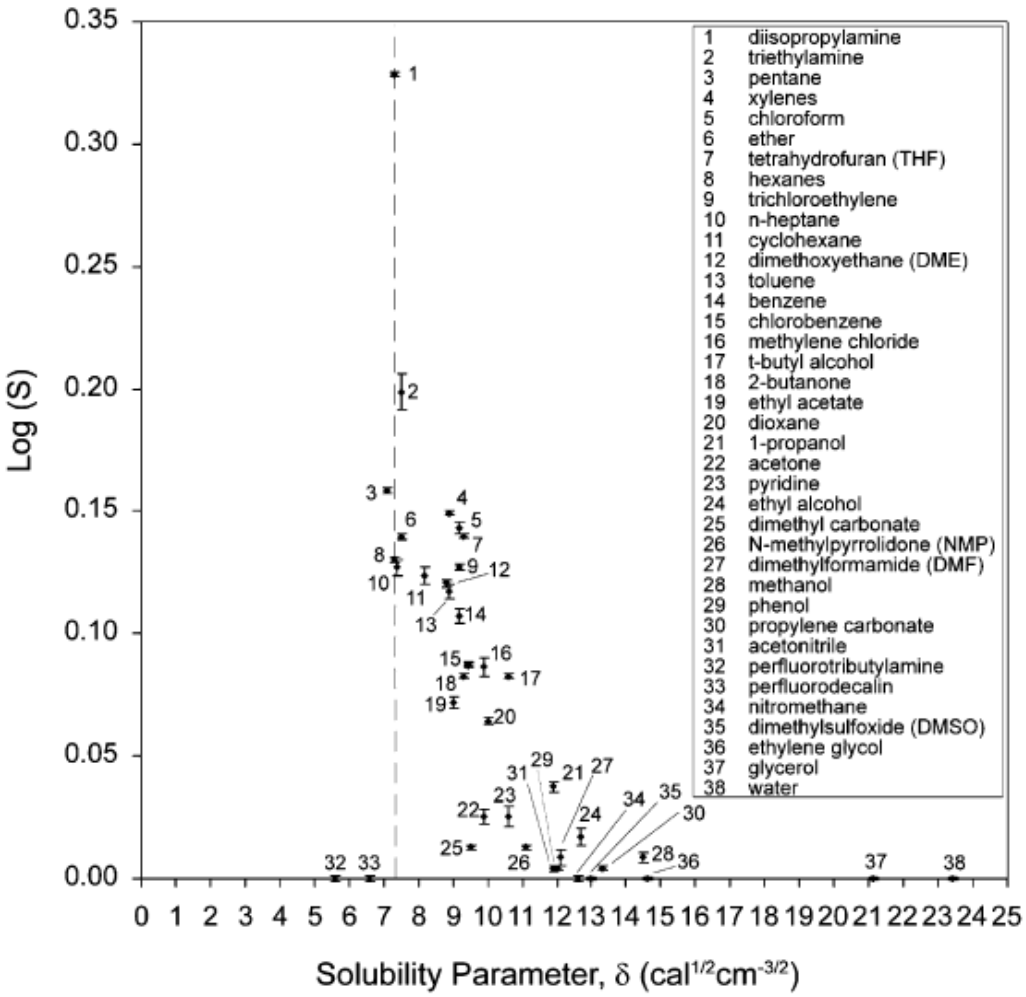

Microfluidics by Soft Lithography

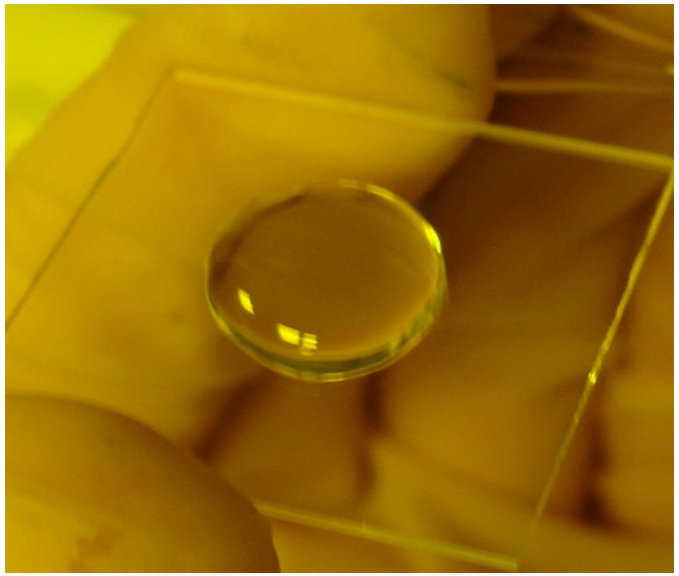

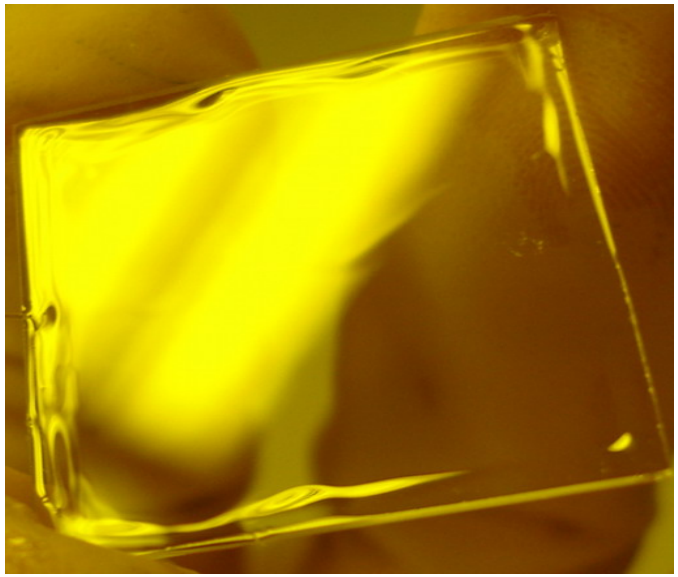

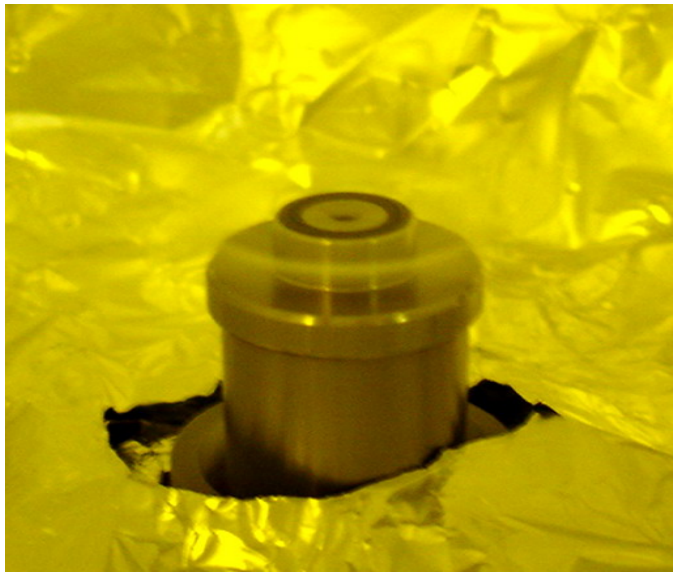

Microfluidics by Soft Lithography

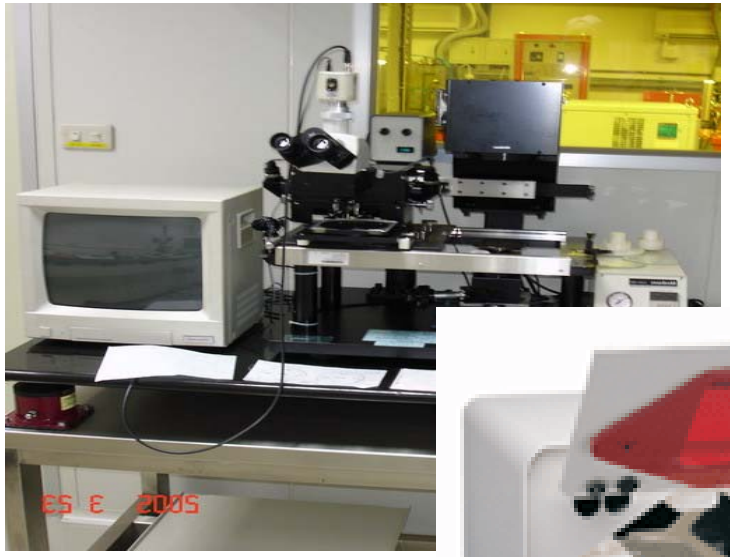

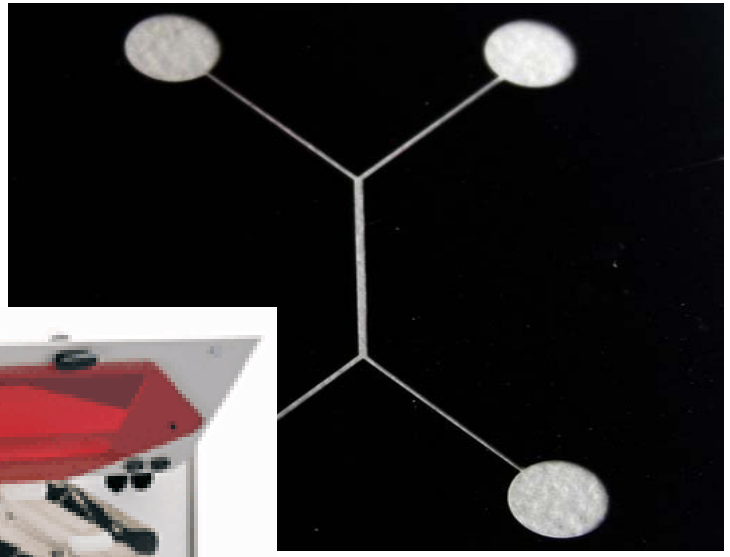

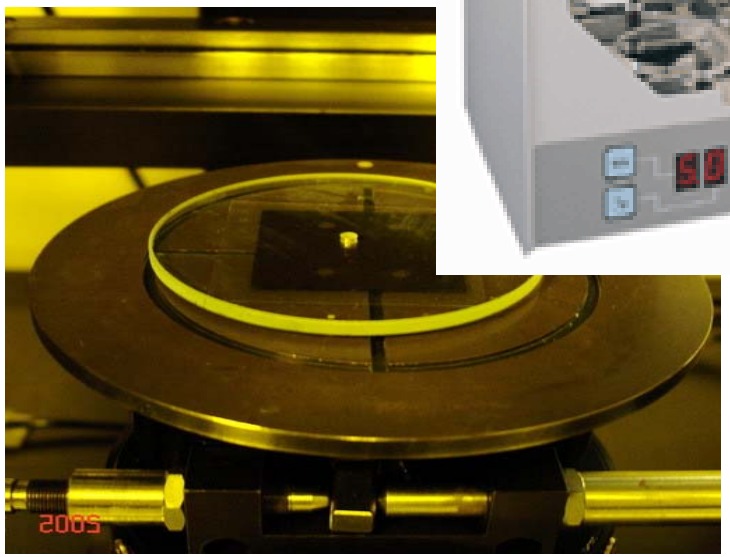

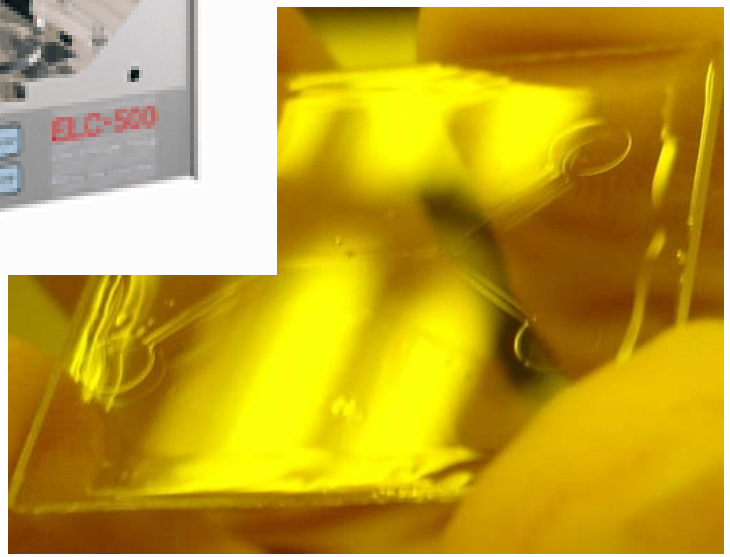

Microfluidics by Soft Lithography

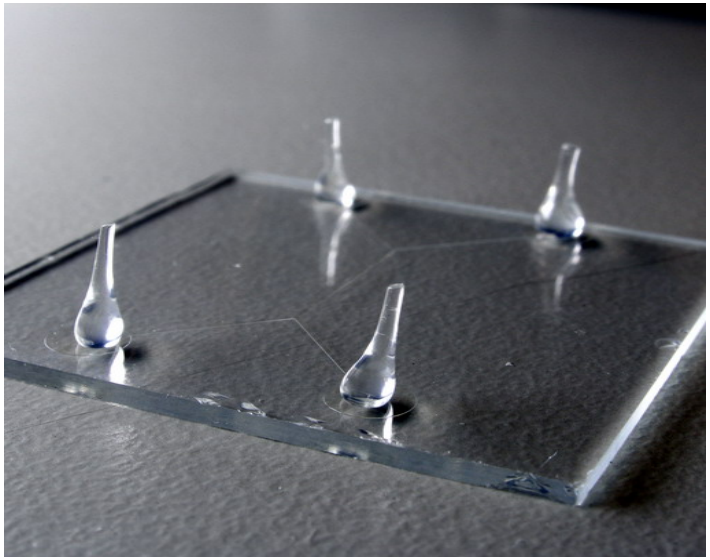

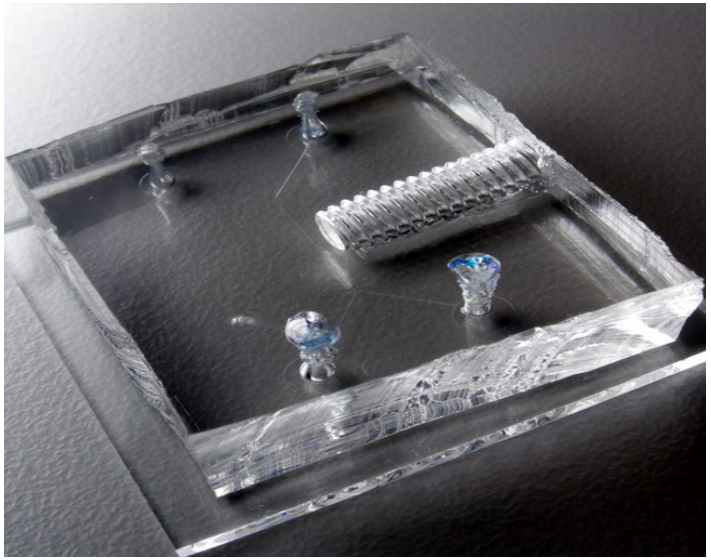

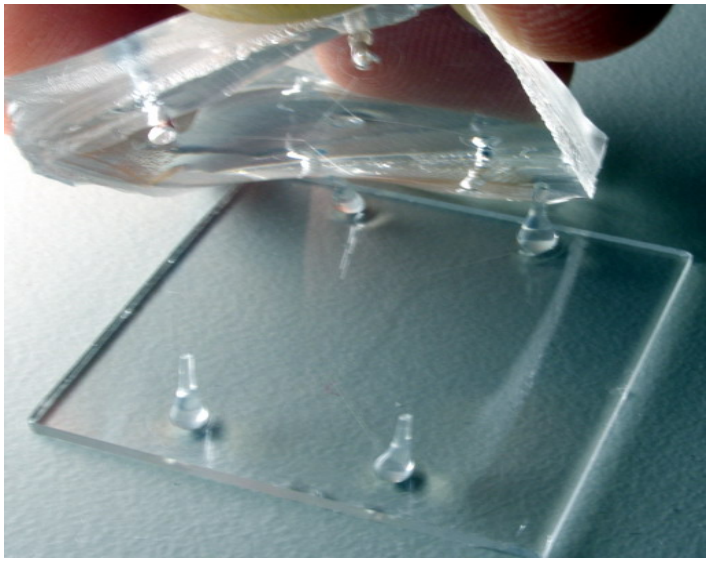

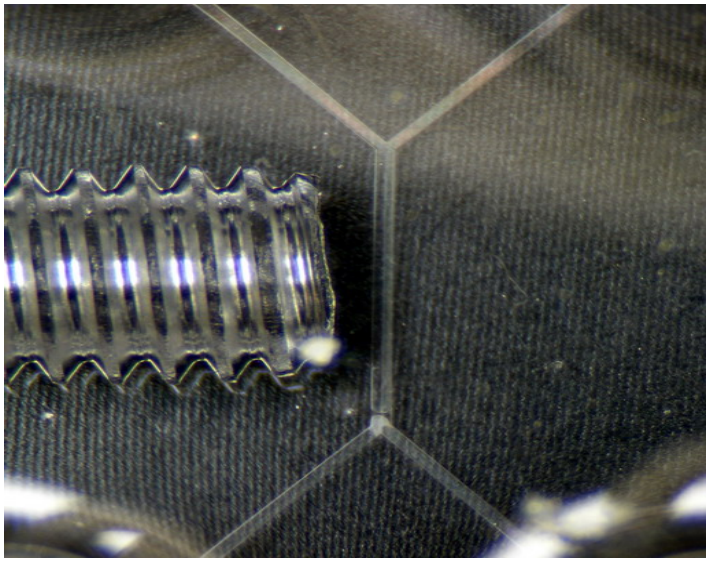

Microfluidics by Soft Lithography

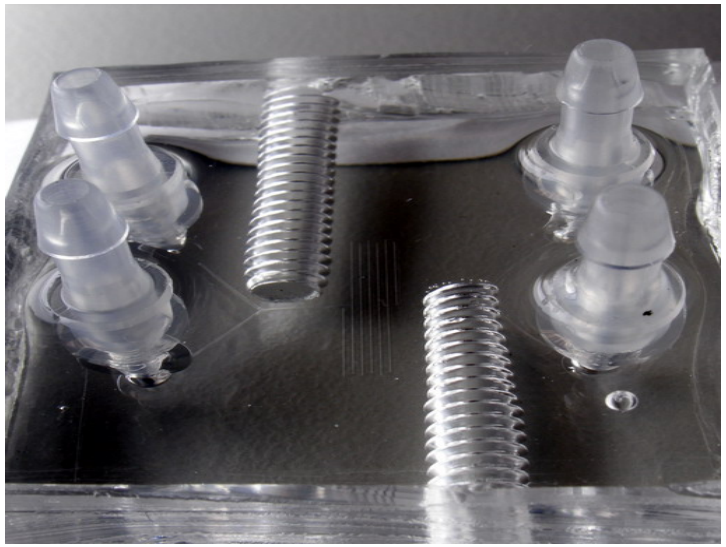

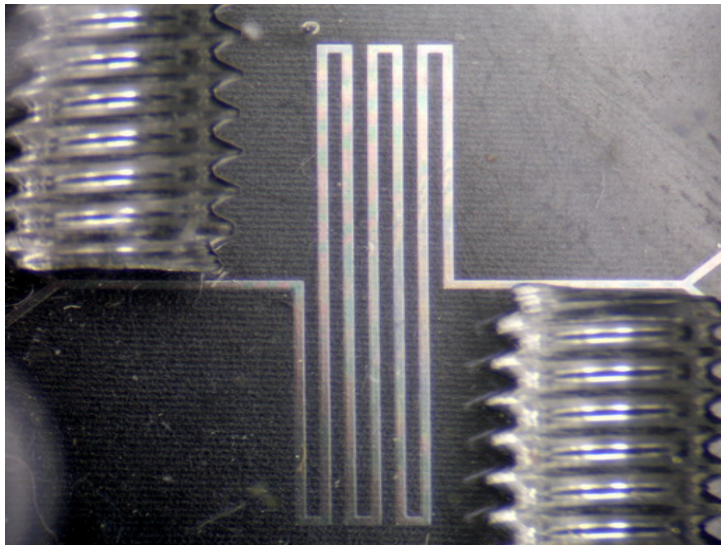

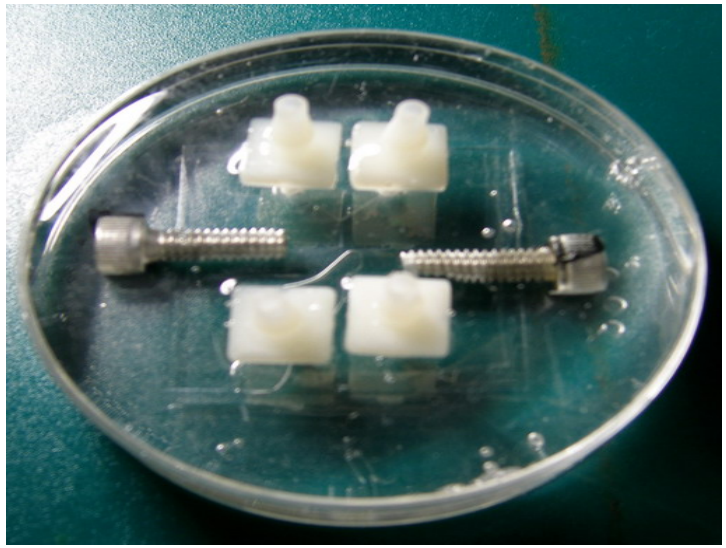

Monolithic Microfabricated Valves and Pumps by Multilayer Soft Lithography

SCIENCE VOL 288 7 APRIL 2000

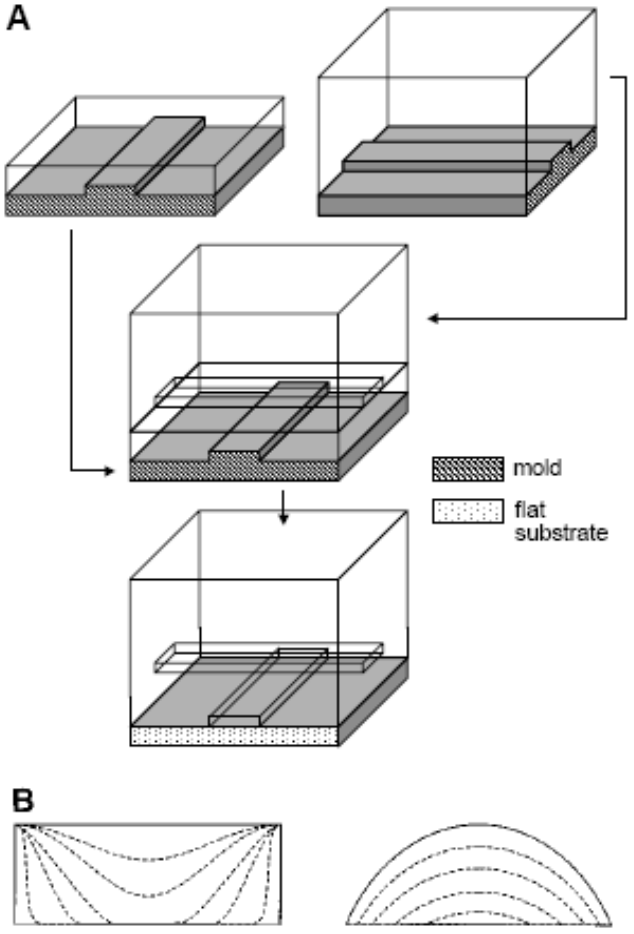

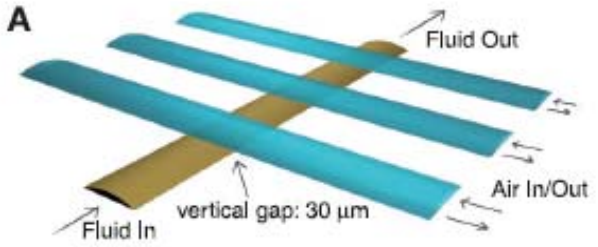

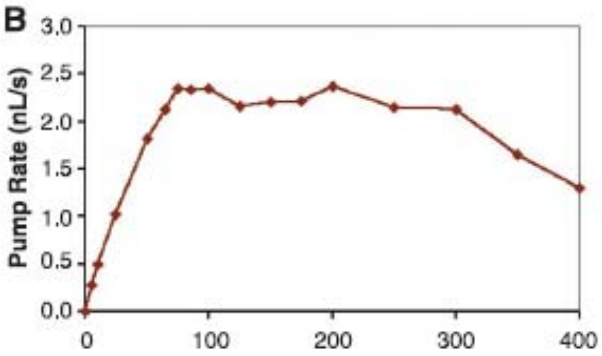

Microfluidic Large-Scale Integration

18 OCTOBER 2002 VOL 298 SCIENCE

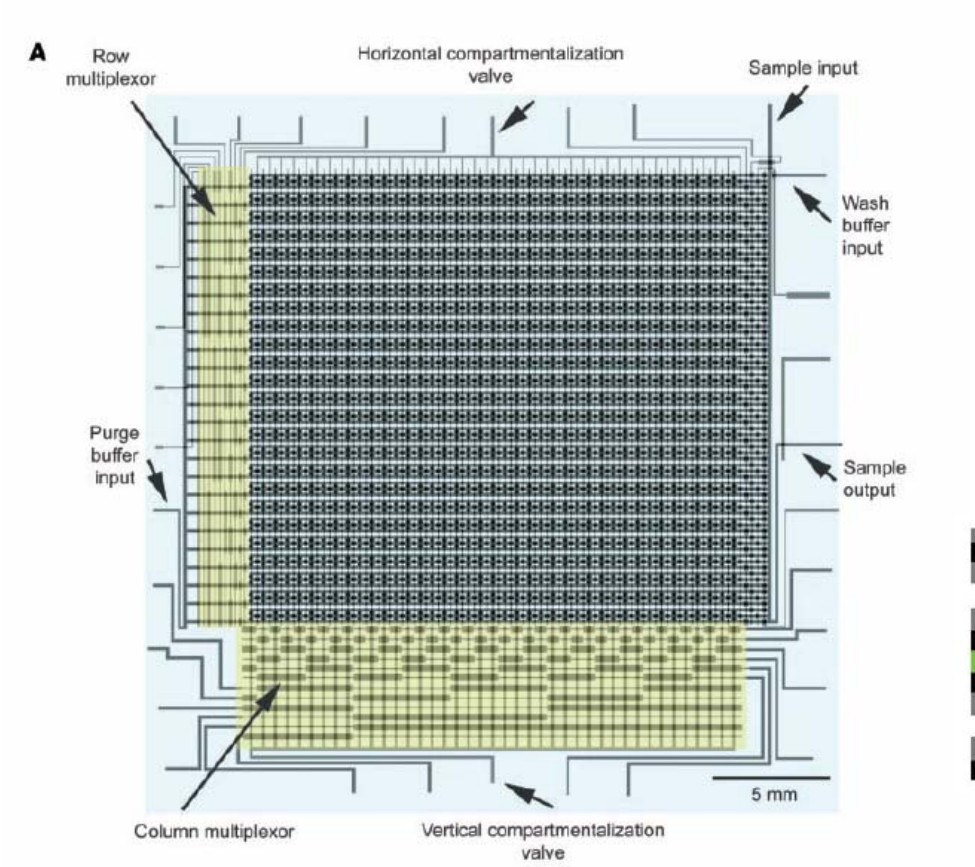

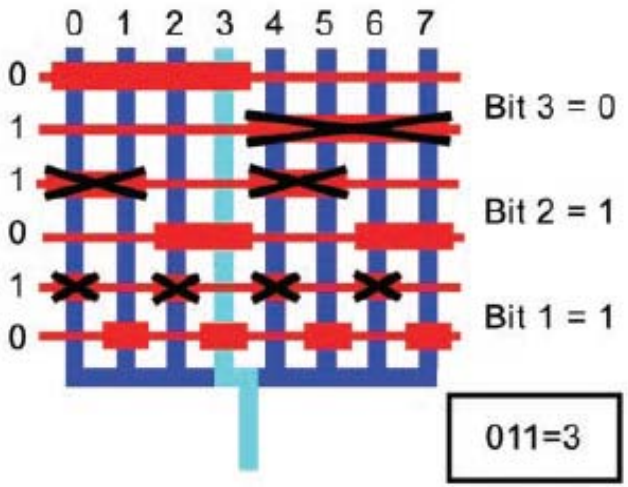

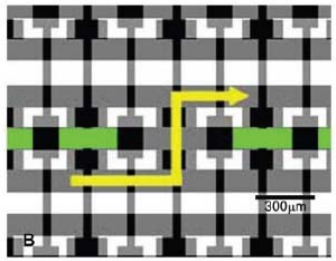

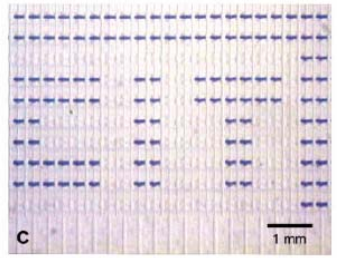

- $2 \log_2 n$ control channels.

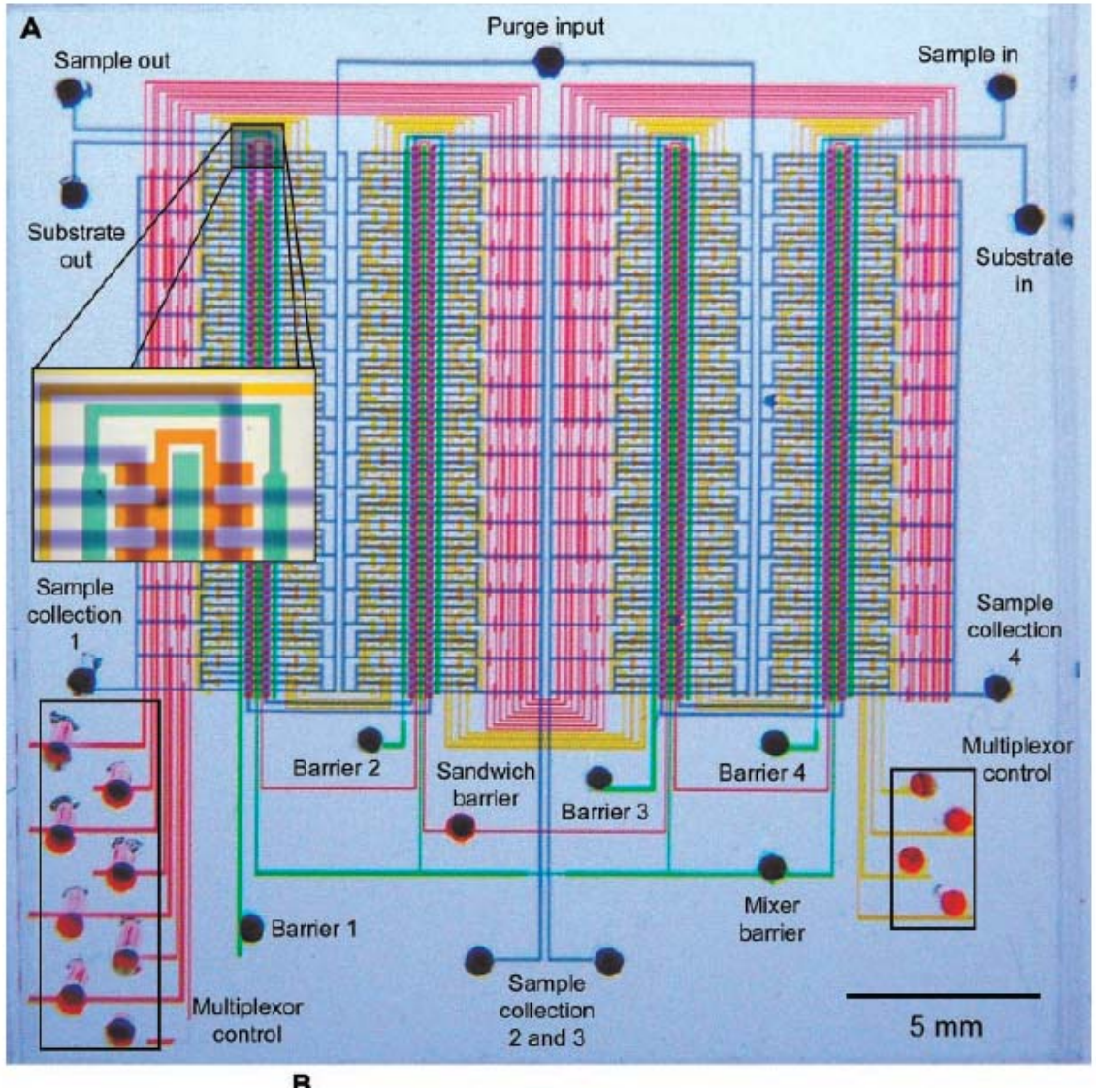
A
Purge input
Sample out
Sample in
Substrate out
Substrate in
Sample collection 1
Sample collection 4
Barrier 2
Sandwich barrier
Barrier 3
Barrier 4
Multiplexor control
Barrier 1
Mixer barrier
Multiplexor control
Sample collection 2 and 3
5 mm
B

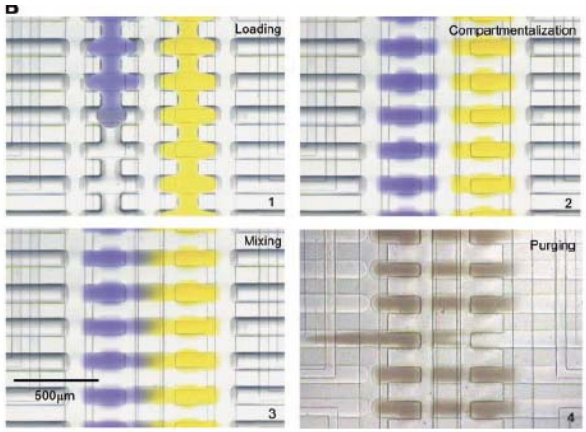
Loading
Compartmentalization
Mixing
Purging
500 µm
1
2
3
4

Multistep Synthesis of a Radiolabeled Imaging Probe Using Integrated Microfluidics

SCIENCE VOL 310 16 DECEMBER 2005

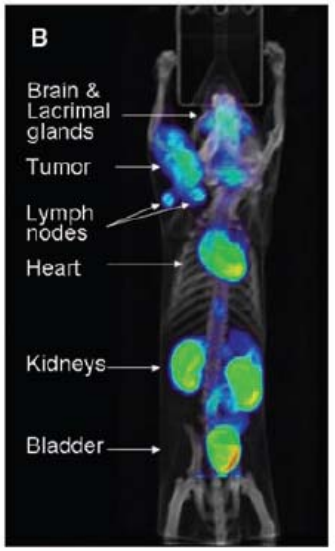

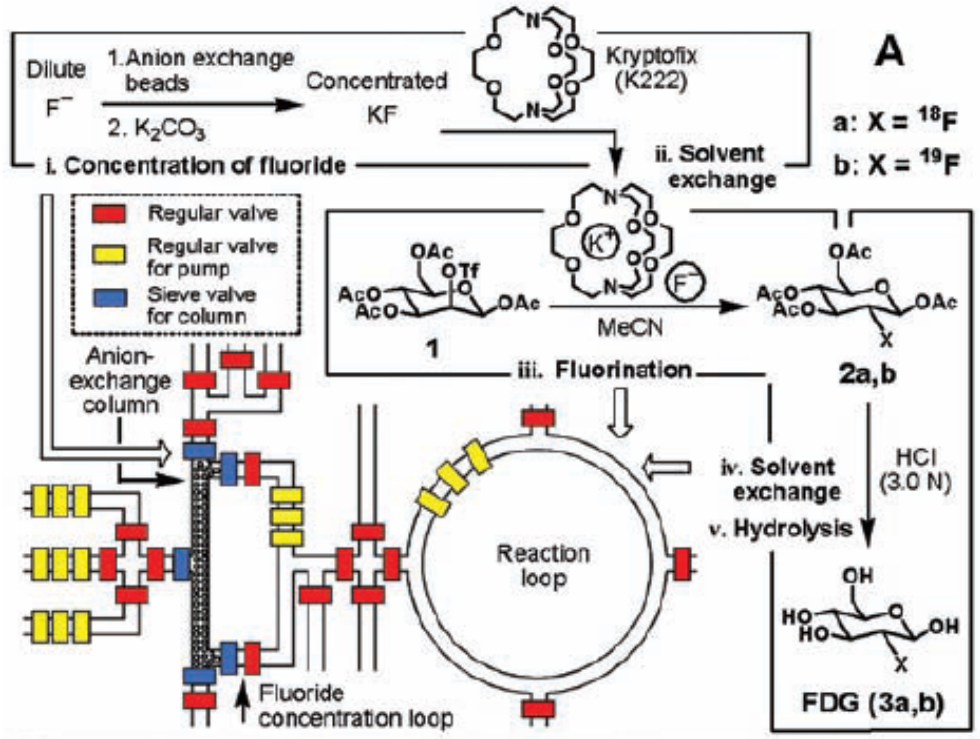

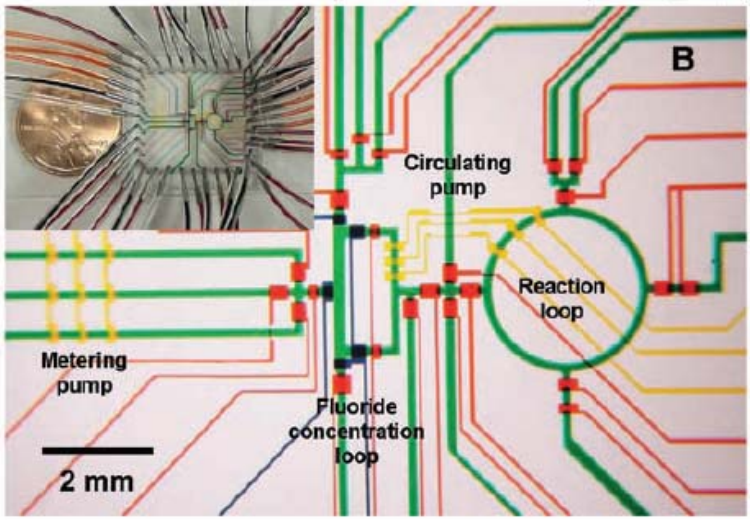

Microfabricated Fluidic System by Soft Lithography

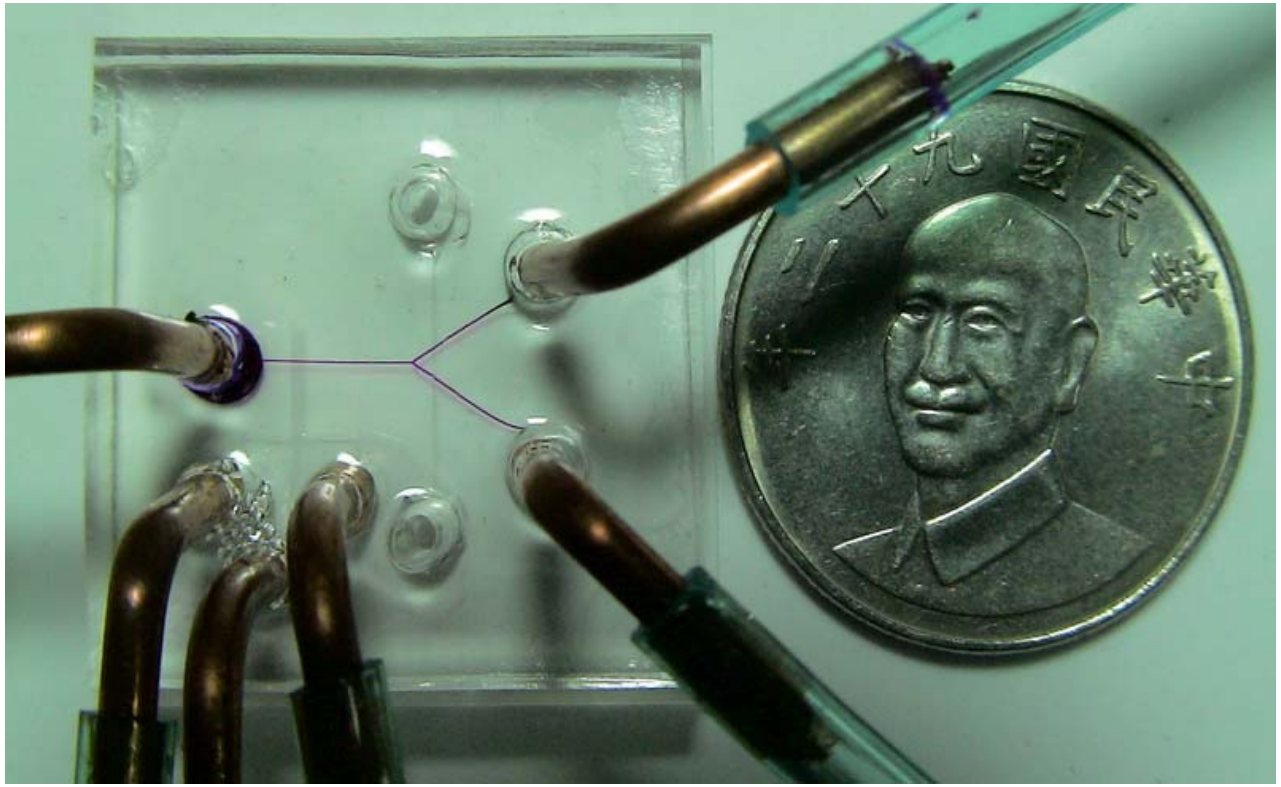

Peristaltic Pump by Soft Lithography

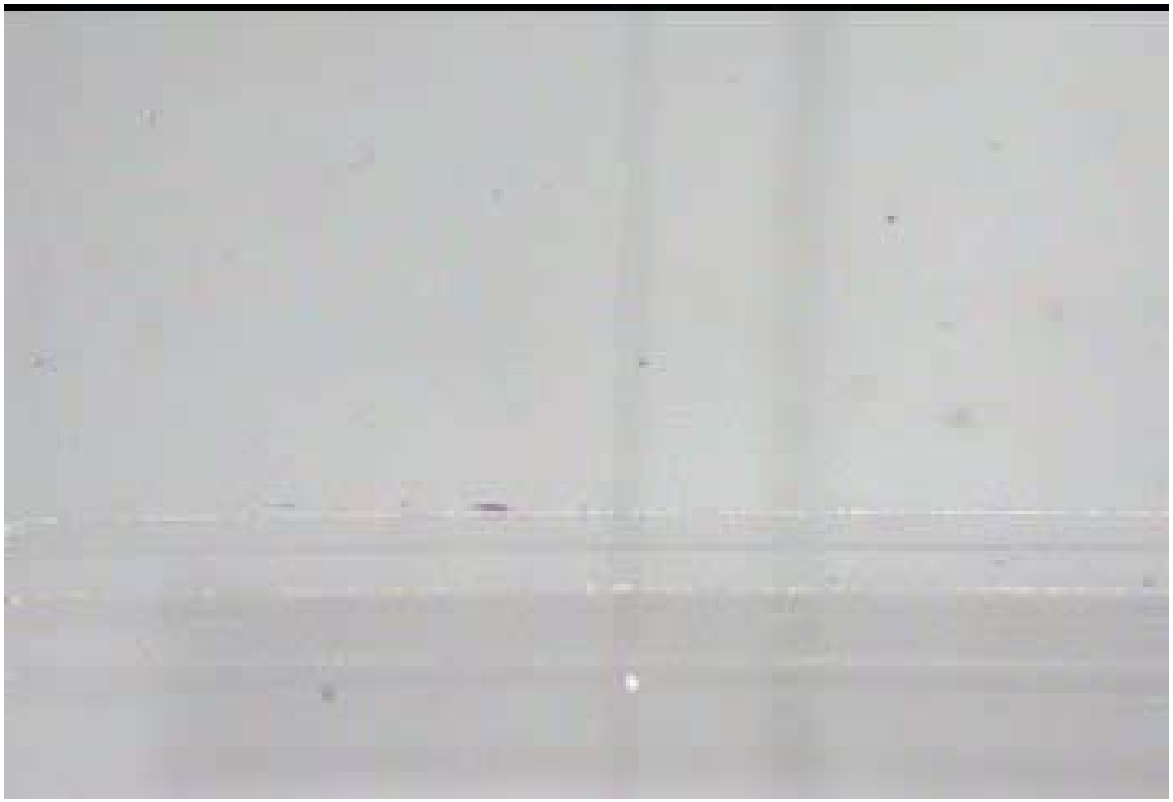

Fluidic Control by Microfabricated Valves

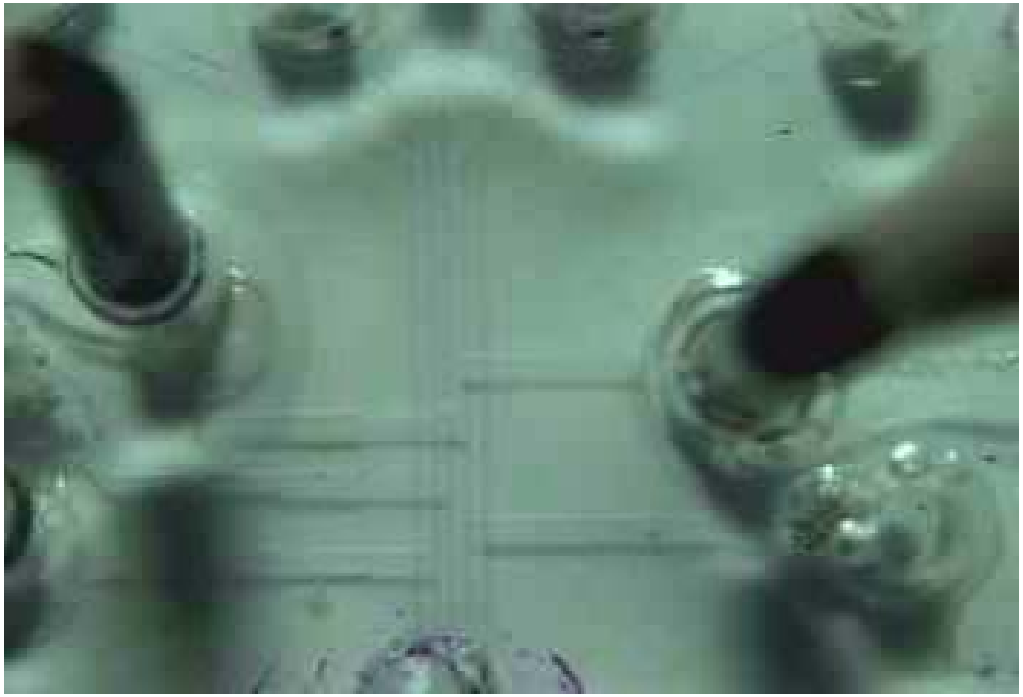

Addressable Microfluidic System

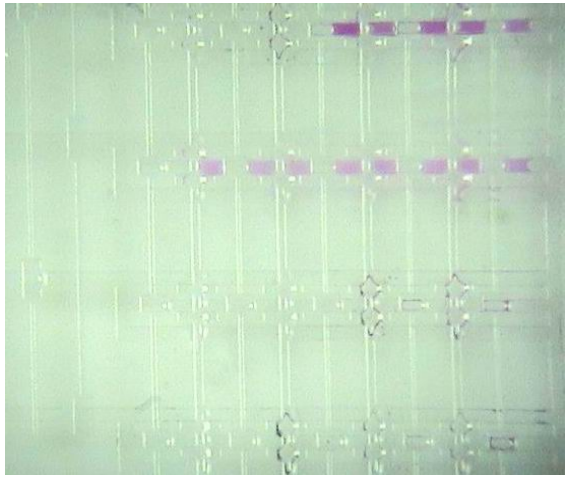

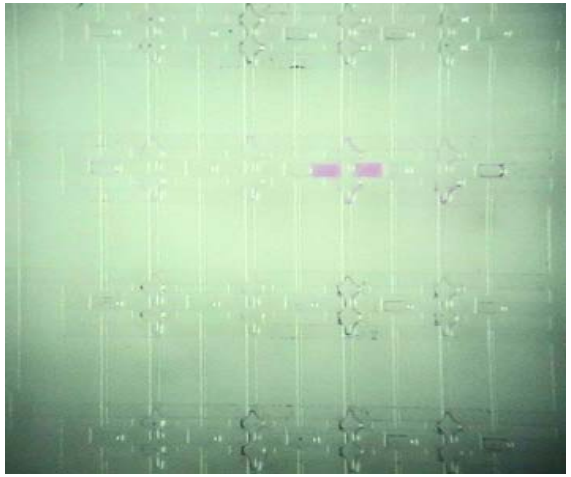

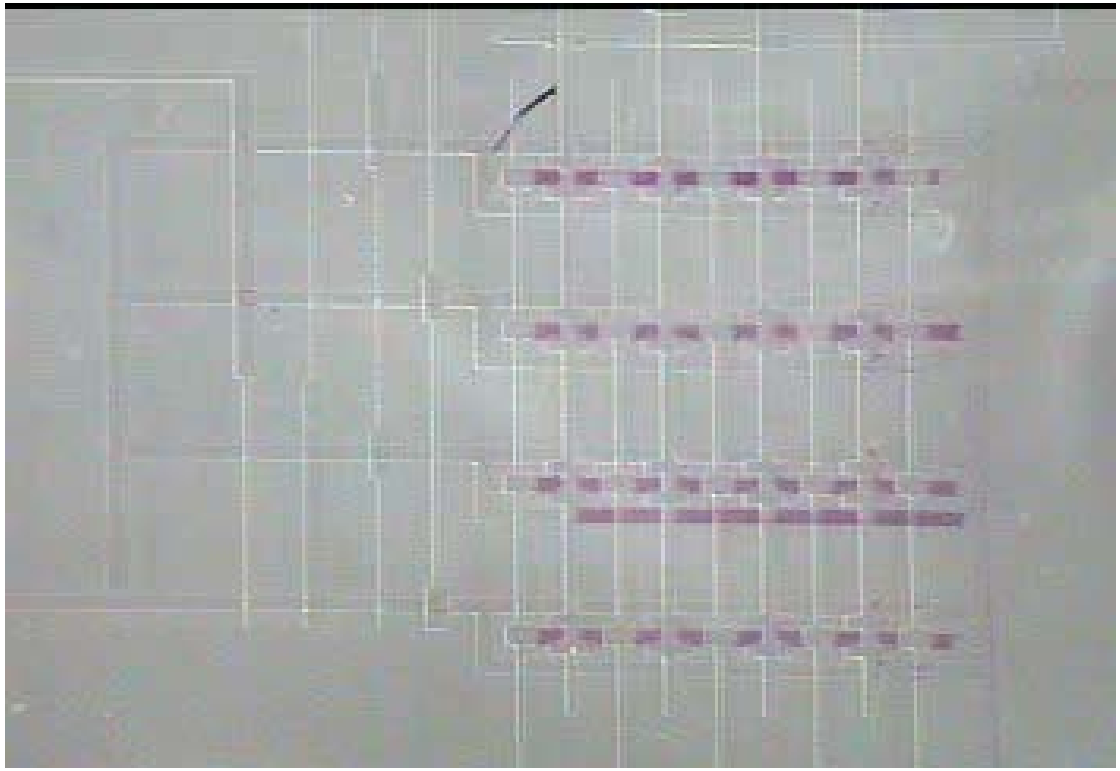

Integrated Detection System in Microchannel

fluidic channel + microlens + fiber

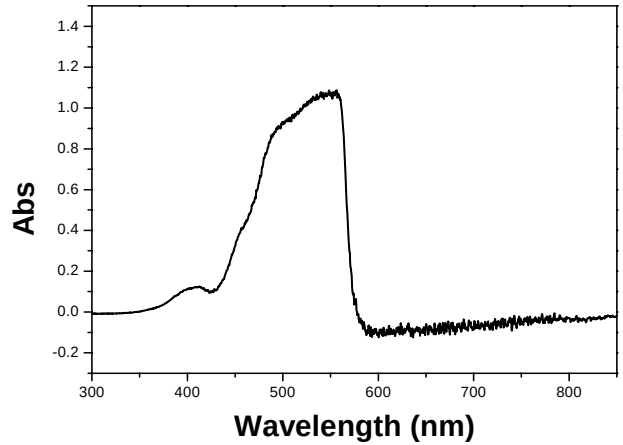

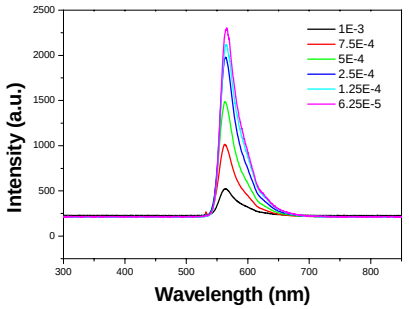

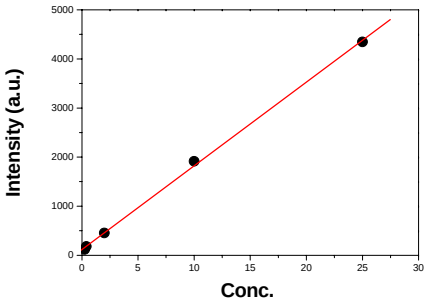

Reference

Adv. Mater. 2004, 16, No. 15, August 4 1249

ADVANCED MATERIALS

Patterning: Principles and Some New Developments**

By *Matthias Geissler* and *Younan Xia**

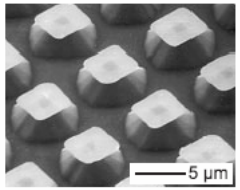

This article provides an overview of various patterning methodologies, and it is organized into three major sections: generation of patterns, replication of patterns, and three-dimensional patterning. Generation of patterns from scratch is usually accomplished by serial techniques that are able to provide arbitrary features. The writing process can be carried out in many different ways. It can be achieved using a rigid stylus; or a focused beam of photons, electrons, and other energetic particles. It can also be accomplished using an electrical or magnetic field; or through localized add-on of materials such as a liquid-like ink from an external source. In addition, some ordered but relatively simple patterns can be formed by means of self-assembly. In replication of patterns, structural information from a mask, master, or stamp is transferred to multiple copies with the use of an appropriate material. The patterned features on a mask are mainly used to direct a flux of radiation or physical matter from a source onto a substrate, whereas a master/stamp serves as the original for replication based on embossing, molding, or printing. The last section of this article deals with three-dimensional patterning, where both vertical and lateral dimensions of a structure need to be precisely controlled to generate well-defined shapes and profiles. The article is illustrated with various examples derived from recent developments in this field.

Direct Writing

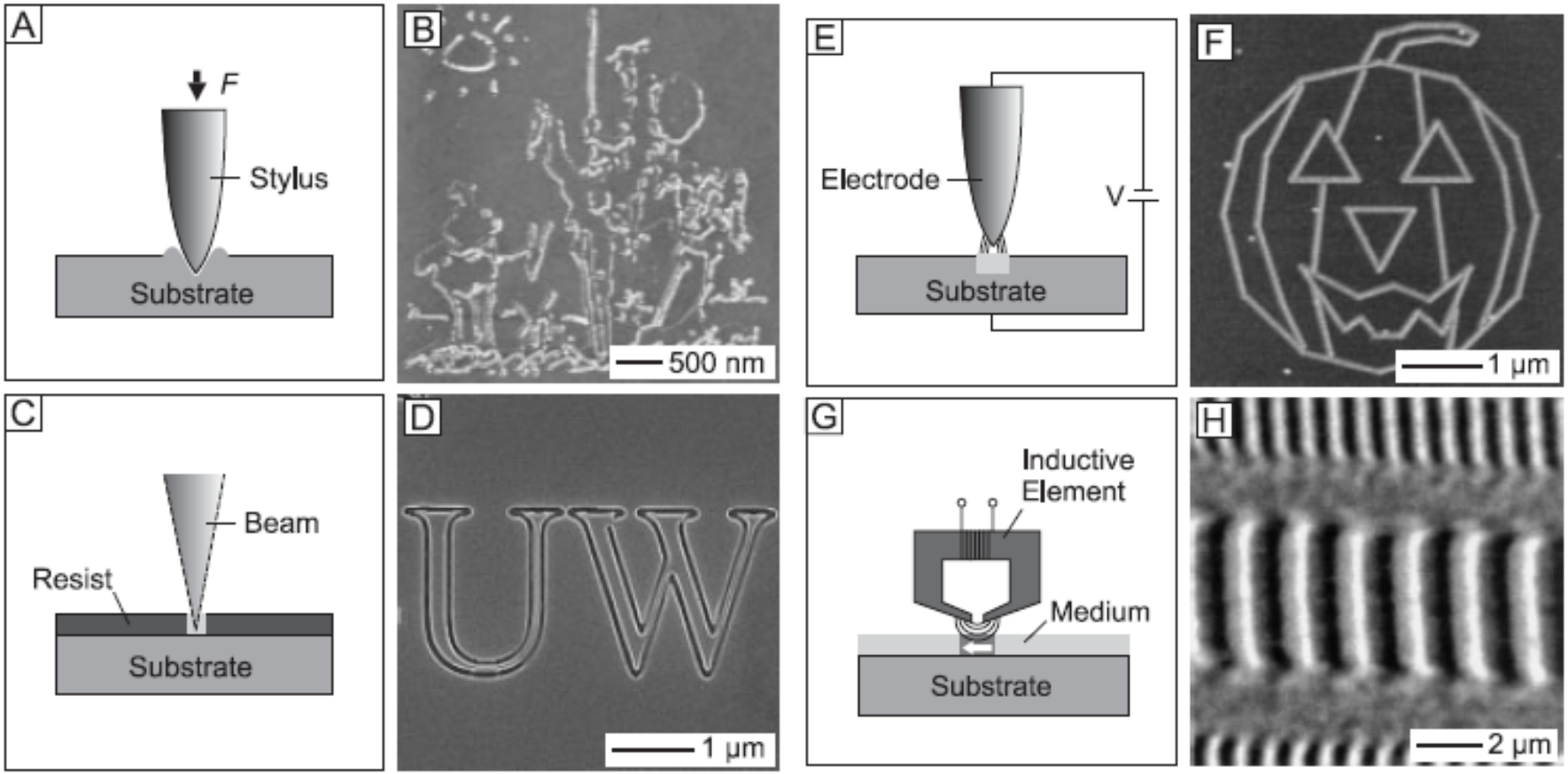

	write head				
	2mm	**4mm**	**10mm**	**20mm**	**40mm**
min. structure size [µm]	0.6	1.0	2.5	5.0	10.0
address resolution [nm]	20	40	100	200	400
writing speed [mm²/min]	1.5	5.7	36	119	416
line width uniformity, 3σ [nm]	80	100	220	440	880
edge roughness, 3σ [nm]	60	80	120	180	280

Electron Microscope

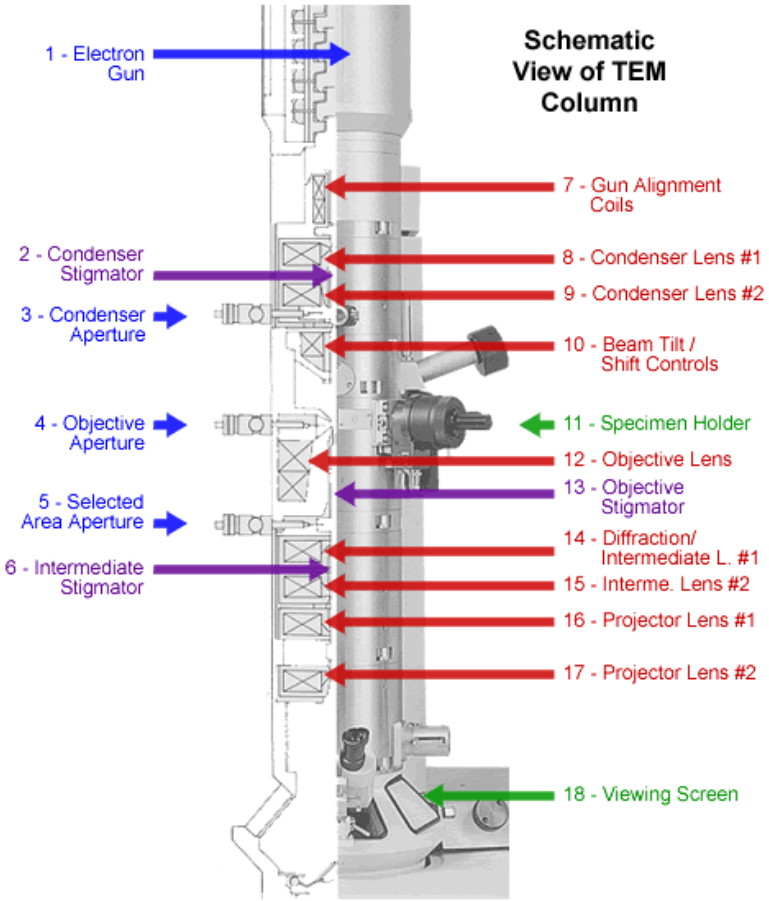

TEM Image

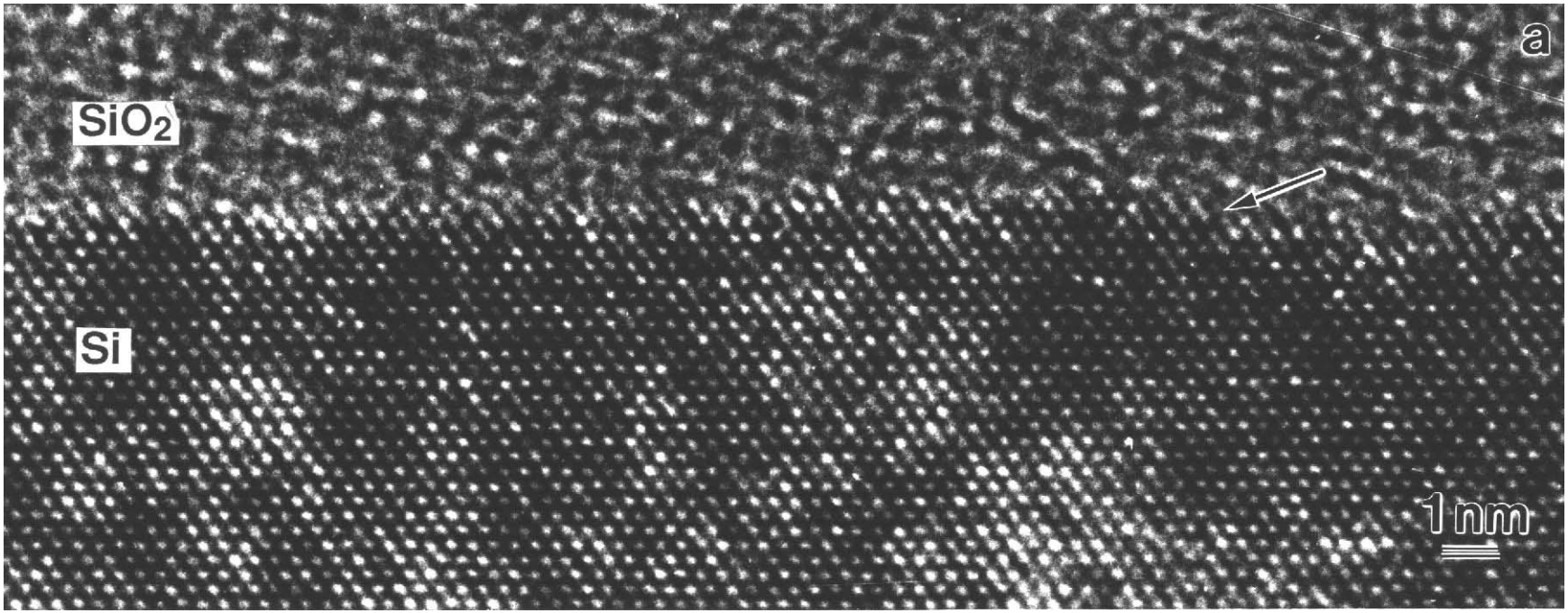

E-Beam Lithography

Resolution:

2 nm @ 20 KeV

2 nm @ 1.0 KeV

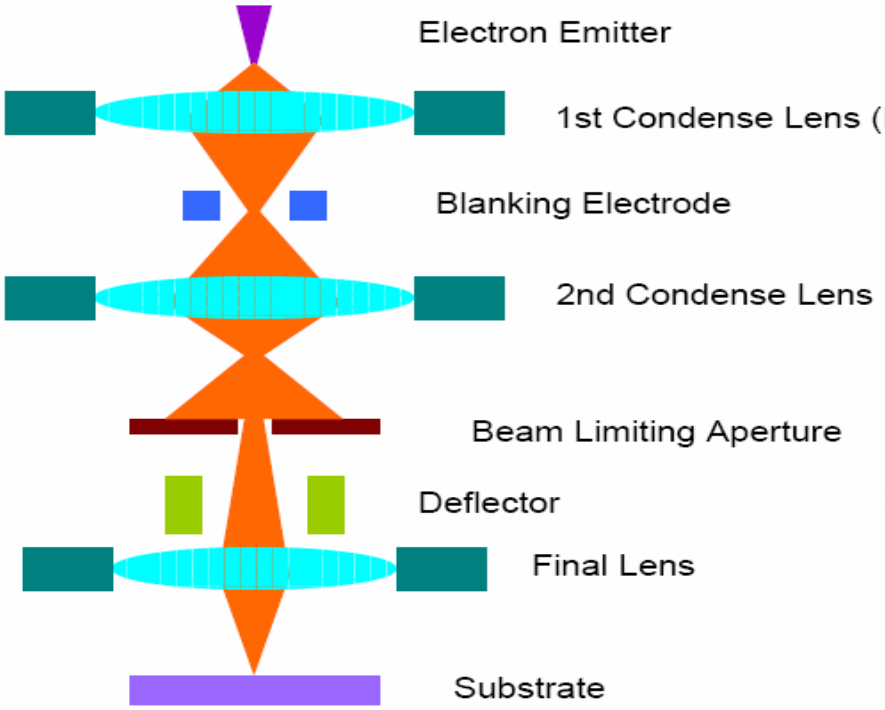

E-beam Writer

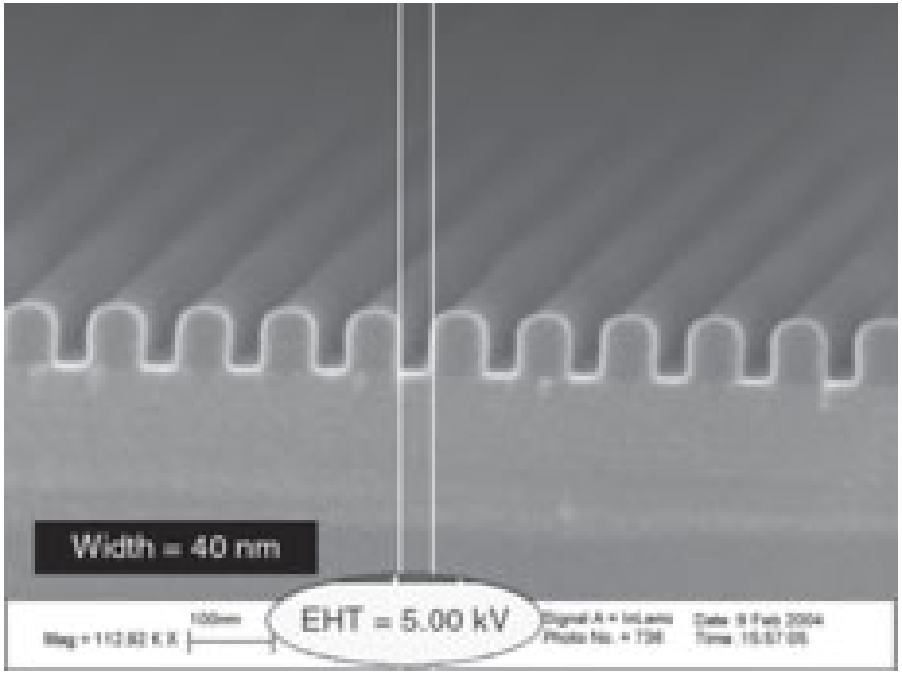

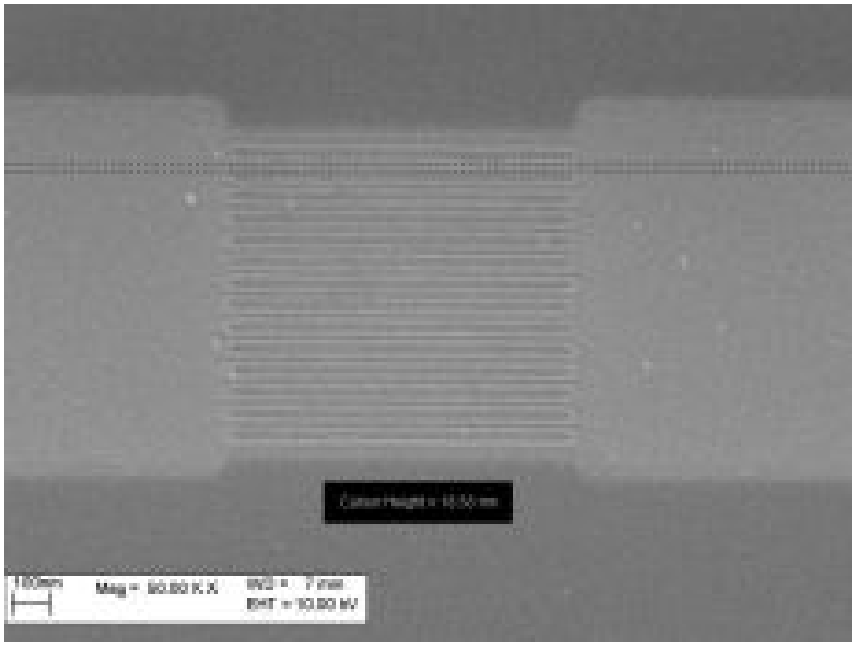

Better than 10 nm lines over 4 inch wafer

EUV System

EUV Source

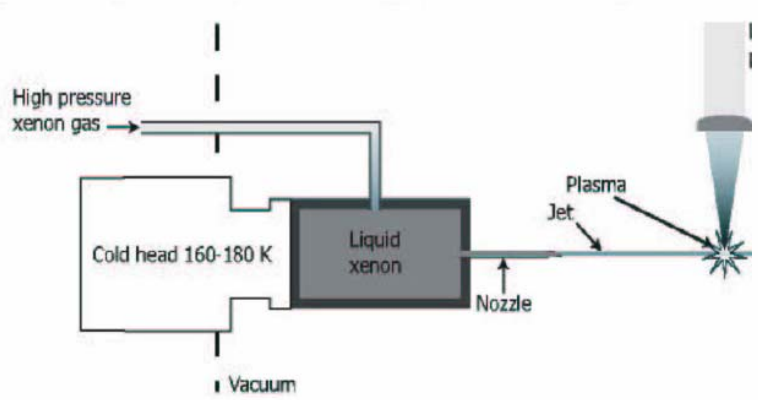

1. 13.4nm source.
2. Laser-produced plasma

Reflective Optics for EUV

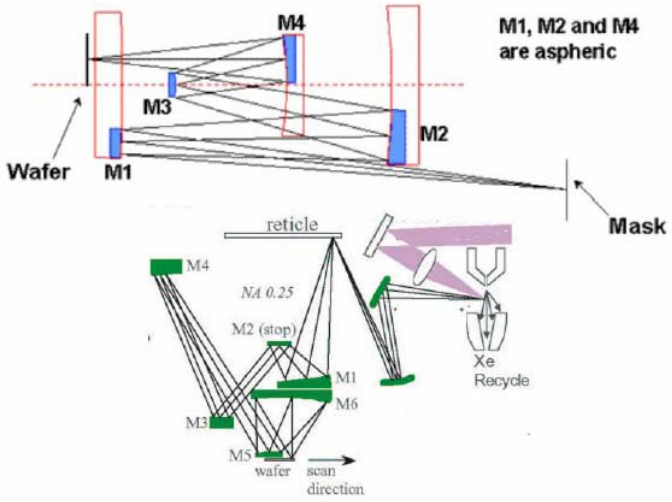

EUV light (< 100nm) is absorbed by almost all materials -> No lens.

Two Photon Writing

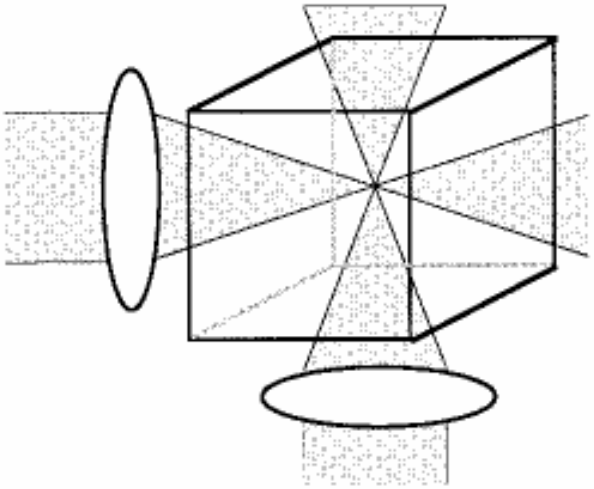

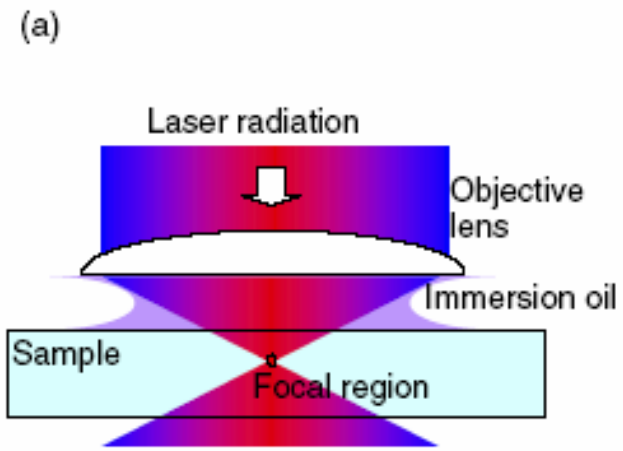

$$D(r) = w_0\sqrt{2\ln\left(\frac{I(r)}{I_{\text{th}}}\right)\frac{1}{N}},$$

$$L(z) = 2z_{\text{R}}\sqrt{\left(\frac{I(z)}{I_{\text{th}}}\right)^{\frac{1}{N}} - 1},$$

Two Photon Writing

NATURE | VOL 412 | 16 AUGUST 2001 |

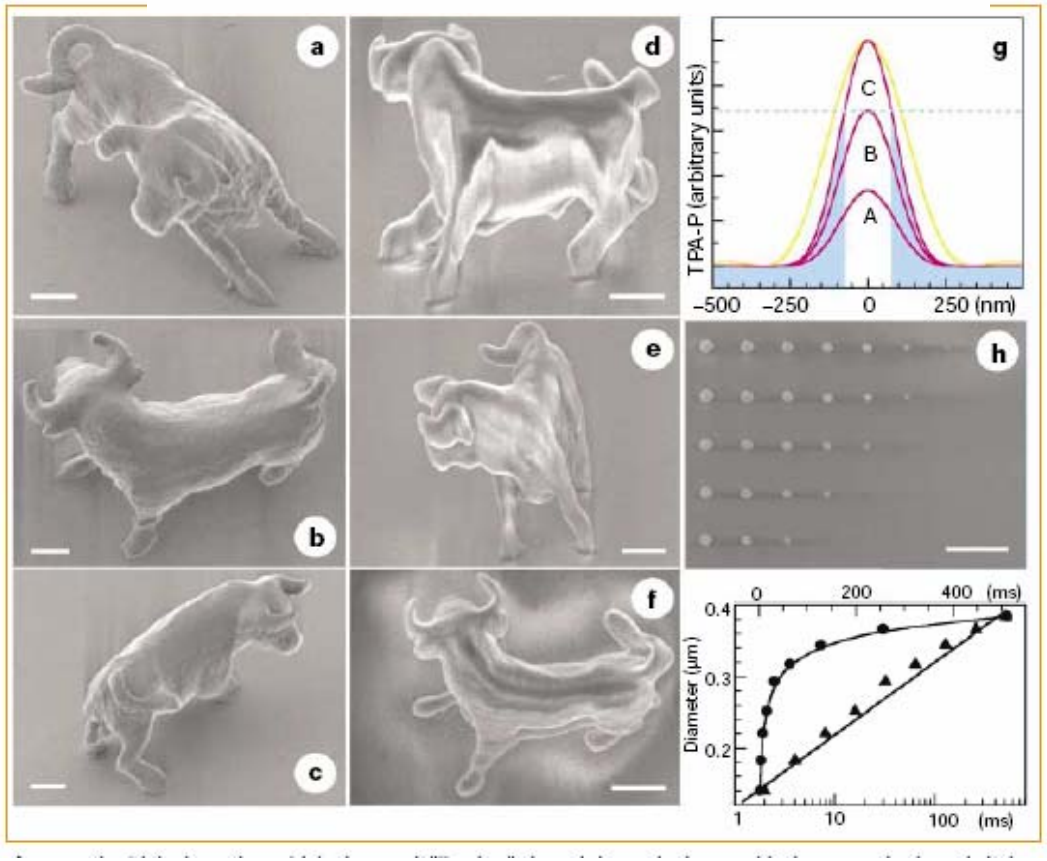

Two Photon Writing

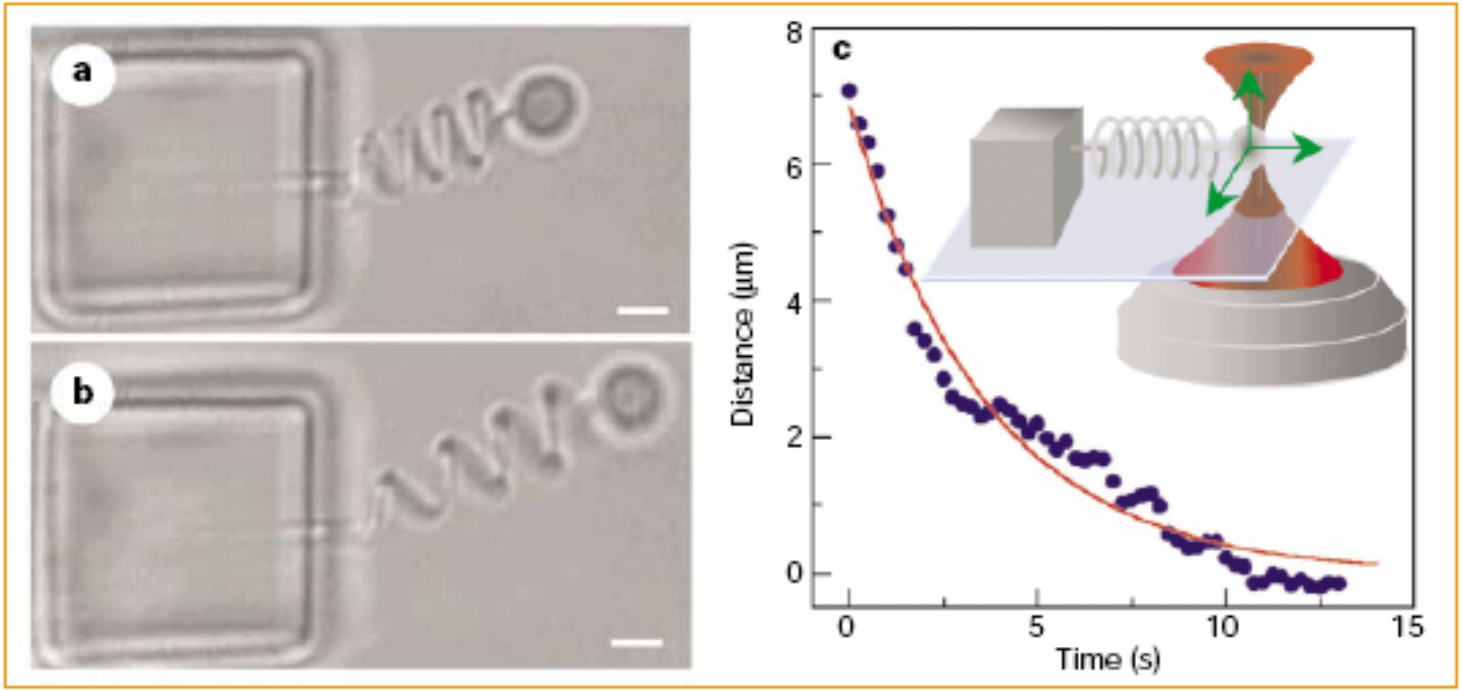

Figure 2 Functional micro-oscillator system, in which not only the spring but also the cubic anchor and the bead were produced using our two-photon absorption system. The oscillator was kept in ethanol so that the buoyancy would balance gravity and eliminate bead–substrate friction. **a**, **b**, The spring in its original (**a**) and extended (**b**) states. Scale bars, 2 μm. **c**, Restoring curve of the damping oscillation; inset, diagram showing driving of the oscillator by using laser trapping.

Introduction To Scanning Probe Microscopy

General features of SPM

The first scanning probe microscope was invented in 1981 by Gerd Binnig and Heinrich Rohrer at the IBM laboratory in Zurich. Since that time, a vast family of scanning probe microscopes has been spawned, a few of which are represented in this family tree. Despite the huge number of types of SPM and modes in which they can be operated, the underlying operation is the same for them all. Each different type of SPM is **characterized by the nature of the local probe and its interaction with the sample surface.**

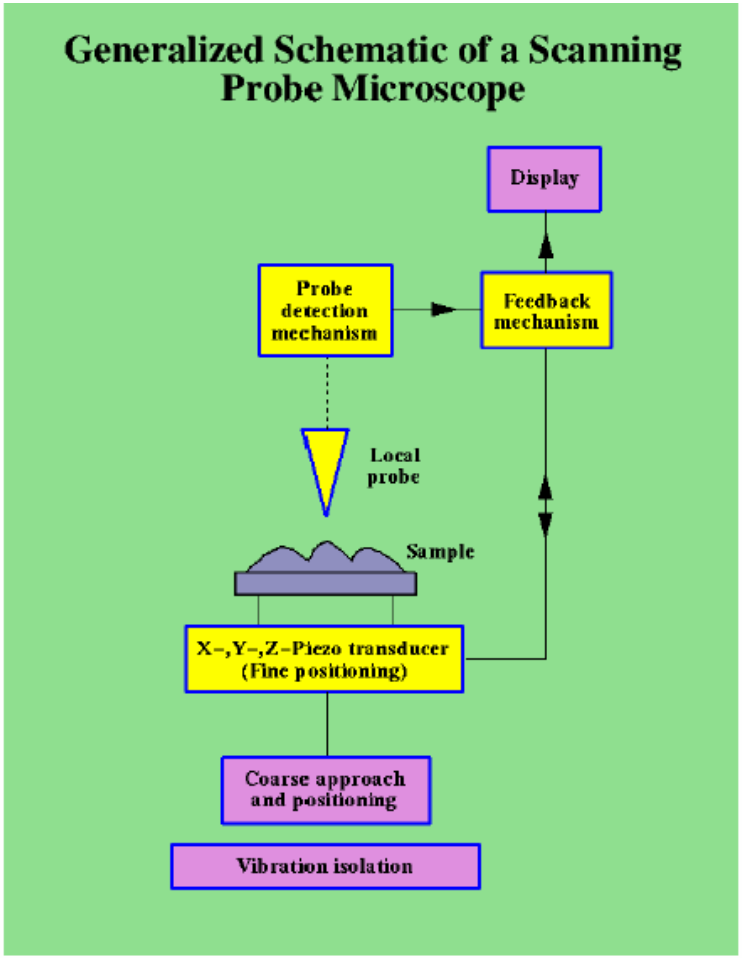

Scanning Tunneling Microscopy

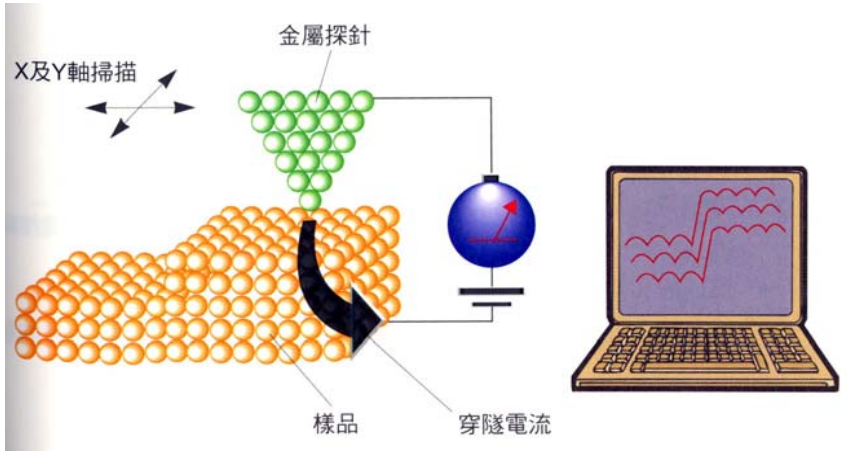

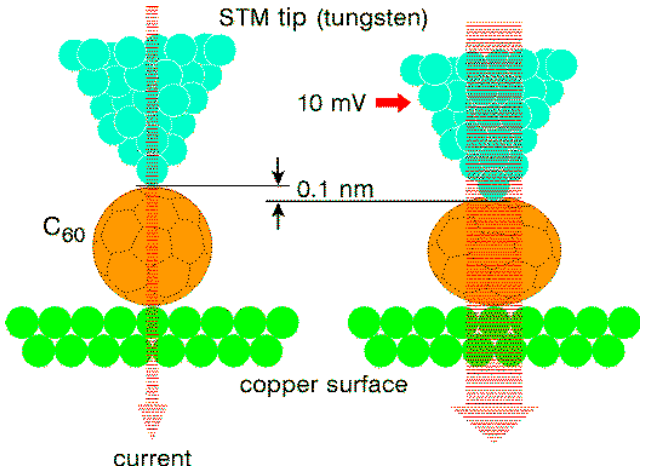

STM Images

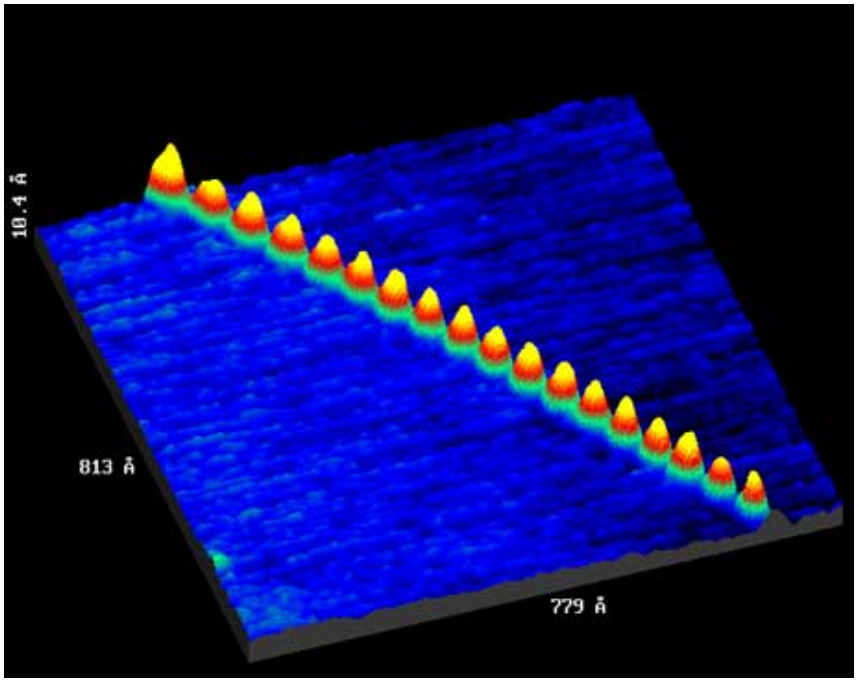

Polymer

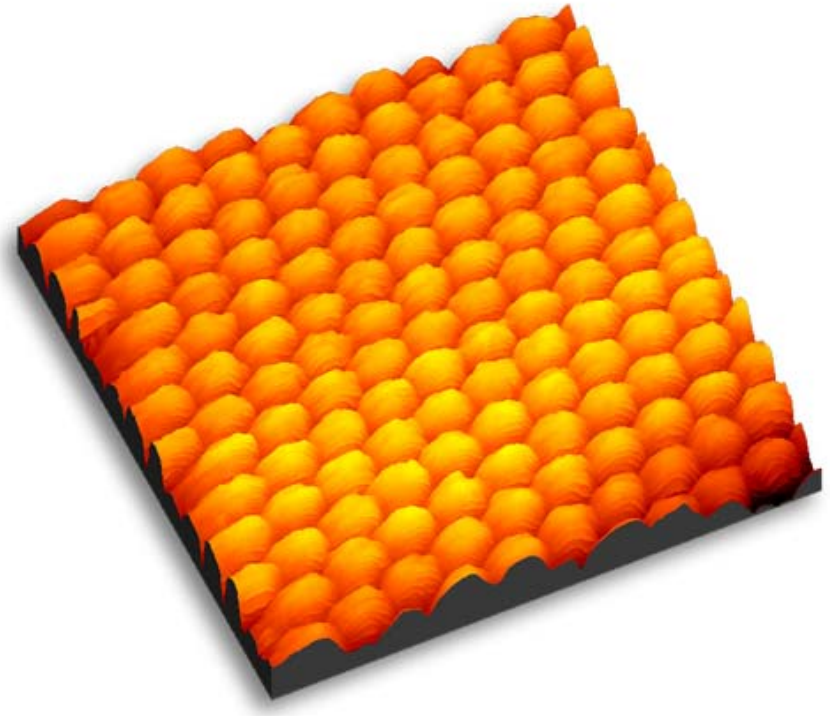

Gold atom

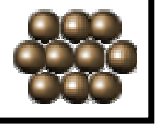

Atomic Force Microscopy

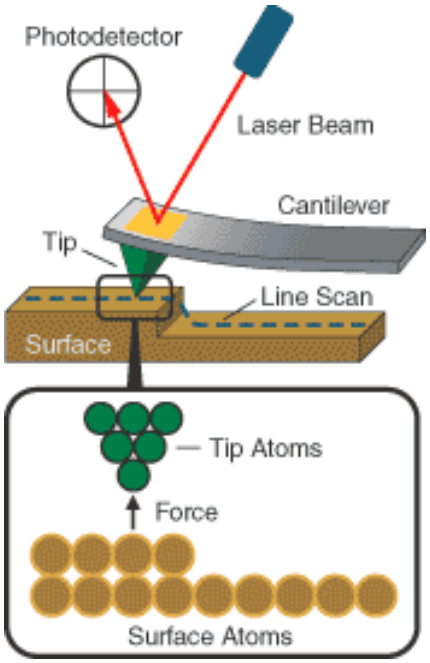

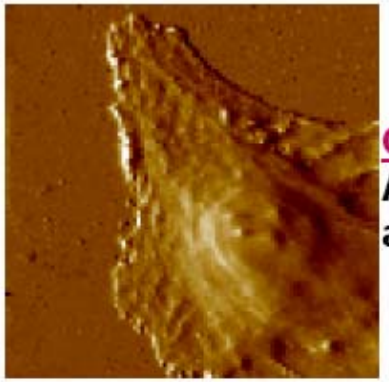

Cell surface imaging
AFM imaging of living and fixed animal cells

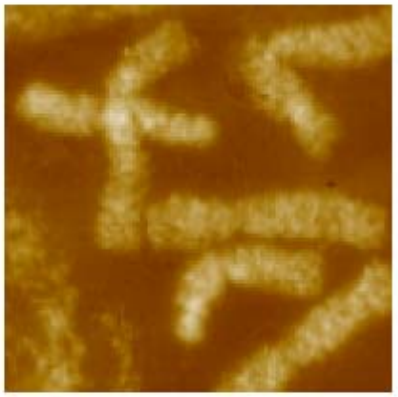

Chromosomes
A large selection of work on both human and plant chromosomes

Scanning Probe Microscope

DNA
AFM images of double-stranded DNA and of some special single-double-stranded DNA constructs

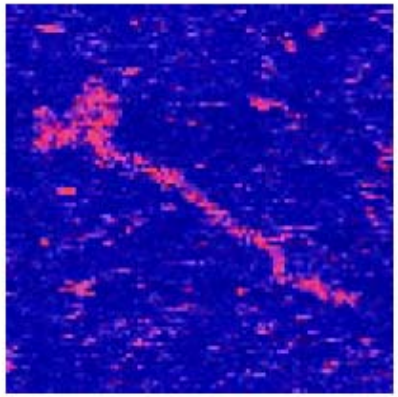

Muscle Proteins
High resolution AFM images of myosin and titin

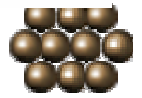

AFM Images

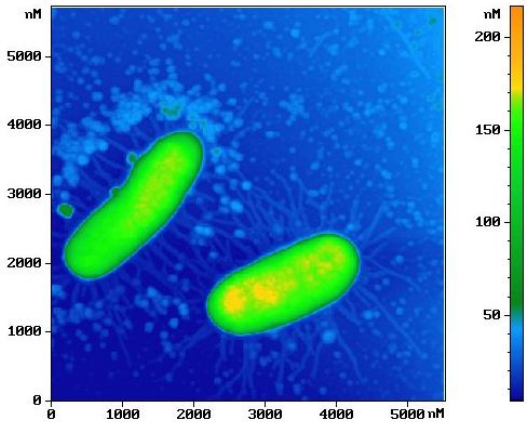

E Coli

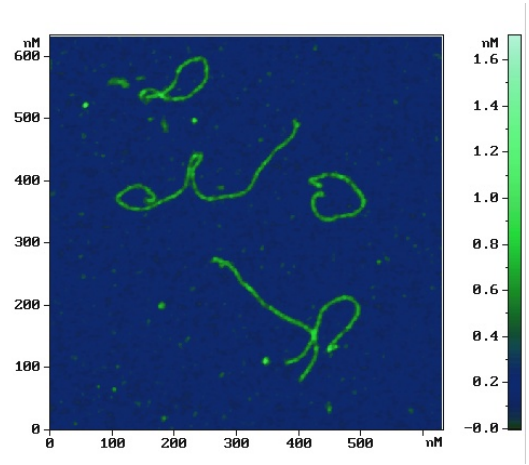

Protein

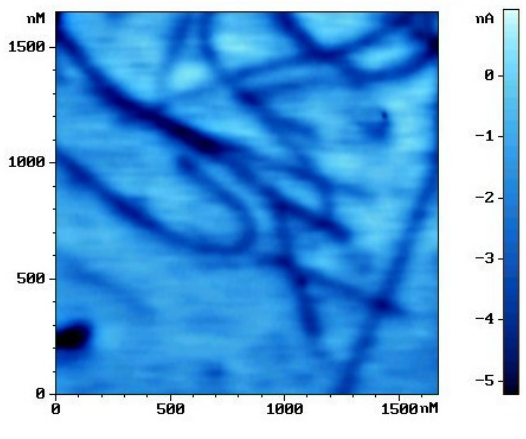

Nanotubes

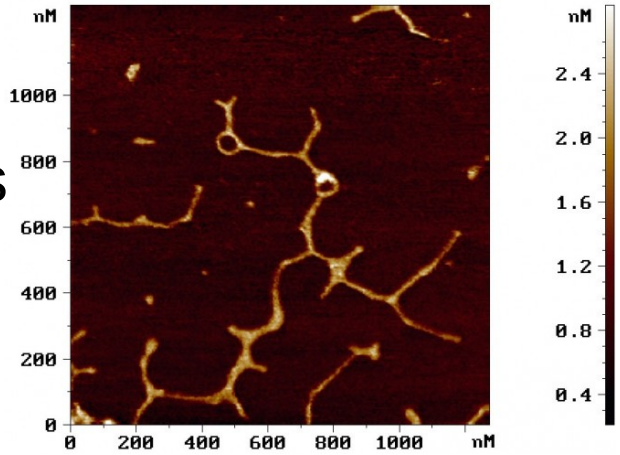

DNA

Scanning Probe Family

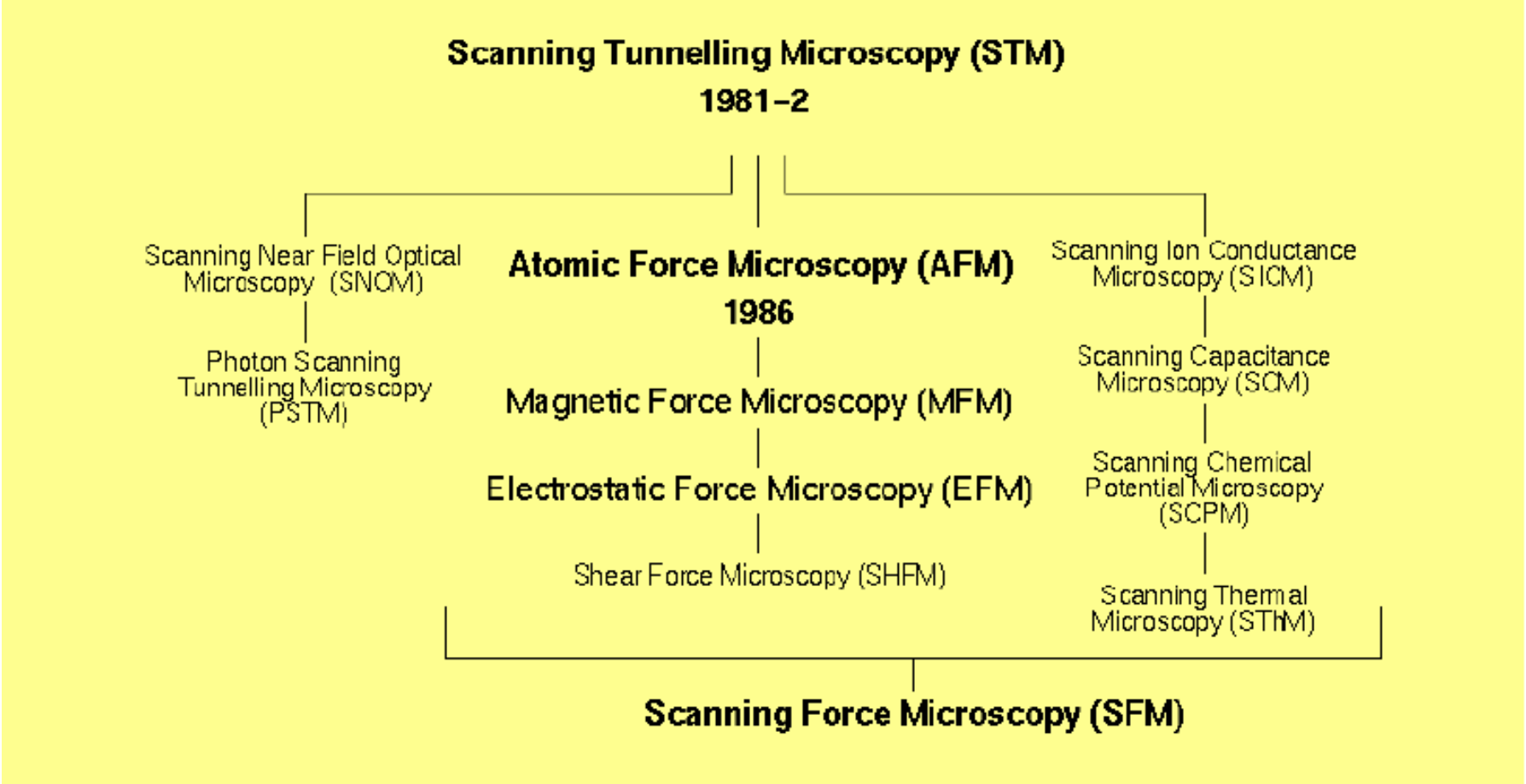

STM Lithography

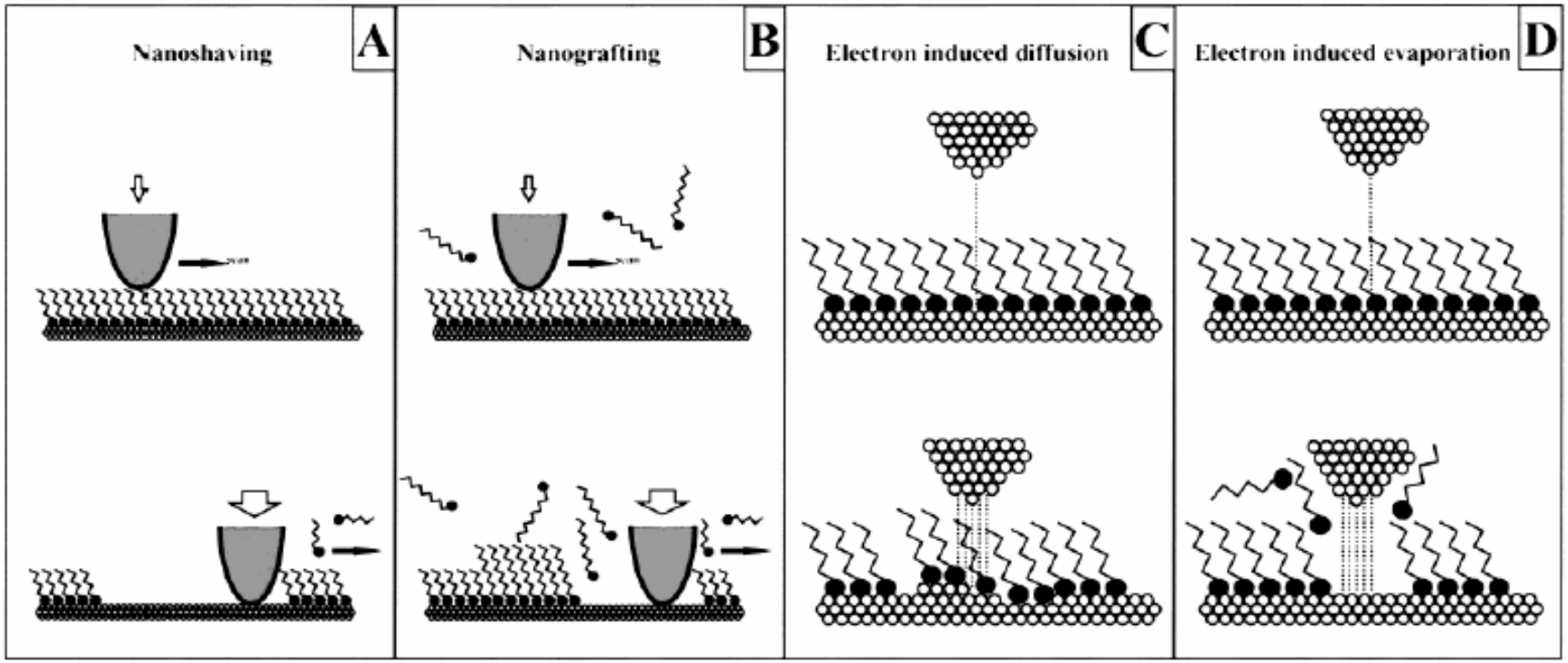

Resist: Thiol

STM Lithography

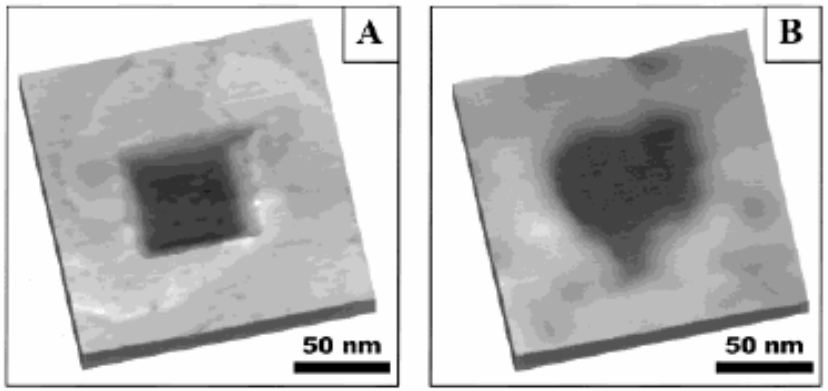

FIGURE 3. (A) 160 × 160 nm² topographic images of $C_{18}S$/Au(111) with the thiols shaved away from the central 50 × 50 nm² square. (B) 160 × 160 nm² topographic images of OTE/mica containing a heart-shaped pattern produced using nanoshaving.

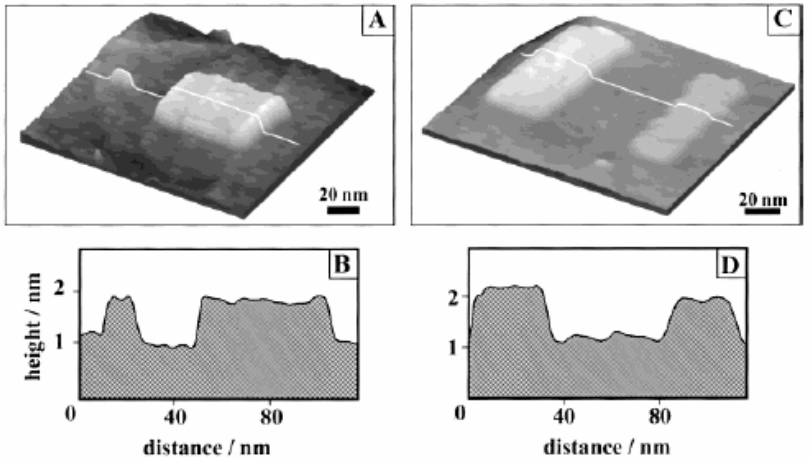

Oxidation Lithography

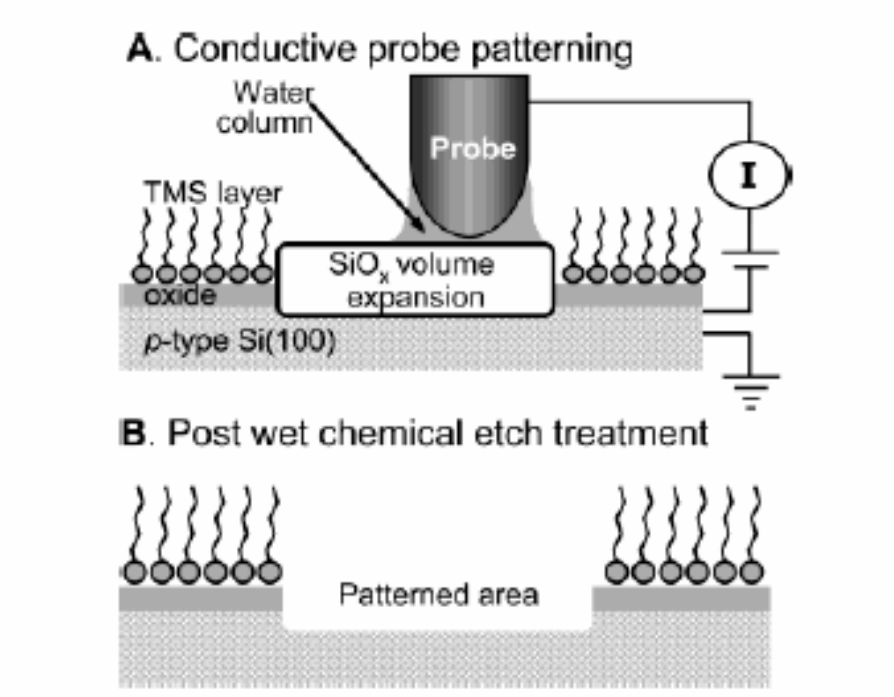

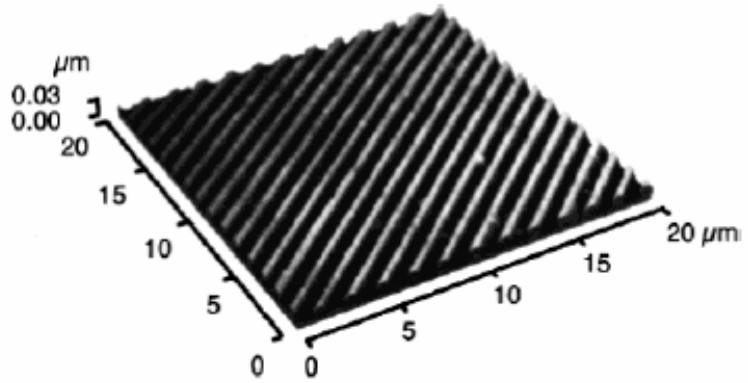

Figure 8. AFM images showing the results of AFM anodic oxidation and wet etching of a pattern in an ODS-SAM on a multilayer resist: scan speed, 10 μm/s; probe current, 5 nA; etching steps with 0.5 wt % hydrofluoric acid (0.5 min) and 25 wt % tetraammonium hydroxide (3 min). Reprinted with permission from ref 111. Copyright 1999 Society of the American Institute of Physics.

AFM Lithography

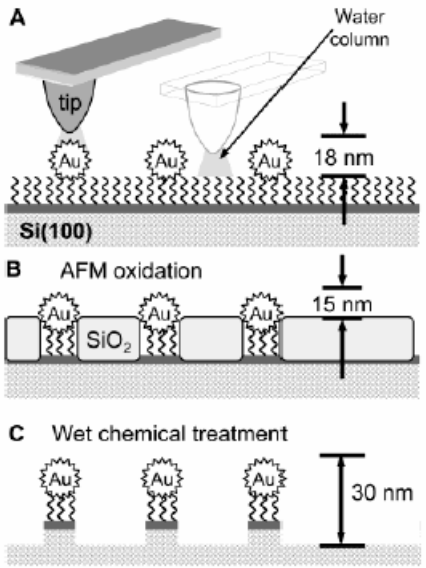

Figure 10. Schematic diagram of (A) selective anodization of the silicon regions not masked by nanoparticles. (B) The volume expansion of the silicon led to a decreased height contrast between the particles and the substrate. (C) After a wet etching step, silicon columns capped with a nanoparticle were formed.

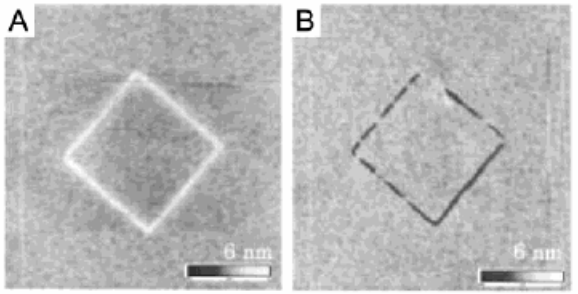

Figure 12. AFM images showing a lithographically defined pattern in a palmitic acid LB layer adsorbed to a SiO_N/Si substrate. Diamond pattern with protruding lines was written with −10 V applied tip bias (A), and that with grooves, with +10 V applied tip bias (B) (*z*-scale: 6 nm). Reprinted with permission from ref 123. Copyright 2002 American Institute of Physics.

Substitution Lithography

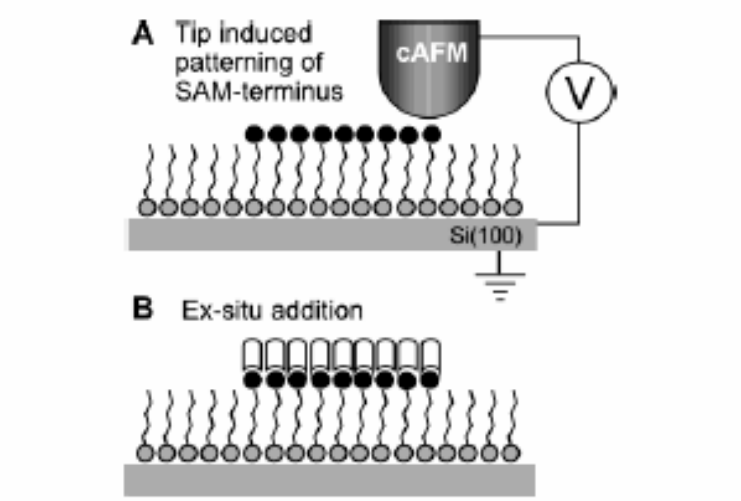

Figure 39. Schematic diagram of substitution lithography through the headgroup modification under an applied bias: (A) conductive AFM tip scanned under an applied bias voltage across a SAM and modified the headgroup without changing the structural integrity of the SAM; (B) altered functionality used for the subsequent binding of a second self-assembly molecule.

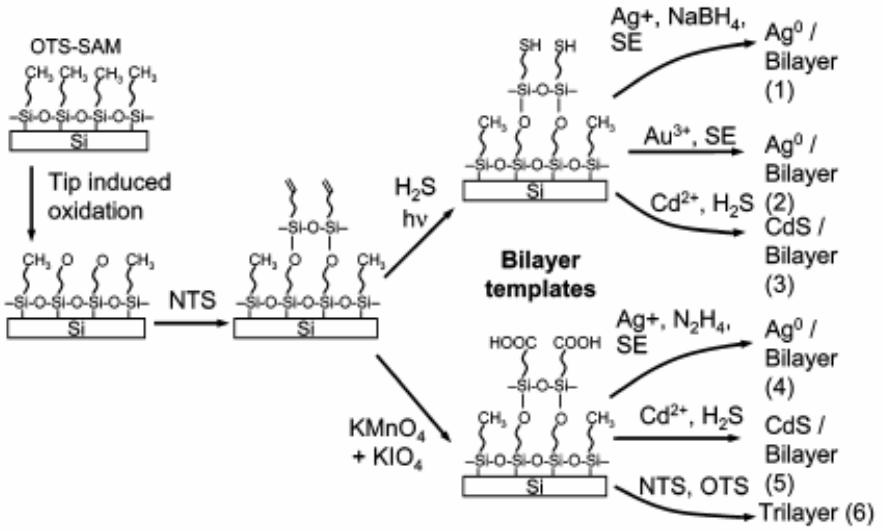

Dip-Pen Lithography

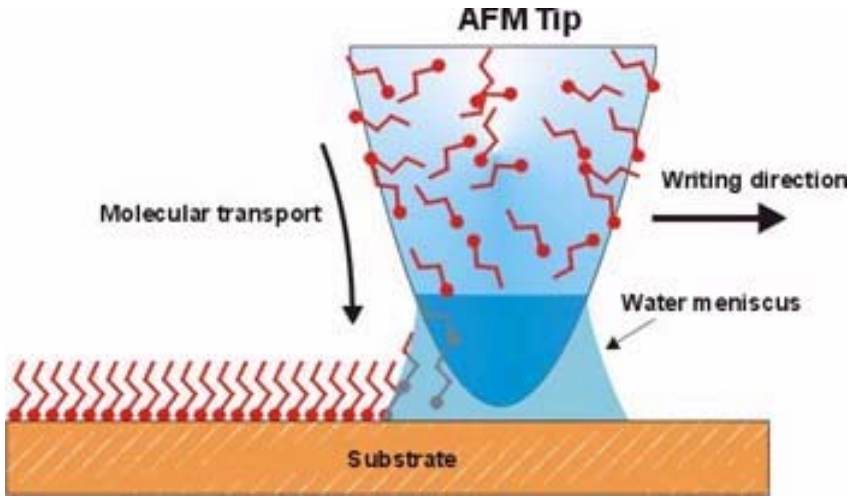

Conducting Polymers

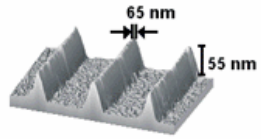

Silicon Nanostructures

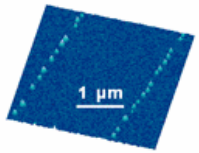

Single Nanoparticle Lines

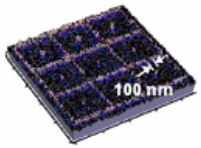

Protein Nanoarrays

Dip-Pen Nanolithograpy

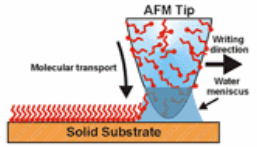

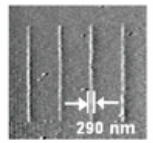

Sol Gel Templates

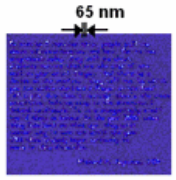

Small Organic Molecules

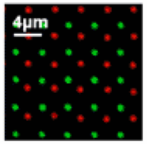

Ultrahigh Density DNA Arrays

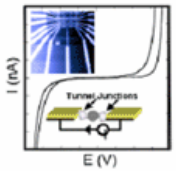

Single Particle Devices

"Dip-Pen" Nanolithography

Richard D. Piner, Jin Zhu, Feng Xu, Seunghun Hong,
Chad A. Mirkin*

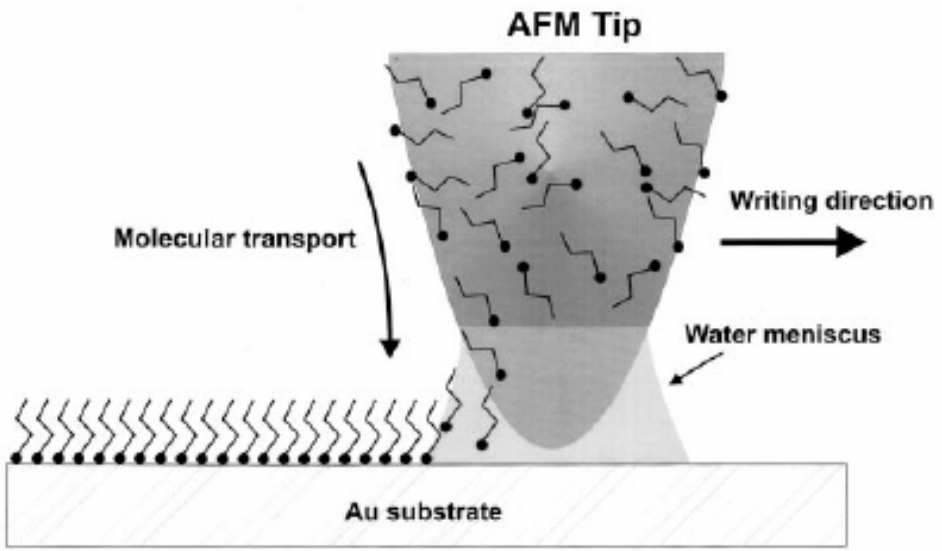

Fig. 1. Schematic representation of DPN. A water meniscus forms between the AFM tip coated with ODT and the Au substrate. The size of the meniscus, which is controlled by relative humidity, affects the ODT transport rate, the effective tip-substrate contact area, and DPN resolution.

SCIENCE VOL 283 29 JANUARY 1999

Dip-Pen Lithography

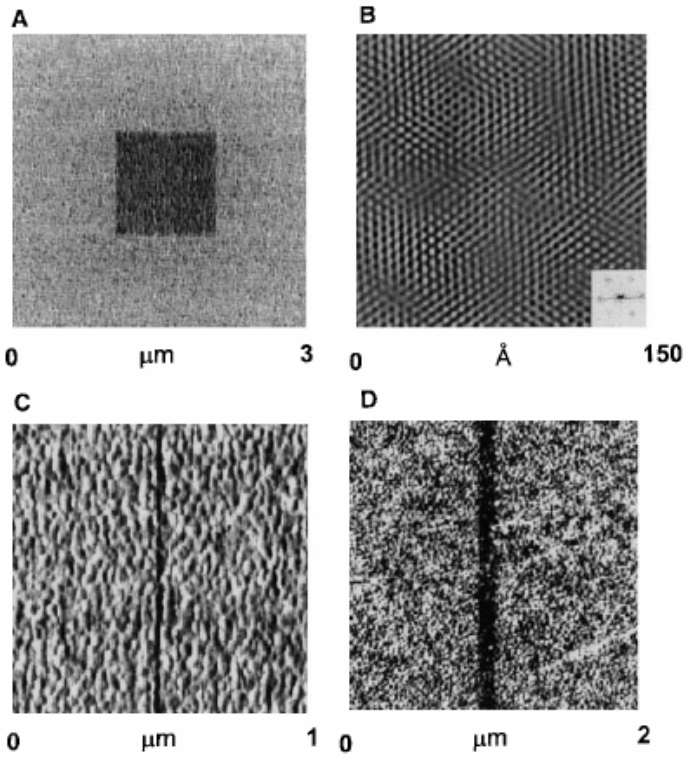

Fig. 2. (A) Lateral force image of a square of ODT measuring 1 µm by 1 µm, deposited onto a Au substrate by DPN. This pattern was generated by scanning the 1-μm^2 area at a scan rate of 1 Hz for a period of 10 min at a relative humidity of 39%. Then the scan size was increased to 3 µm, and the scan rate was increased to 4 Hz while the image was recorded. The faster scan rate prevents ODT transport. (B) Lattice-resolved, lateral force image of an ODT SAM deposited onto Au(111)/mica by DPN. The image has been filtered with a fast Fourier transform (FFT), and the FFT of the raw data is shown in the lower right insert. The monolayer was generated by scanning a 1000 Å square area of the Au(111)/mica five times at a rate of 9 Hz at 39% relative humidity. (C) Lateral force image of a 30-nm-wide line (3 µm long) deposited onto Au/mica by DPN. The line was generated by scanning the tip in a vertical line repeatedly for 5 min at a scan rate of 1 Hz. (D) Lateral force image of a 100-nm line deposited on Au by DPN. The method of depositing this line is analogous to that used to generate the image in (C), but the writing time was 1.5 min. In all images, darker regions correspond to areas of relatively lower friction.

Dip-Pen Lithography

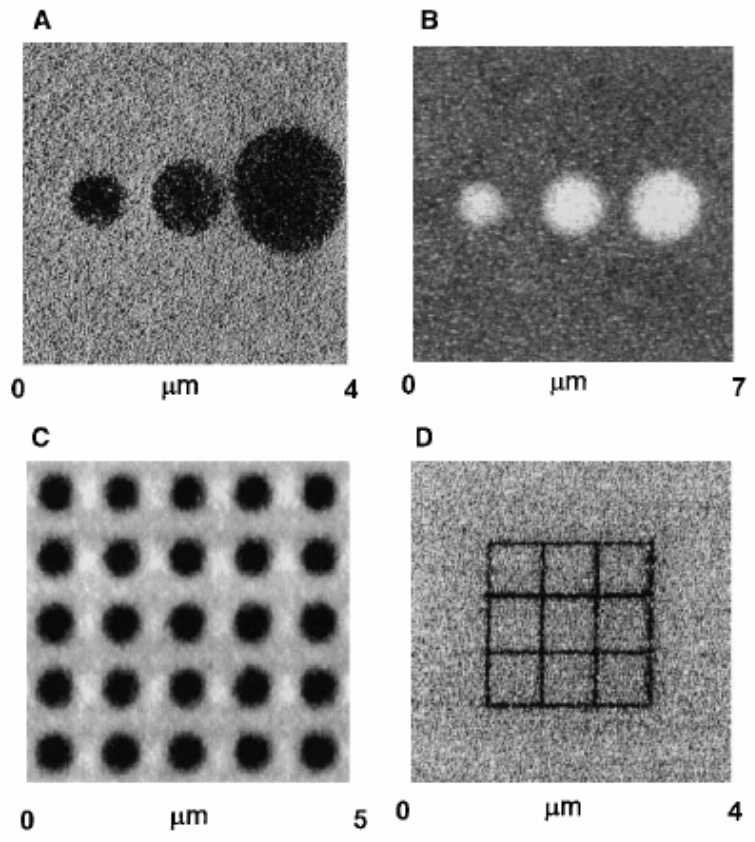

Fig. 3. (A) Lateral force image of an Au substrate after an AFM tip, which was coated with ODT, had been in contact with the substrate for 2, 4, and 16 min (left to right); the relative humidity was held constant at 45%, and the image was recorded at a scan rate of 4 Hz. (B) Lateral force image of dots of 16-mercaptohexadecanoic acid on a Au substrate. To generate the dots, an AFM tip coated with 16-mercaptohexadecanoic acid was held on the Au substrate for 10, 20, and 40 s (left to right). The relative humidity was 35%. The images show that the transport properties of 16-mercaptohexadecanoic acid and of ODT differ substantially. (C) Lateral force image of an array of dots generated by DPN. Each dot was generated by holding an ODT-coated tip in contact with the surface for ~20 s. Writing and recording conditions were the same as in (A). (D) Lateral force image of a molecule-based grid. Each line is 100 nm in width and 2 μm in length and required 1.5 min to write.

Dip-pen Lithography

SCIENCE VOL 288 9 JUNE 2000

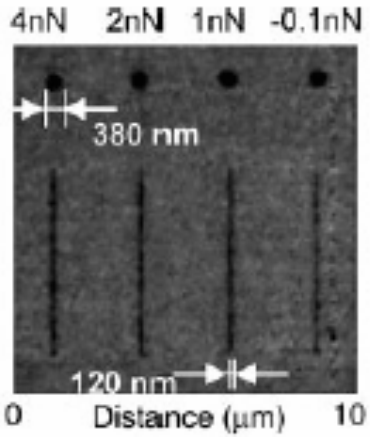

Fig. 1. Lateral force microscopy (LFM) images of ODT monolayer nanodot and line features on gold generated by the same tip but under different tip-substrate contact forces. Feature sizes vary less than 10%.

Fig. 4. LFM images of eight identical patterns generated with one imaging tip and eight writing tips coated with ODT molecules.

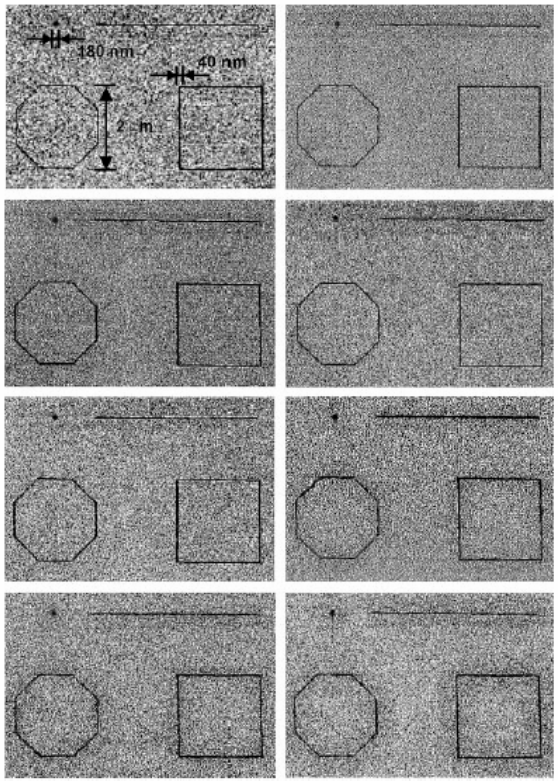

Protein Nanoarrays Generated By Dip-Pen Nanolithography

Ki-Bum Lee,[1] So-Jung Park,[1] Chad A. Mirkin,[1]* Jennifer C. Smith,[2] Milan Mrksich[2]*

1 MARCH 2002 VOL 295 SCIENCE

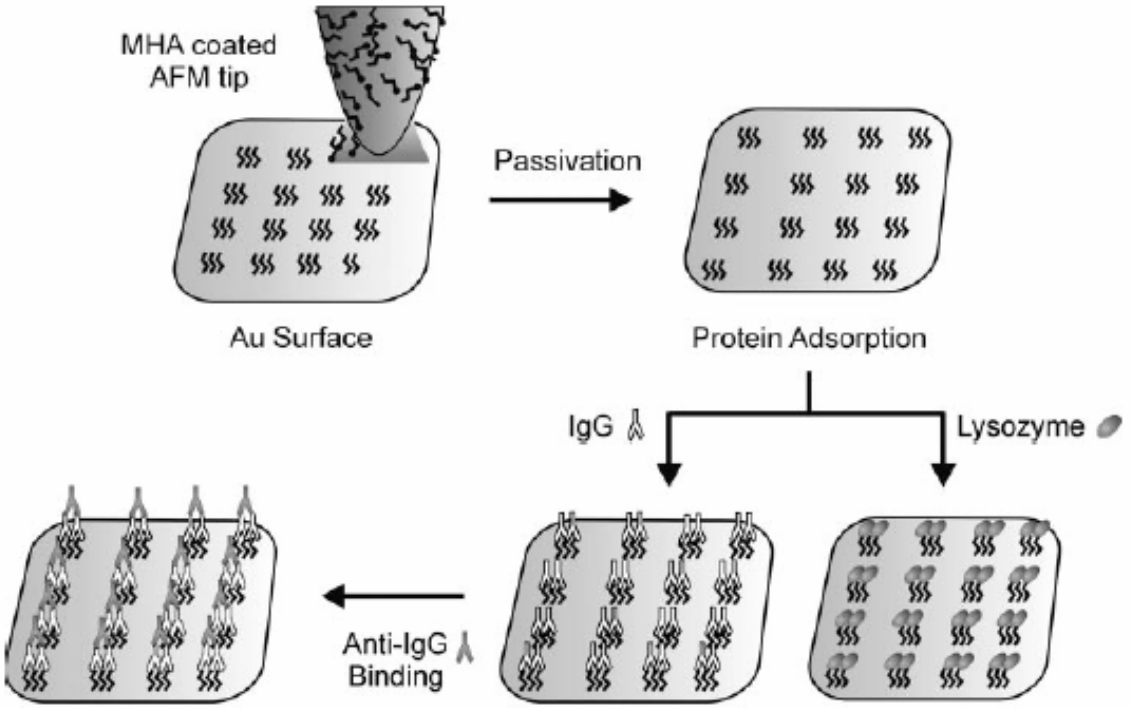

Fig. 2. Diagram of proof-of-concept experiments, in which proteins were absorbed on preformed MHA patterns. The resulting protein arrays were then characterized by AFM.

Protein Nanoarrays Generated By Dip-Pen Nanolithography

Ki-Bum Lee,[1] So-Jung Park,[1] Chad A. Mirkin,[1]* Jennifer C. Smith,[2] Milan Mrksich[2]*

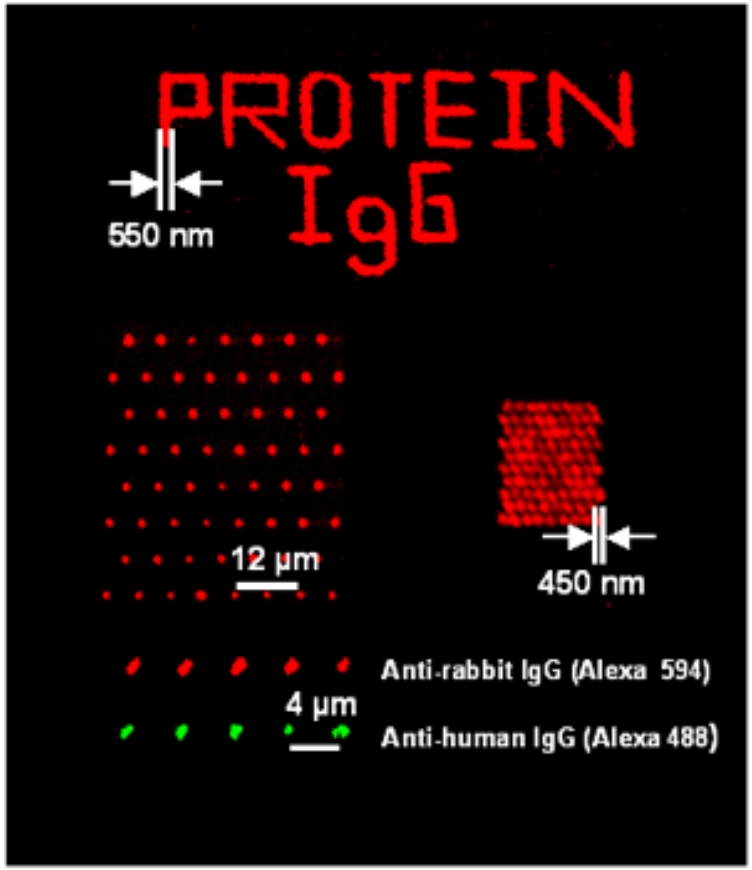

Protein Nanoarrays Generated By Dip-Pen Nanolithography

Ki-Bum Lee,[1] So-Jung Park,[1] Chad A. Mirkin,[1]* Jennifer C. Smith,[2] Milan Mrksich[2]*

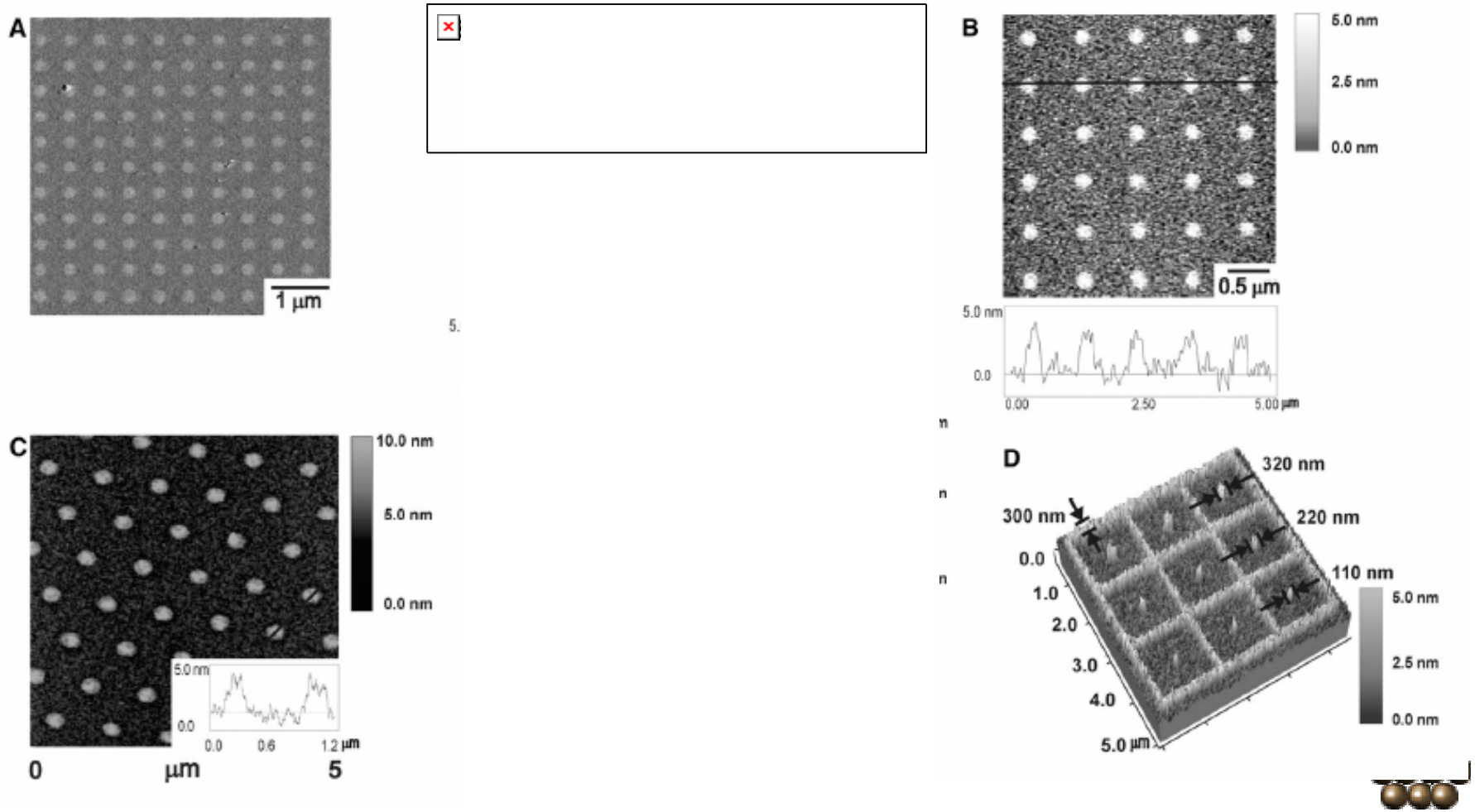

Protein Nanoarrays Generated By Dip-Pen Nanolithography

Ki-Bum Lee,[1] So-Jung Park,[1] Chad A. Mirkin,[1]* Jennifer C. Smith,[2] Milan Mrksich[2]*

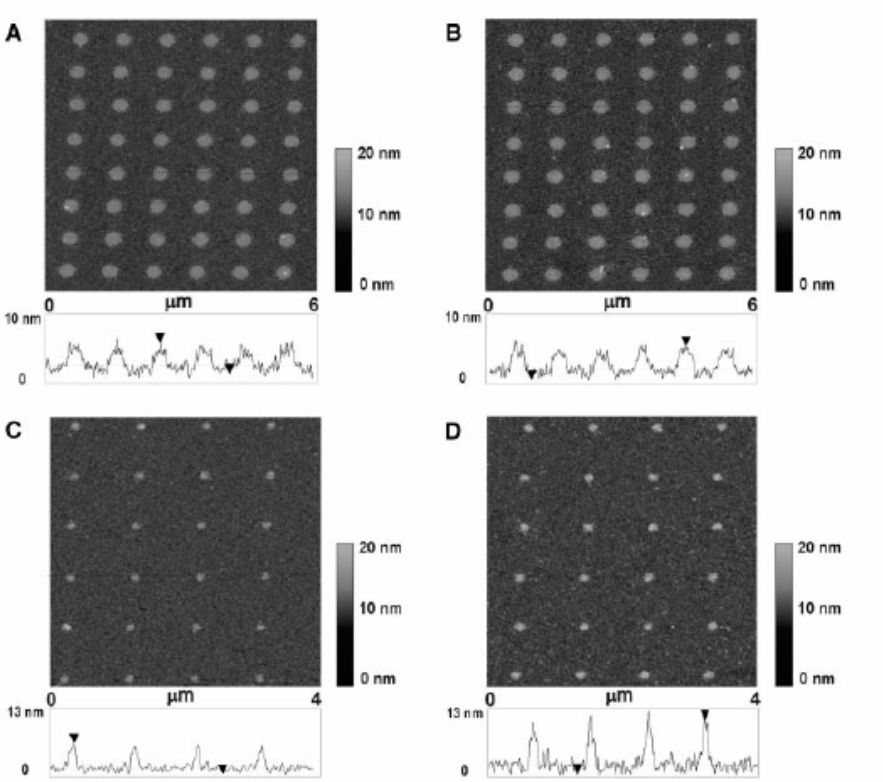

Fig. 3. AFM tapping mode image and height profile of rabbit IgG assembled onto an MHA dot array generated by DPN before (**A**) and after (**B**) exposure to a solution containing lysozyme, Retronectin, goat/sheep anti-IgG, and human anti-IgG. An IgG nanoarray before (**C**) and after (**D**) treatment with a solution containing lysozyme, goat/sheep anti-IgG, human anti-IgG, and rabbit anti-IgG. All images were taken at a 0.5-Hz scan rate in tapping mode.

Protein Nanoarrays Generated By Dip-Pen Nanolithography

Ki-Bum Lee,[1] So-Jung Park,[1] Chad A. Mirkin,[1]* Jennifer C. Smith,[2] Milan Mrksich[2]*

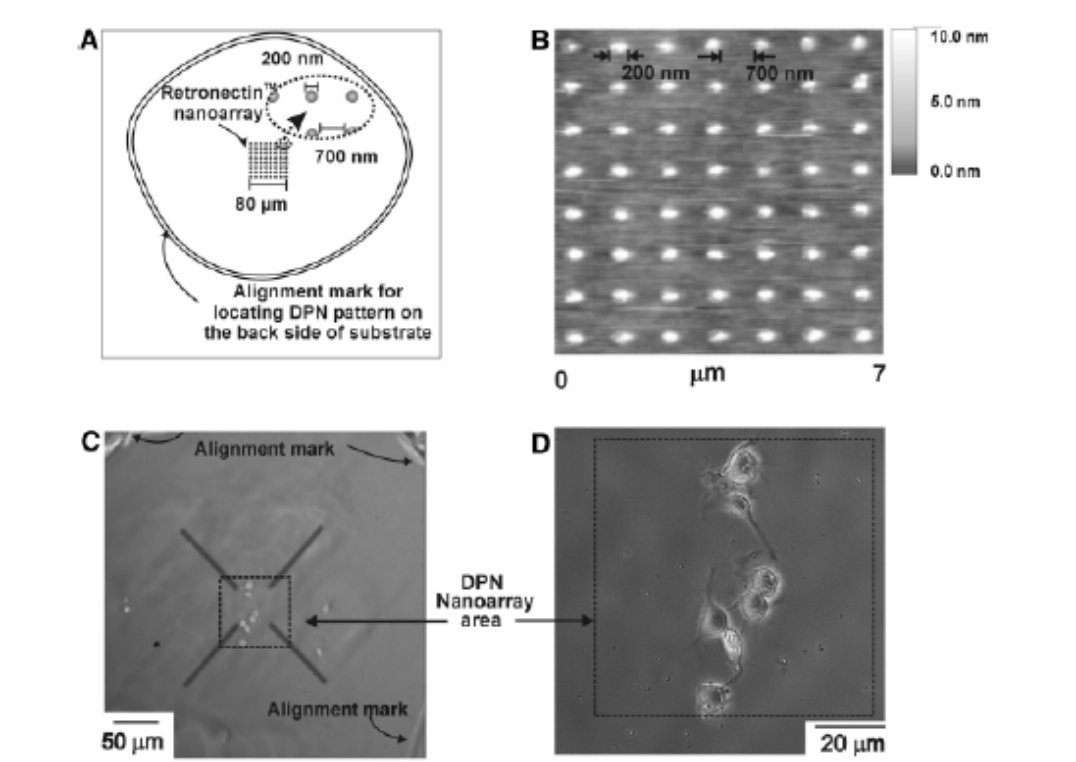

Fig. 4. (A) Diagram describing the cell adhesion experiment on the DPN-generated pattern. The total patterned area is 6400 μm^2. The alignment marks were generated by scratching a circle into the backside of the Au-coated glass substrate. (B) Topography image (contact mode) of the Retronectin protein array. Imaging conditions were the same as in Fig. 1B. (C) Large-scale optical microscope image showing the localization of cells in the nanopatterned area. (D) Higher resolution optical image of the nanopatterned area, showing intact cells.

Dip-Pen Array

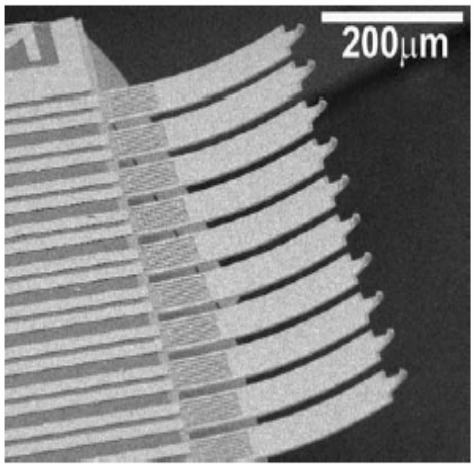

FIG. 2. An array of ten thermally actuated DPN probes showing the power lead and heater layout. Each probe is 300 μm long, 80 μm wide, and 1.3 μm thick.

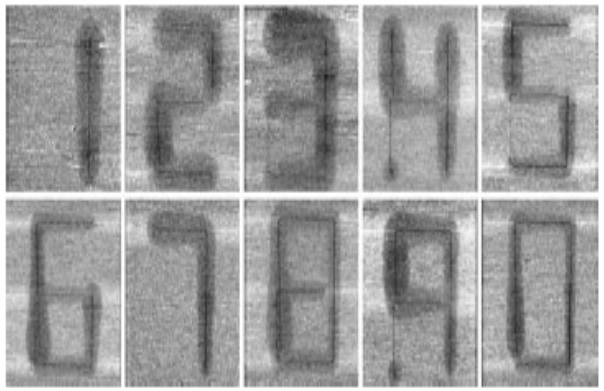

FIG. 4. LFM scans, 8 μm square, of ten simultaneously generated ODT patters on a gold surface. Each numeral is 6 μm tall, 4 μm wide, and was written at 1 μm/s.

Ultimate STM Lithography

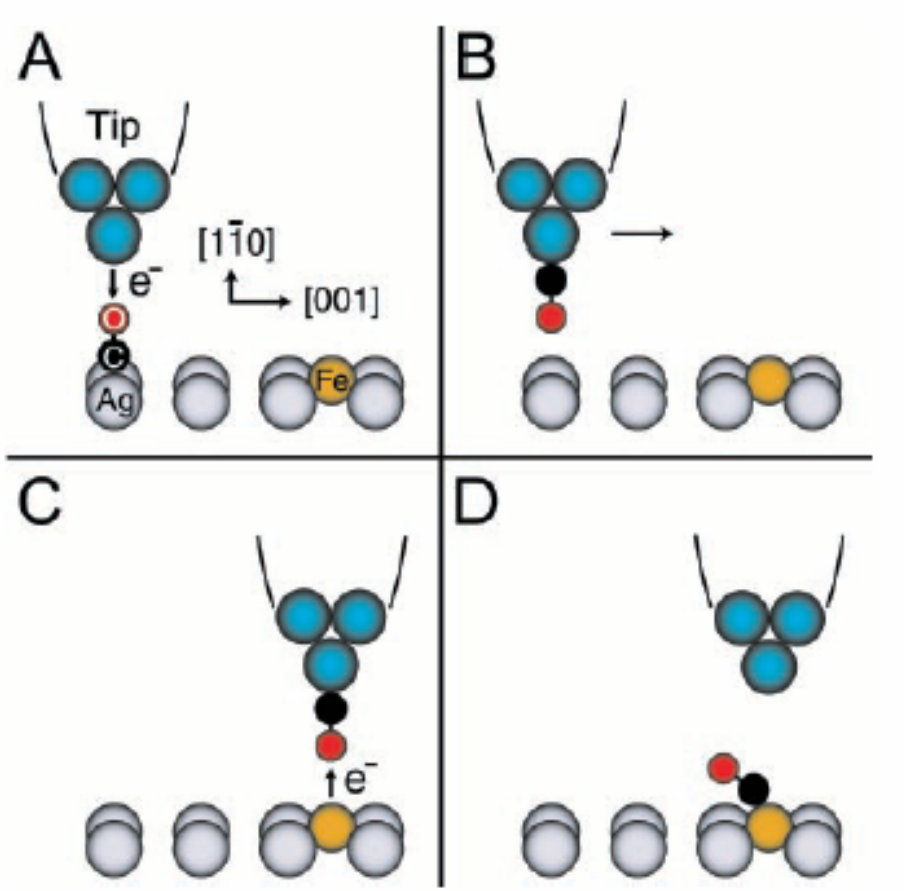

Single Atomic Manipulation

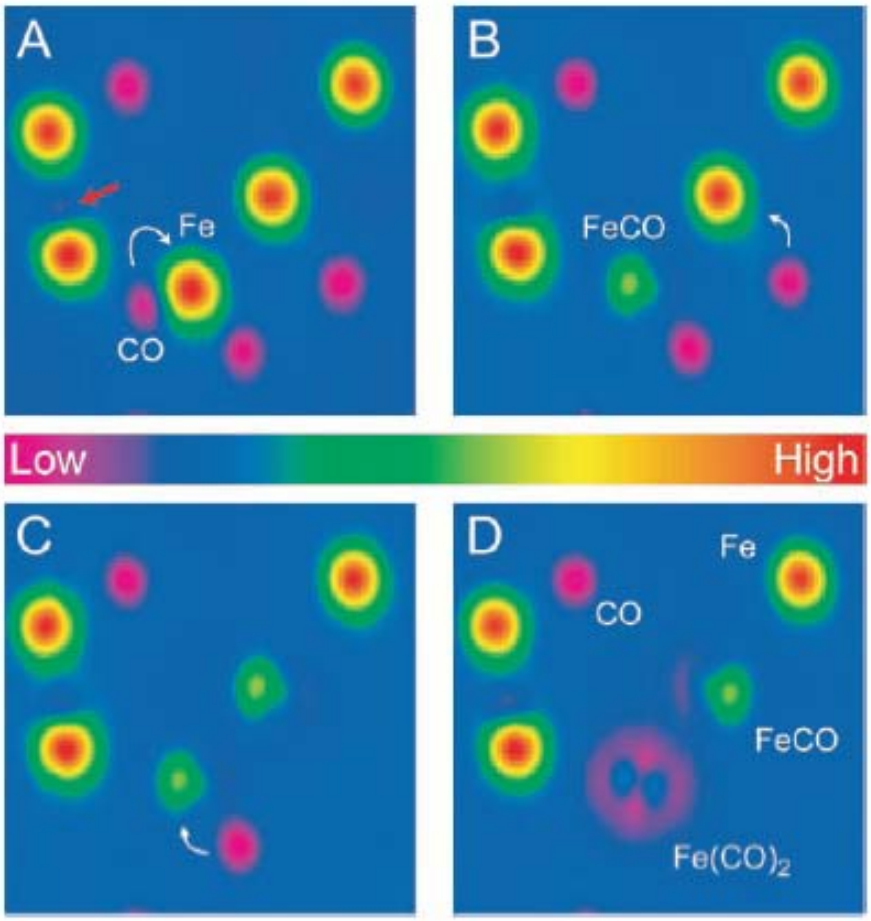

Single Molecular Vibrational Spectra by STM

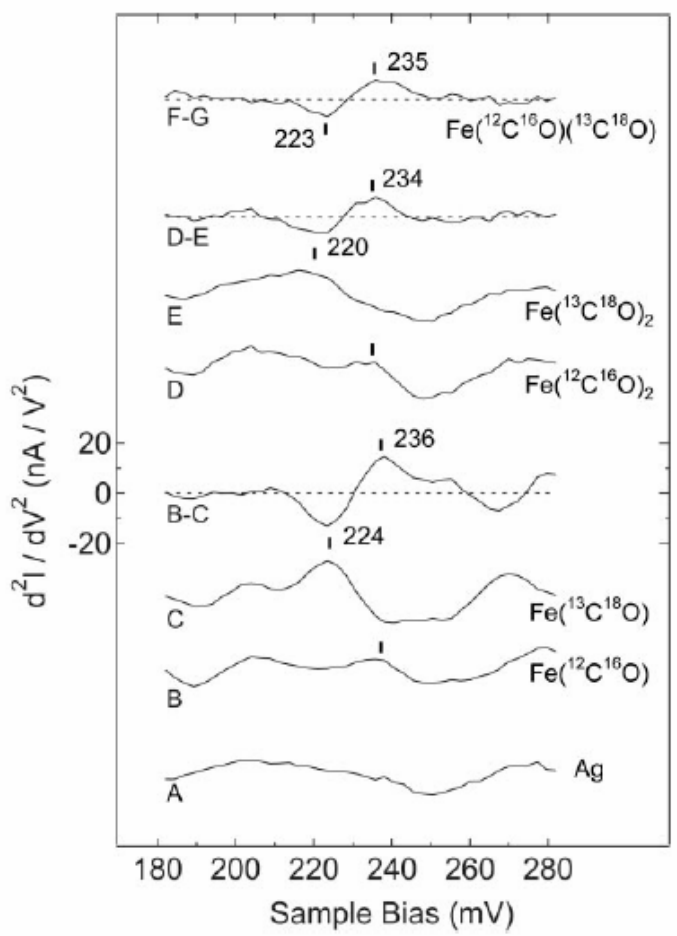

Building Molecule Step by Step

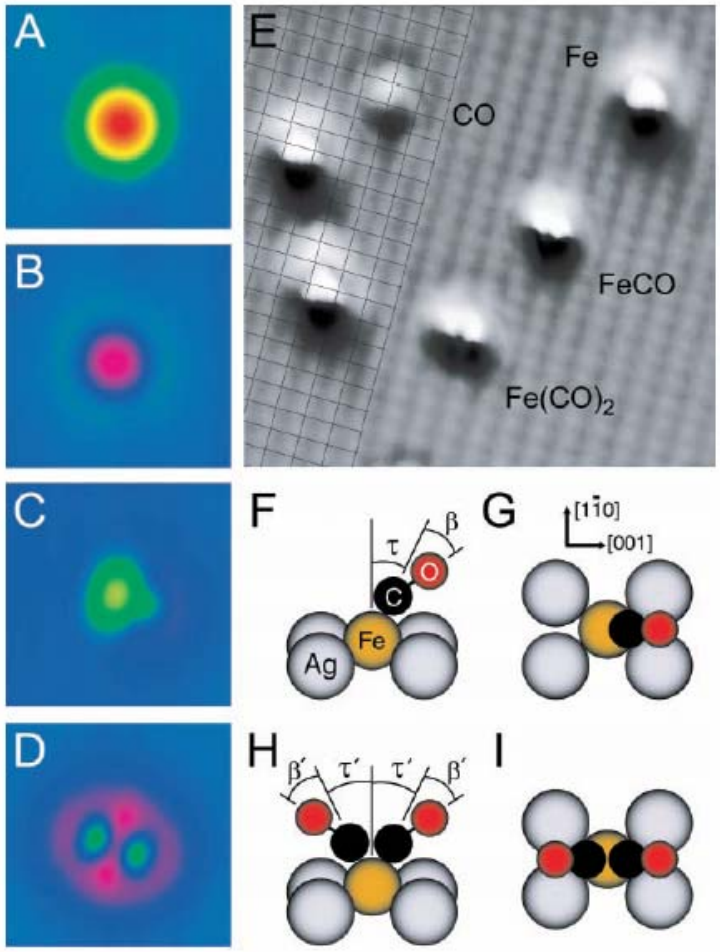

Atomic Manipulation

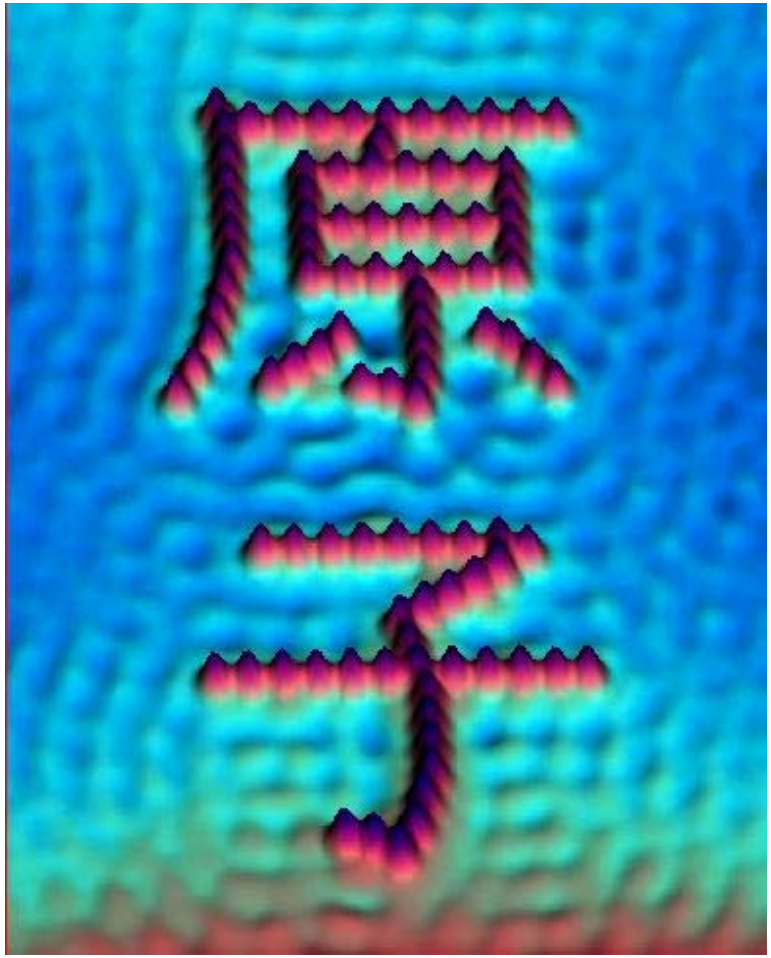

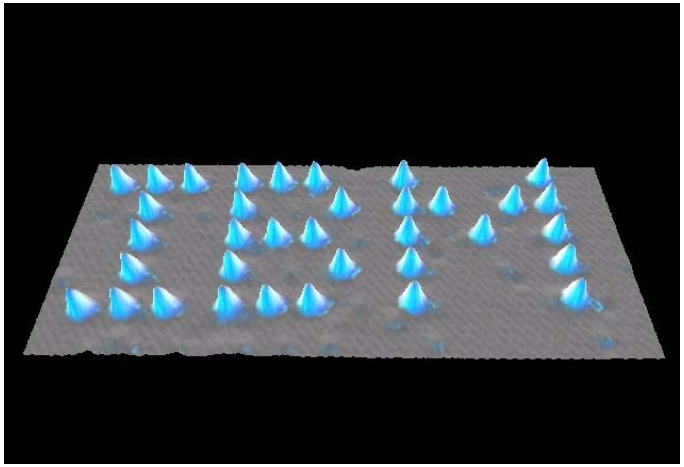

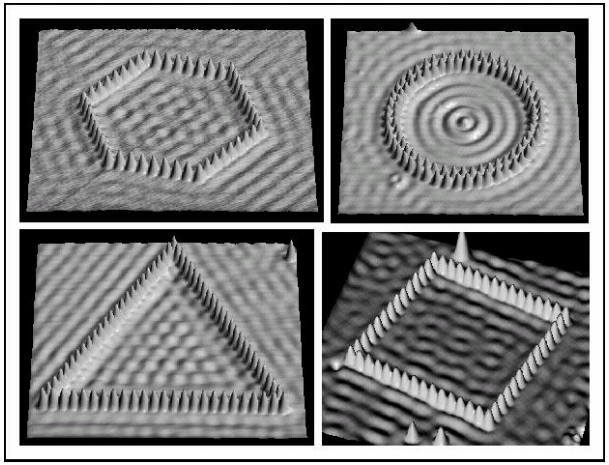

Near-Field Microscope

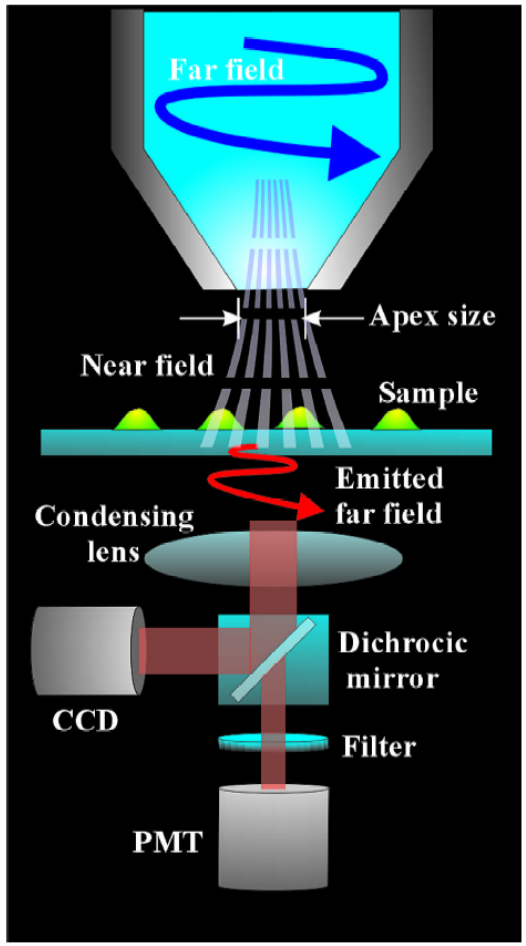

Near-Field Images

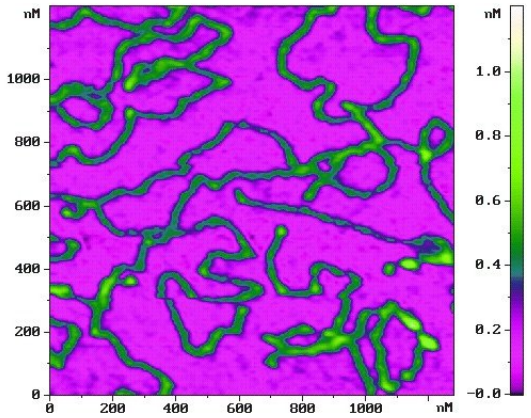

DNA

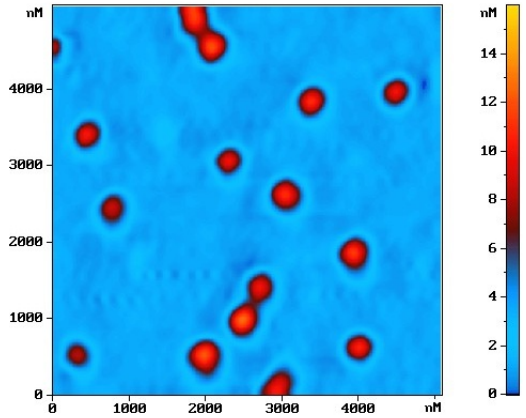

Nanosphere

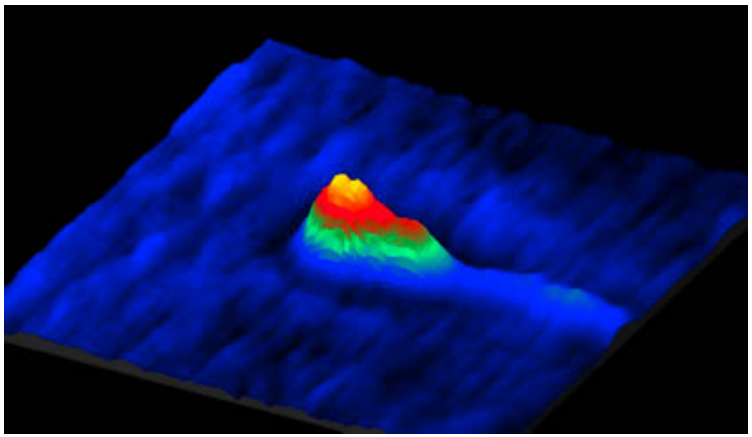

Sperm

Near-Field Lithography

Figure 2. TappingMode image of a lithography test pattern. The Aurora-3 used nanolithography software to write into S1805 photoresist. 25μm scan.

Add on Writing

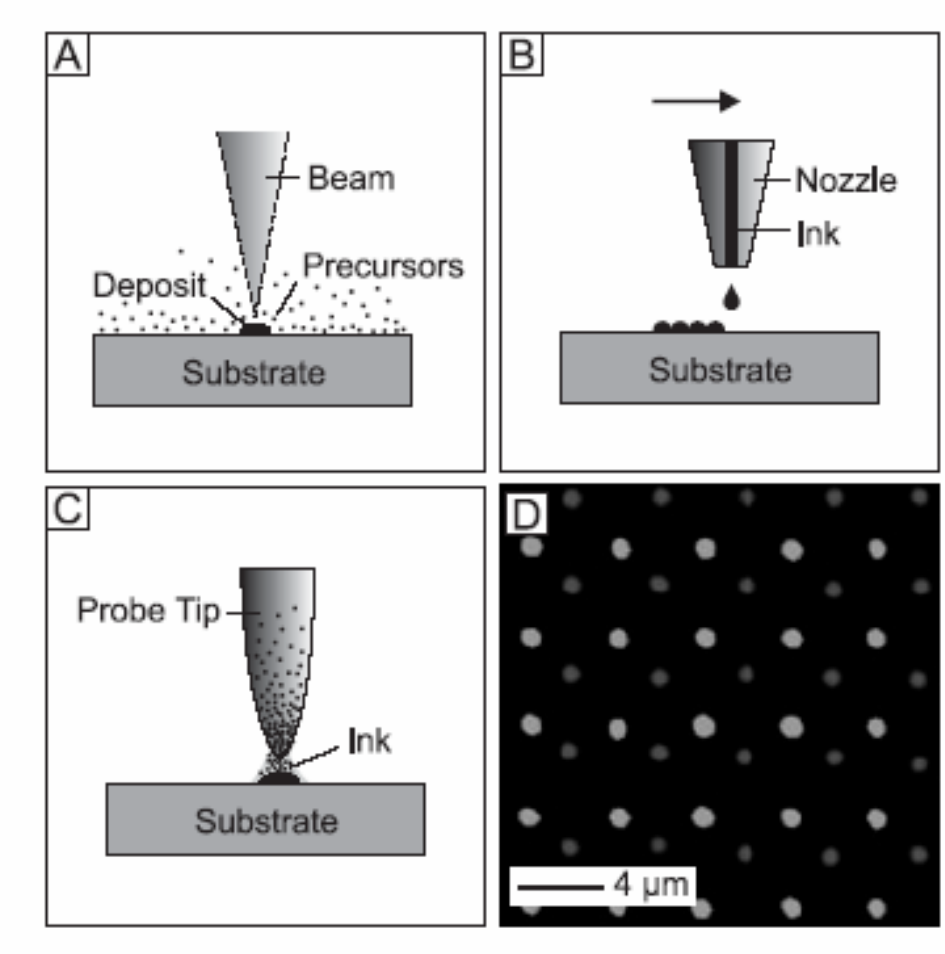

Direct Writing 3D

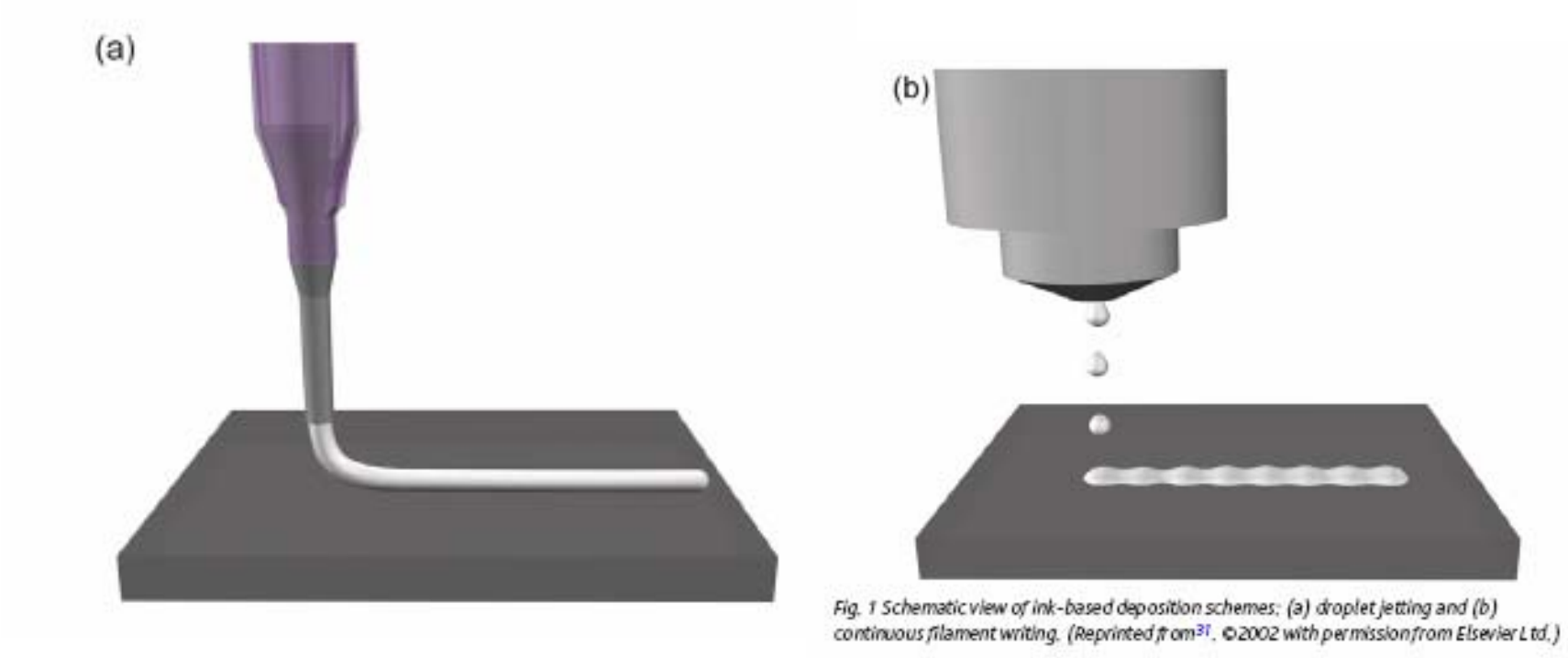

Fig. 1 Schematic view of ink-based deposition schemes: (a) droplet jetting and (b) continuous filament writing. (Reprinted from[31]. ©2002 with permission from Elsevier Ltd.)

Direct Writing

Table 1 *Capabilities of ink-writing techniques.*

Technique	Ink design	Minimum printed feature size	3-D periodic structures
Robotic Deposition[11]	Concentrated colloidal gel[13,14]	200 μm diameter	Yes
"	Concentrated nanoparticle gel[15]	100 μm diameter	Yes
"	Viscous polymer solution[16-18]	200 μm diameter	Yes
"	Concentrated polyelectrolyte complexes[3]	<1 μm	Yes
Three-dimensional printing[19]	Binder solution printed on powder bed	170 μm lateral, 45 μm depth	Yes
Ink-jet printing[20]	Dilute fluid[21]	20 μm lateral, 100 nm height	No
"	Concentrated fluid (max. solids ~40%)[22-25]	70 μm lateral, < 1 μm height	No
Fused deposition	Thermoplastic polymer melt[26]	100 μm diameter	Yes
"	Particle-filled polymer melt[27] (max. solids ~50%)	100 μm diameter	Yes
Micropen writing[28]	Concentrated, shear-thinning colloidal fluid	25 μm diameter	No
Dip-pen nanolithography[29]	Dilute fluid	20 nm	No
Scanning probe contact printing[30]	Dilute fluid	<500 nm	No

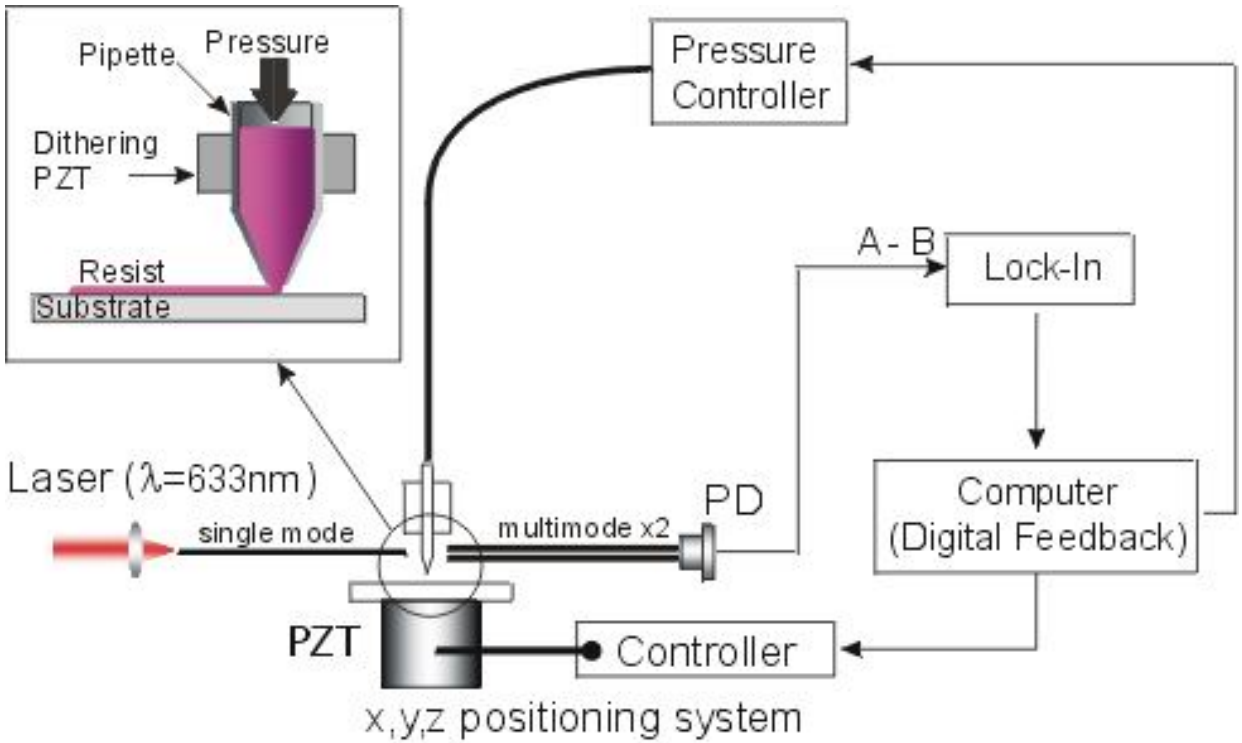
Pipette
Pressure
Dithering
PZT
Resist
Substrate
Pressure
Controller
A - B
Lock-In
Laser (λ=633nm)
single mode
multimode x2
PD
Computer
(Digital Feedback)
PZT
Controller
x,y,z positioning system

Direct Writing

NATURE | VOL 428 | 25 MARCH 2004 |

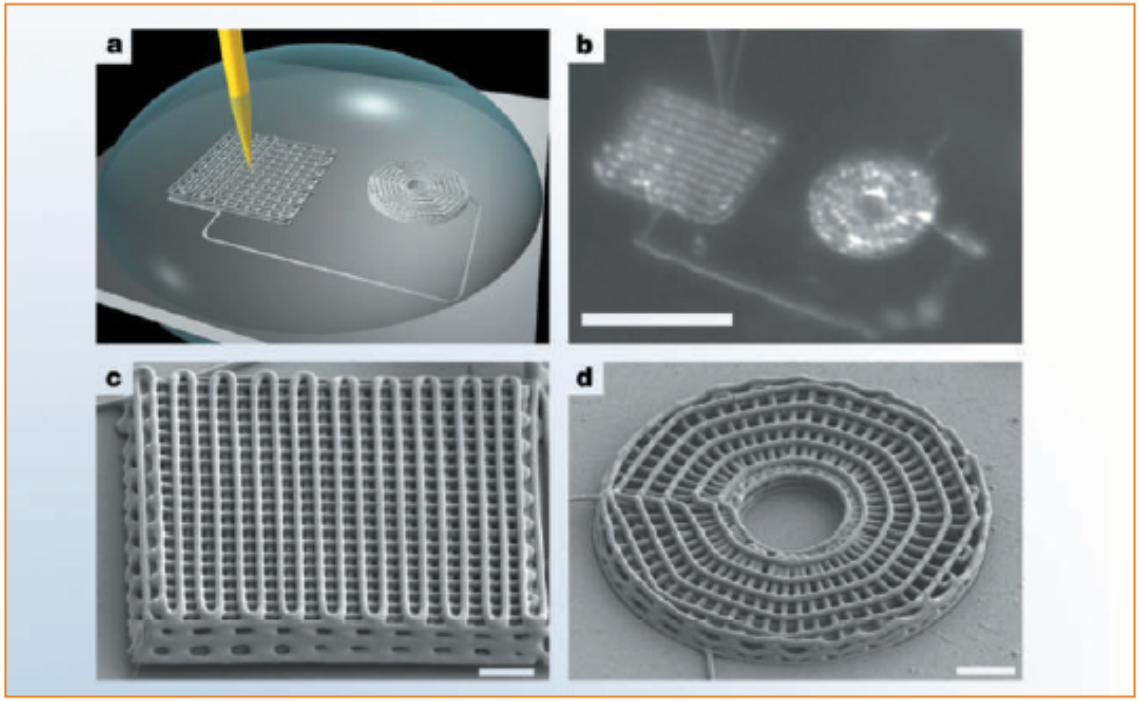

Figure 1 Direct-write assembly of three-dimensional microperiodic structures. **a,** The ink-deposition process (not drawn to scale). A concentrated polyelectrolyte ink is housed in a syringe (yellow) immersed in a coagulation reservoir (grey hemispherical drop) and deposited on to a glass substrate (light grey). **b,** Optical image acquired *in situ* during deposition reveals the features drawn in **a**, including the deposition nozzle that is patterning a three-dimensional lattice, as well as a completed radial array. This image is blurred by the reservoir (scale bar: 100 μm). **c,** Three-dimensional periodic structure with a face-centred tetragonal geometry (filament diameter: 1 μm; 10 layers; scale bar: 10 μm). **d,** Three-dimensional radial array (filament diameter: 1 μm; 5 layers; scale bar: 10 μm).

Inkjet Printer

Figure 1. Microdrop Autodrop Platform (courtesy Microdrop GmbH, Germany).

Inkjet Printing

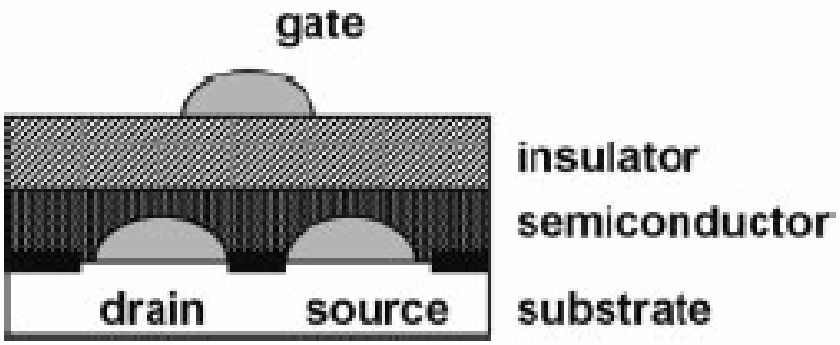

Figure 5. Schematic picture of inkjet printed all-polymer thin film transistor, as constructed by Sirringhaus et al. [41]. Source and drain electrode, consisting of PEDOT/PPS are inkjet printed on a pre-patterned surface. Two spin-coated layers of semiconducting and insulating polymer respectively cover the electrodes. Finally the gate electrode is printed on top.

Inkjet Printing

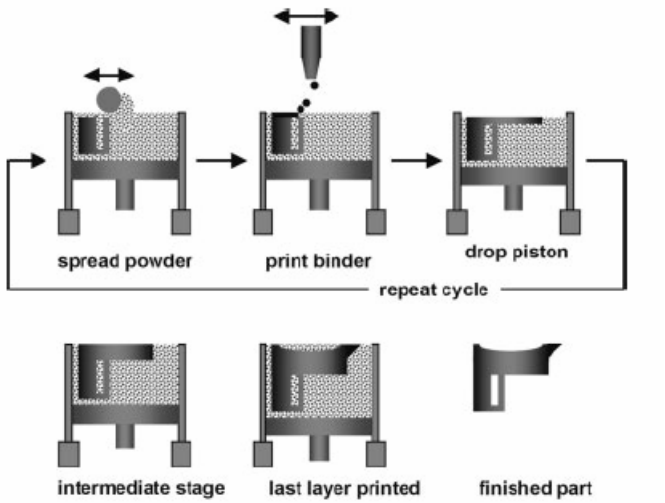

Figure 7. Schematic picture of the three-dimensional printing process.

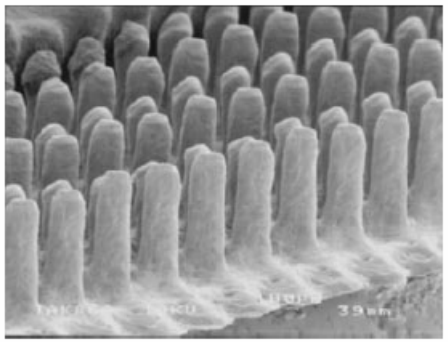

Figure 8. Electron microscopy picture of an array of pillars from lead zirconium titanate, inkjet printed by Bhatti et al. The pillars have an approximate height of 400 μm. (Reprinted from [59] with permission. Copyright 2001 Kluwer Academic Publishers).

Inkjet Printing

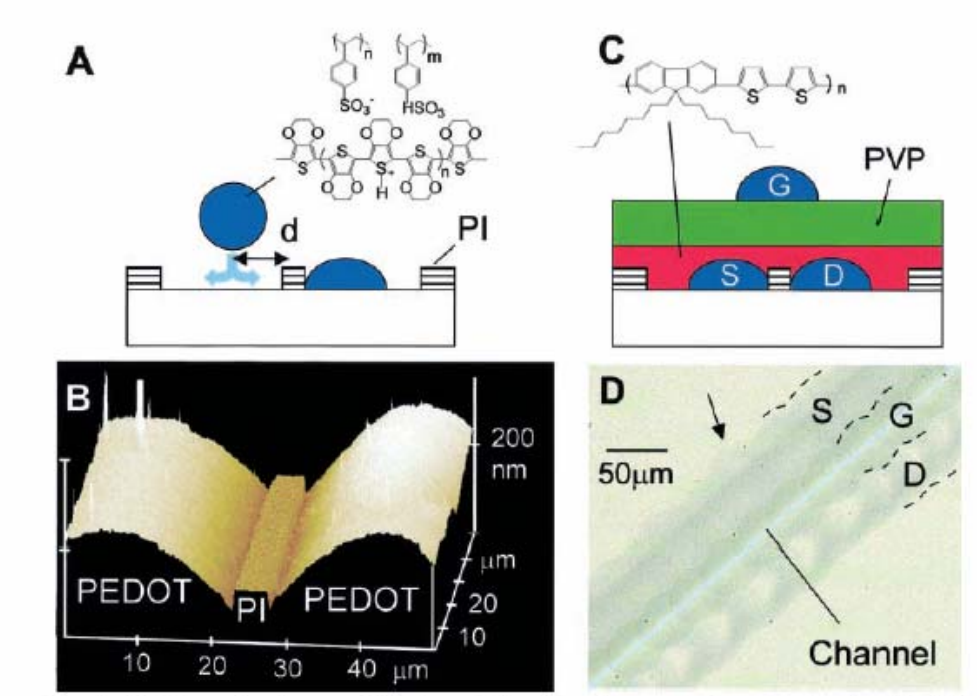

Fig. 1. (**A**) Schematic diagram of high-resolution IJP onto a prepatterned substrate. (**B**) AFM showing accurate alignment of inkjet-printed PEDOT/PSS source and drain electrodes separated by a repelling polyimide (PI) line with $L = 5$ μm. (**C**) Schematic diagram of the top-gate IJP TFT configuration with an F8T2 semiconducting layer (S, source; D, drain; and G, gate). (**D**) Optical micrograph of an IJP TFT ($L = 5$ μm). The image was taken under crossed polarizers so that the TFT channel appears bright blue because of the uniaxial monodomain alignment of the F8T2 polymer on top of rubbed polyimide. Unpolarized background illumination is used to make the contrast in the remaining areas visible, where the F8T2 film is in an isotropic multidomain configuration. The arrow indicates pronounced roughness of the unconfined PEDOT boundary.

Inkjet Printing

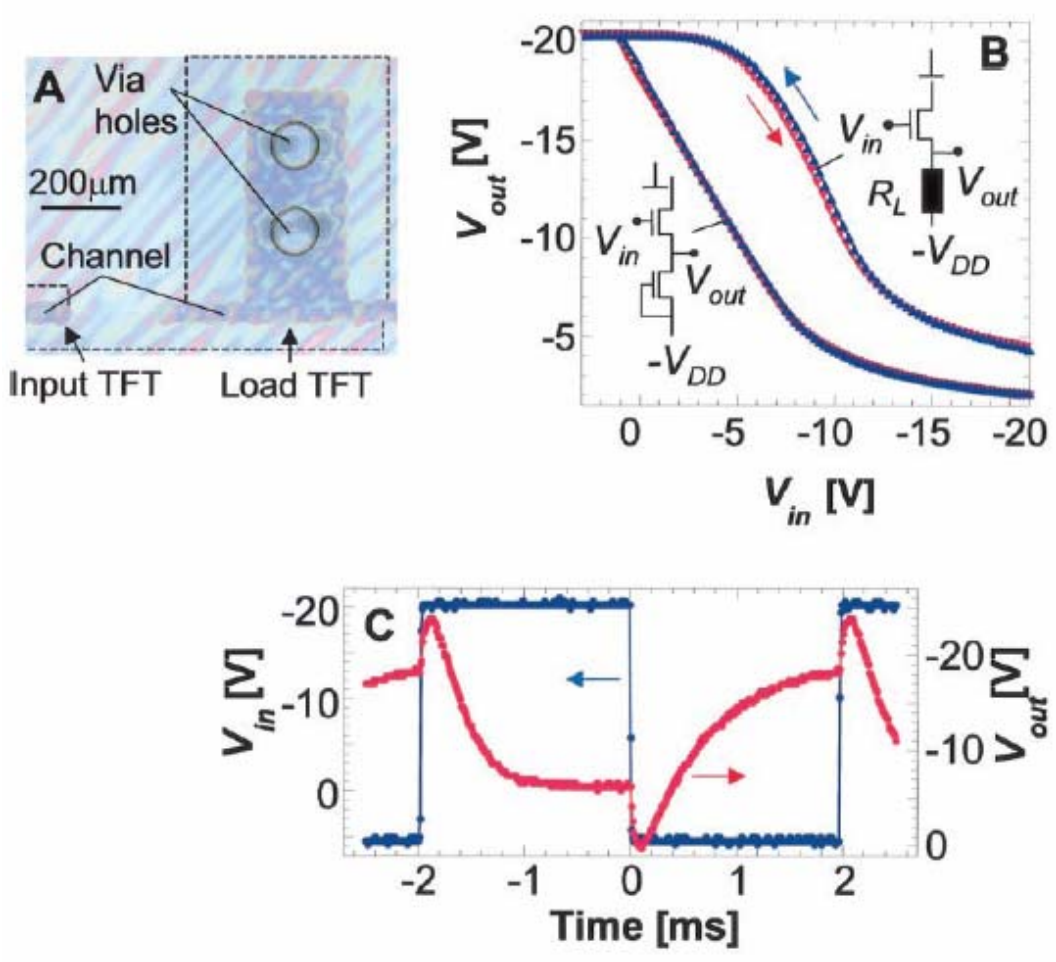

Replication

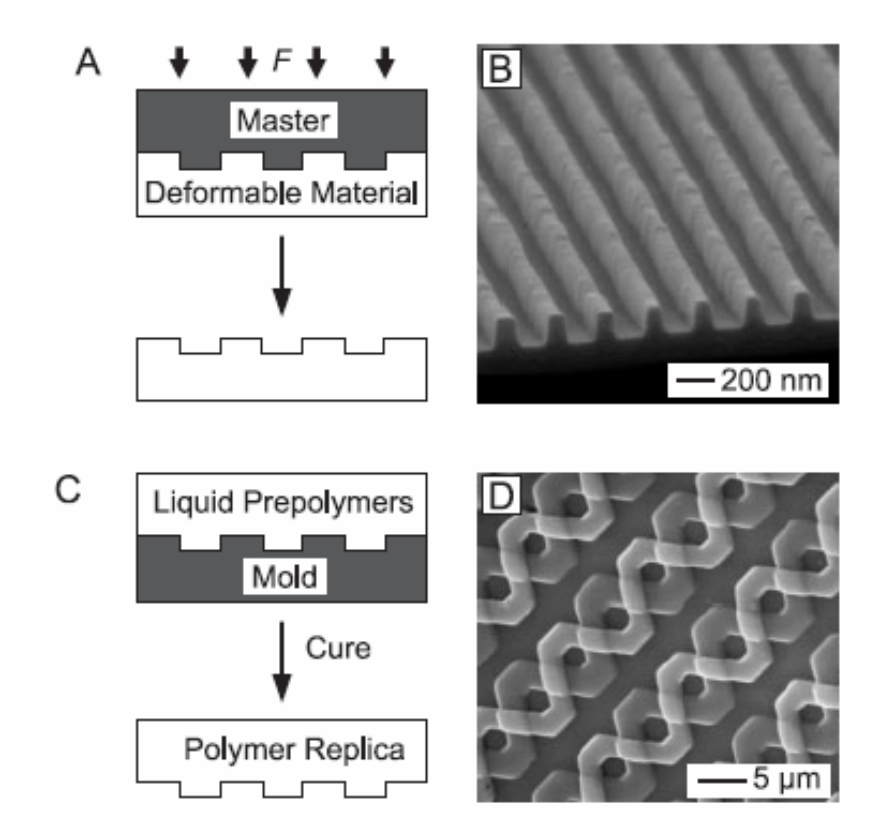

Align the pattern and Exposure

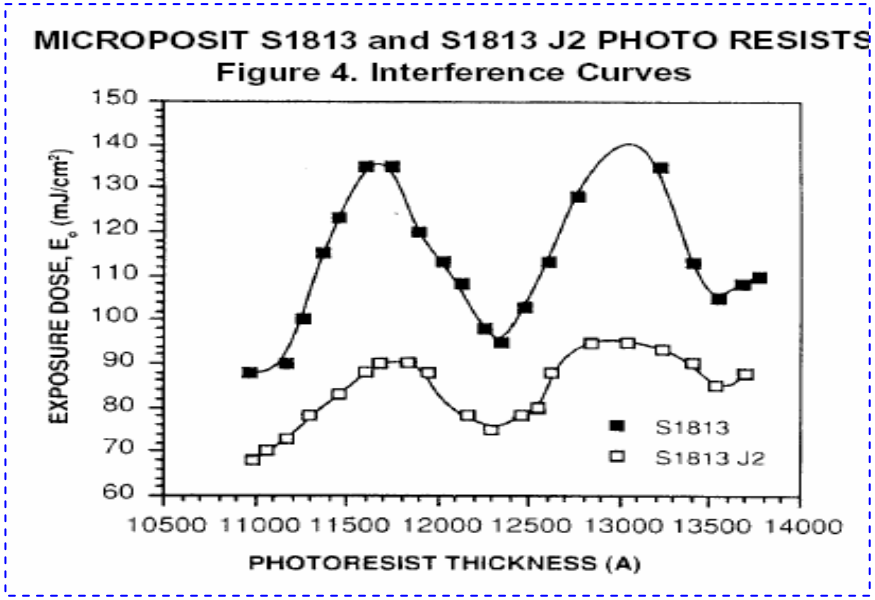

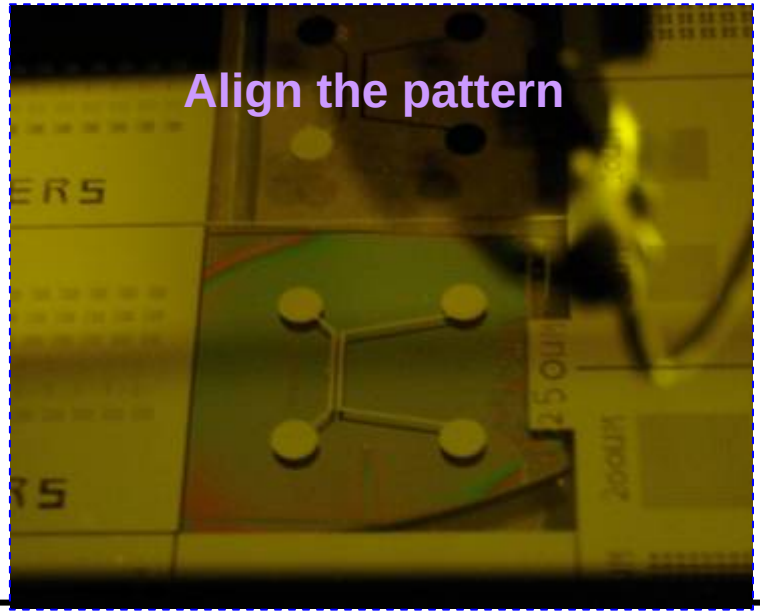

Stepper

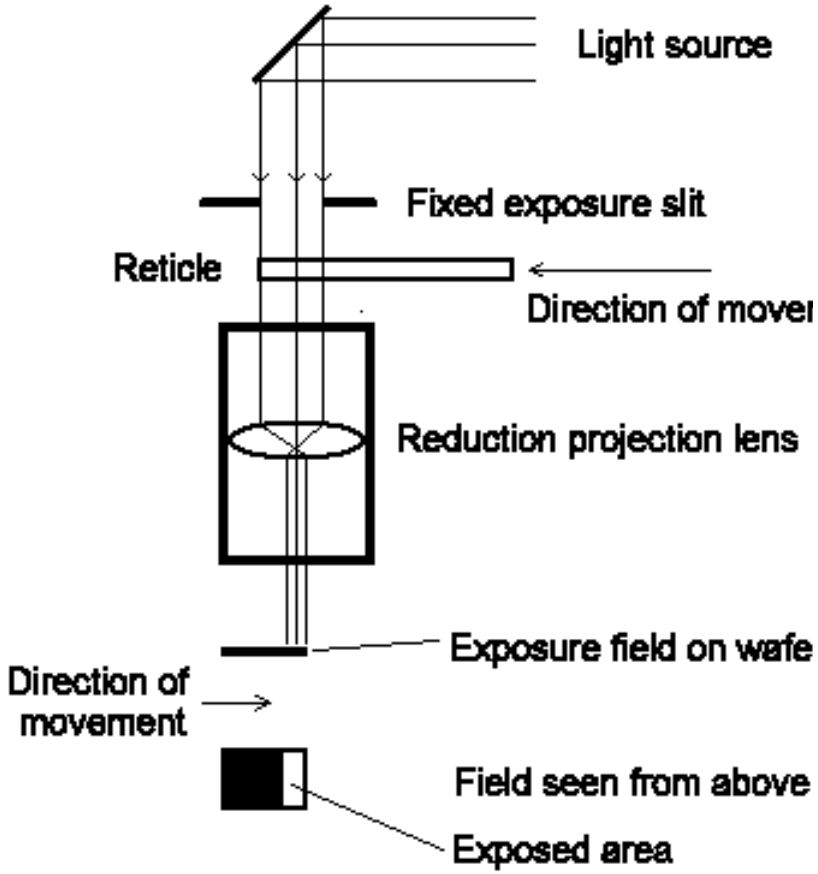
Light source
Fixed exposure slit
Reticle
Direction of move
Reduction projection lens
Exposure field on wafe
Direction of movement
Field seen from above
Exposed area

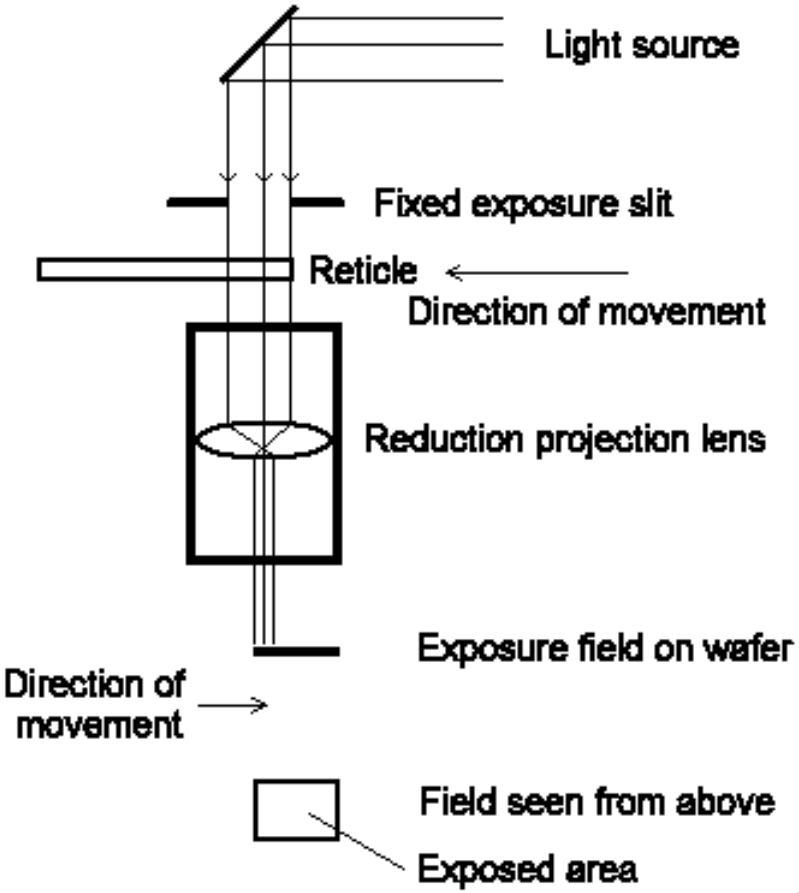
Light source
Fixed exposure slit
Reticle
Direction of movement
Reduction projection lens
Exposure field on wafer
Direction of movement
Field seen from above
Exposed area

E-beam Projection

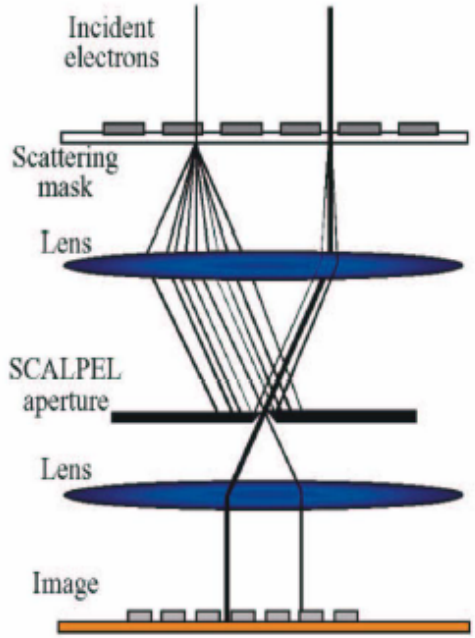

Bell Lab (1999)
There 'was' a consortium including Applied Materials, Inc. and ASM Lithography Holding N.V.; Lucent Technologies Inc.; Motorola, Semiconductor Products Sector; Samsung Electronics Co., Ltd.; and Texas Instruments Incorporated (TI).

Imprint Lithography with 25-Nanometer Resolution

Stephen Y. Chou; Peter R. Krauss; Preston J. Renstrom

Science, New Series, Volume 272, Issue 5258 (Apr. 5, 1996), 85-87.

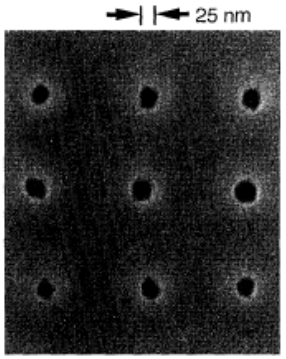

Fig. 2. SEM micrograph of a top view of holes 25 nm in diameter with a period of 120 nm, formed by compression molding into a PMMA film.

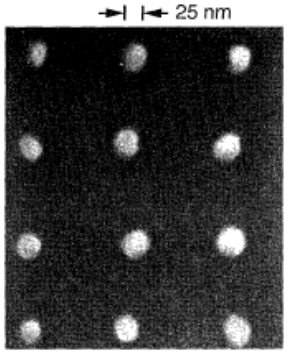

Fig. 5. SEM micrograph of the substrate in Fig. 2, after deposition of metal and a lift-off process. The diameter of the metal dots is 25 nm, the same as that of the original holes created in the PMMA.

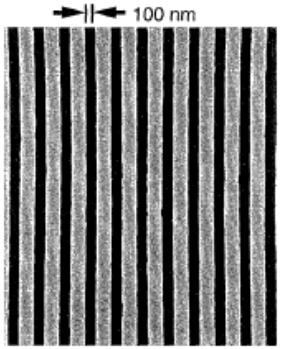

Fig. 3. SEM micrograph of a top view of trenches 100 nm wide with a period of 250 nm, formed by compression molding into a PMMA film.

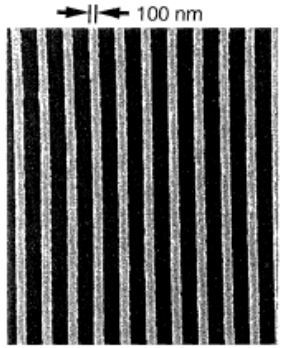

Fig. 6. SEM micrograph of the substrate in Fig. 3, after deposition of metal and a lift-off process. The metal linewidth is 100 nm, the same as the width of the original PMMA trenches.

Nanoimprint Lithography

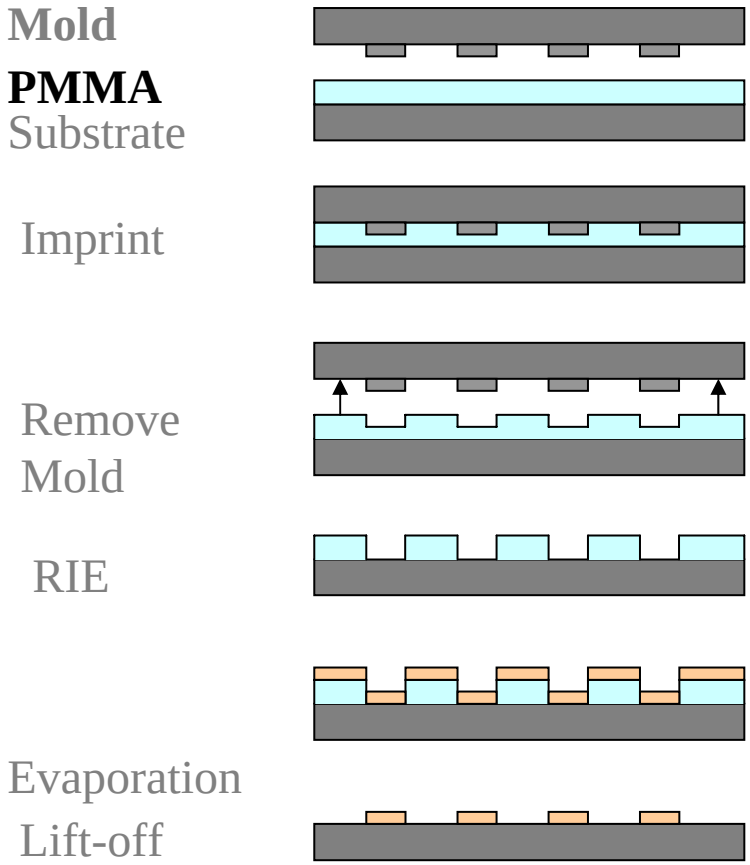

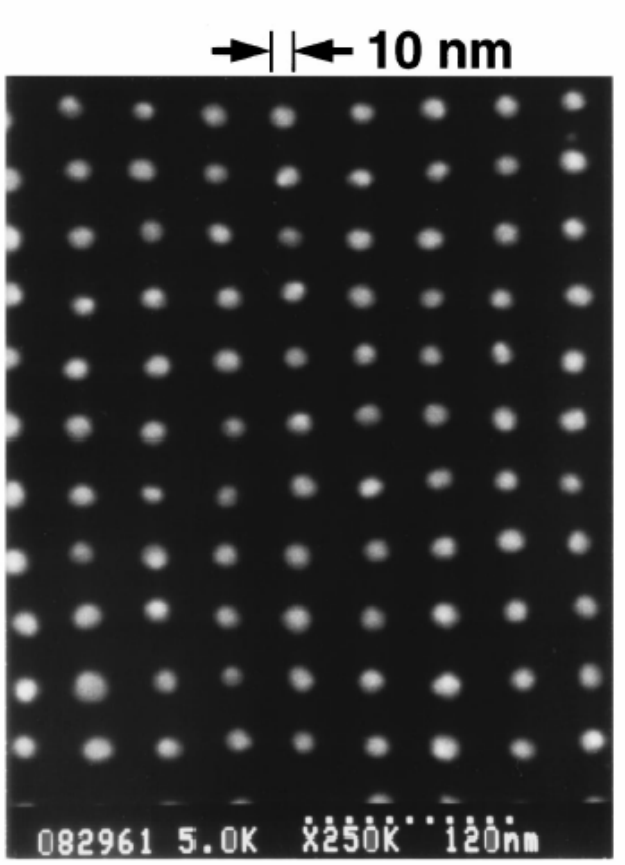

Ultrafast and direct imprint of nanostructures in silicon

NATURE | VOL 417 | 20 JUNE 2002 |

Stephen Y. Chou*, Chris Keimel & Jian Gu

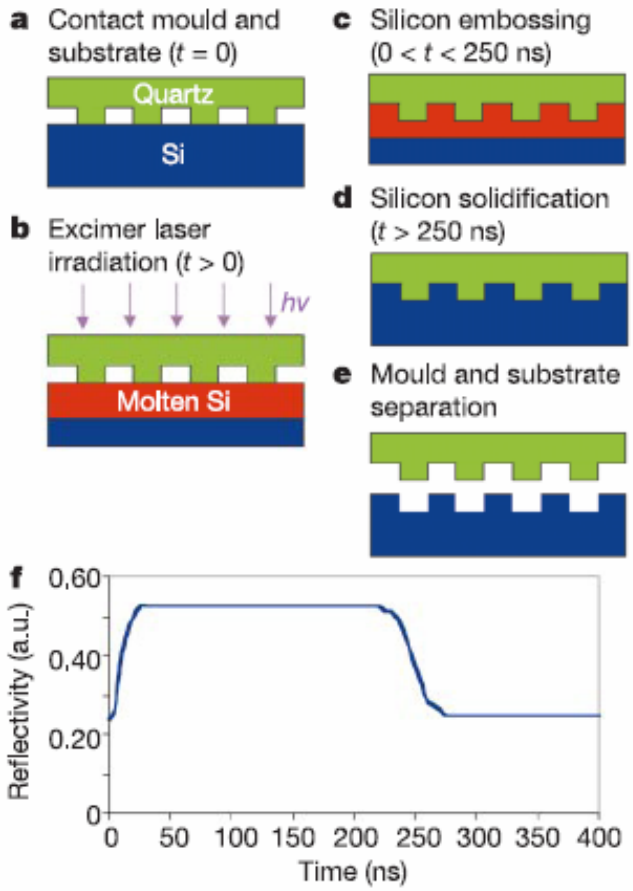

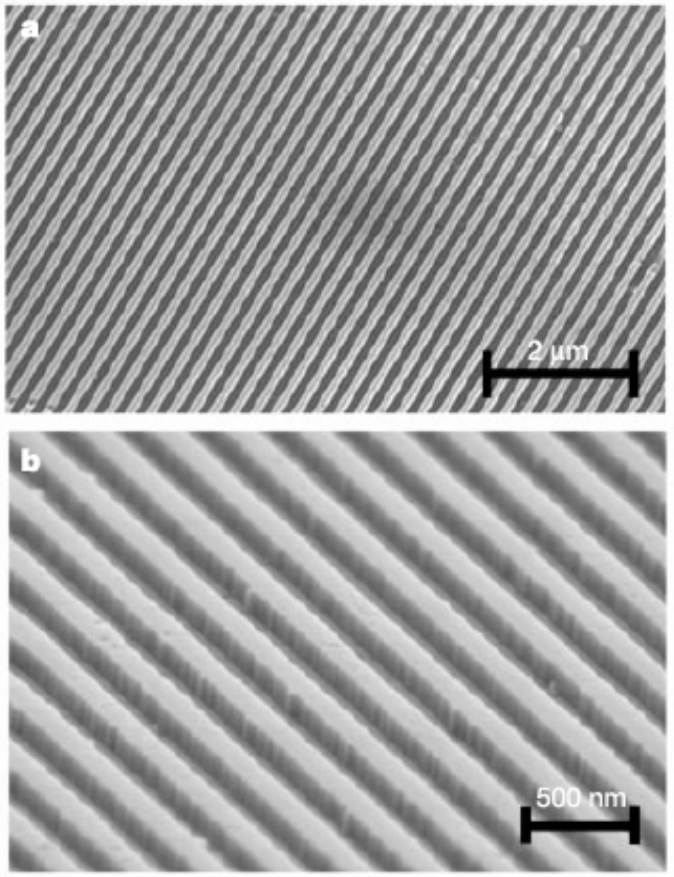

Step and Flash Imprint Lithography

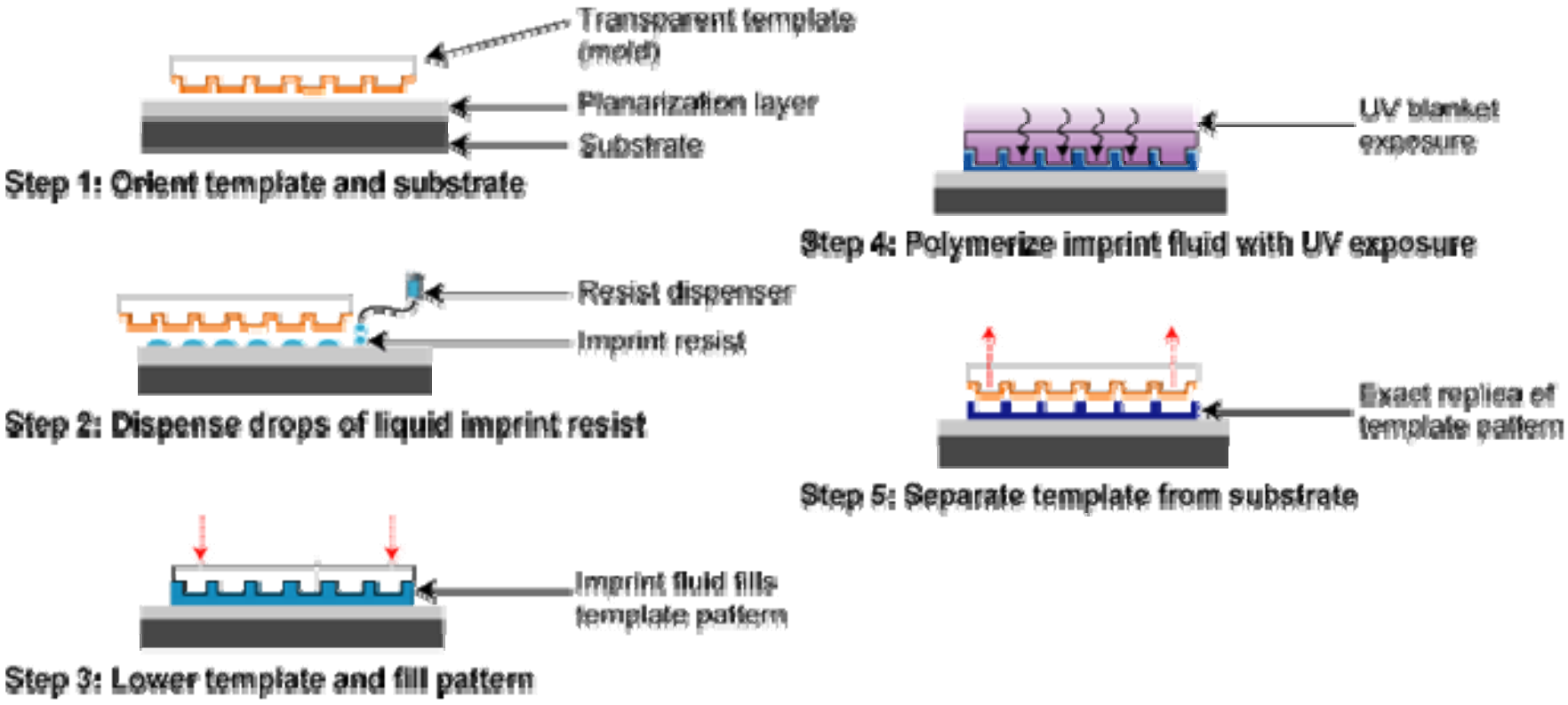

Nanoimprintors

NX-2000, Nanoimprintor, Nanonex

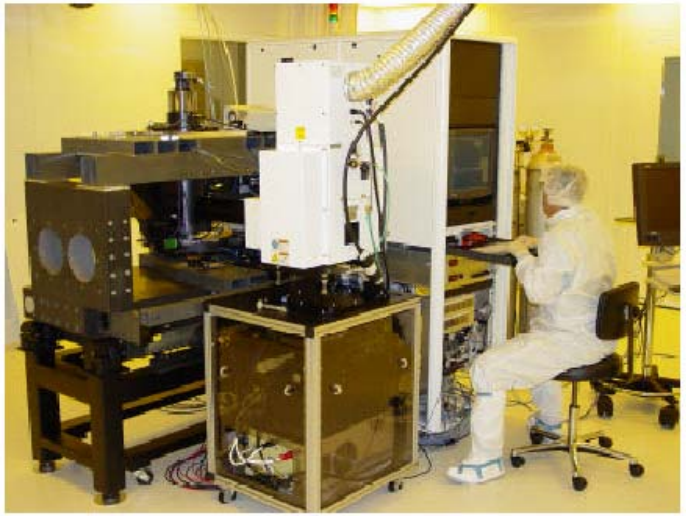

IMPRIO 100

Molecular Imprints, Inc.™

- Resolution: Sub-50 nanometers, imprint template (mold) limited.
- Alignment: < 500 nm, 3σ (X, Y, and Rotation).
- Flexibility: Handles up to 8 inch wafers, including fragile substrates.
- Field size: 25 x 25 mm full active print area, 100 μm street width.

Imprinting Result

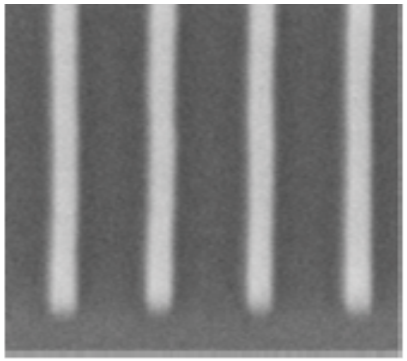

Imprinted 20 nm isolated lines

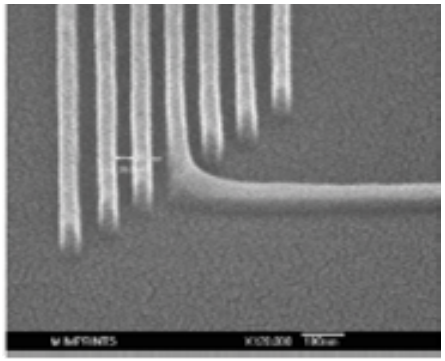

Imprinted 30 nm dense lines

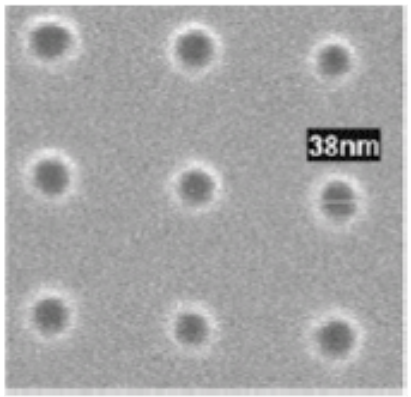

Imprinted sub-40 nm contacts

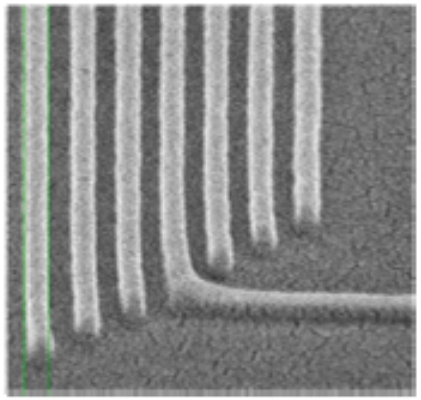

Imprinted 50 nm dense lines

Challenges

- Mask Fabrication (1:1)
- Lift-off process
- Resist
- Mask Design